UNIVERSITÄTSKLINIKUM HAMBURG-EPPENDORF

The Influence of Cytoadhesion of *P. falciparum* Infected Erythrocytes on Human Lung Endothelial Cells

Dissertation

zur Erlangung des Grades eines Doktors der Medizin
an der Medizinischen Fakultät der Universität Hamburg

vorgelegt von:

Tabea Schell
aus Bühl

Hamburg 2024

Angenommen von der
Medizinischen Fakultät der Universität Hamburg am: 15.05.2025

Veröffentlicht mit Genehmigung der
Medizinischen Fakultät der Universität Hamburg.

Prüfungsausschuss, der/die Vorsitzende: PD Dr. Hans F. E. Klose

Prüfungsausschuss, zweite/r Gutachter/in: Prof. Dr. Jürgen May

Table of Contents

Aim of this Study **3**

1. Introduction **4**

1.1. Malaria disease **4**

1.1.1. Clinical picture of *P. falciparum* infection 5

1.1.2. Prophylaxis 7

1.1.3. Treatment 8

1.1.4. Vaccine 9

1.2. Life cycle of *P. falciparum* **11**

1.2.1. Overview 11

1.2.2. Asexual stages 12

1.2.2.1. Merozoite stage 12

1.2.2.2. Ring stage 14

1.2.2.3. Trophozoite stage 14

1.2.2.4. Schizont stage 15

1.2.3. Sexual stage 17

1.2.4. Mosquito stage 18

1.3. Pathogenesis of *P. falciparum* **19**

1.3.1. Cytoadhesion 20

1.3.2. Sequestration 21

1.3.3. Vascular endothelial dysfunction 21

1.3.4. Inflammation 22

1.3.5. *Pf*EMP1 and *var* genes 22

1.4. Lungs during *P. falciparum* infection **25**

1.4.1. Pulmonary manifestations 25

1.4.2. Acute lung injury / acute respiratory distress syndrome 26

1.4.3. Lung endothelia in *P. falciparum* malaria 27

2. Materials and Methods **29**

2.1. Materials **29**

2.1.1. Technical devices 29

2.1.2. Software 30

2.1.3. Labware and disposables 30

2.1.4. Kits 31

2.1.5. Chemical and biological reagents 31

2.1.6. stock solutions, buffers and mediums 32

2.1.7. HULEC-5a cell culture 34

2.1.8. Lung primary cell culture 35

2.1.9. *P. falciparum* isolates 35

2.2. Methods **36**

2.2.1. Cell biological methods 36

2.2.1.1. HULEC-5a culture methods 36

2.2.1.2. Lungs primary cell culture methods 37

2.2.1.3. P. falciparum culture methods 39

2.2.1.4. Selection and enrichment of P. falciparum 42

2.2.1.5. Harvest of P. falciparum culture after selection 43

2.2.1.6. Harvest using TRIzol reagent 43

2.2.1.7. Co-incubation of iRBCs with HMVEC-L 44

2.2.2. Molecular biology methods 45

2.2.2.1. RNA isolation of P. falciparum and lung endothelial cells 45

2.2.2.2. Measurement of RNA concentration via NanoDrops 46

2.2.2.3. Synthesis of cDNA from plasmodia RNA 46

2.2.2.4. Fluorescence activated cell sorting 46

2.2.2.5. Real-time quantitative polymerase chain reaction 47

2.2.2.6. Next generation sequencing 49

3. Results 50
3.1. Enrichment of infected erythrocytes over lung endothelial cells (HULEC-5a) 51
3.1.1. Selection and enrichment via panning assay 51
3.1.2. Next generation sequencing of HULEC-5a enriched infected erythrocytes 53
3.1.2.1. Var genes 53
3.1.2.2. Rifin genes 54
3.1.2.3. Stevor genes 57
3.2. Enrichment of infected erythrocytes over lung primary cells 58
3.2.1. Selection and enrichment via panning assay 58
3.3. Co-Incubation of enriched iRBCs and lung primary cells (HMVEC-L) 60
3.3.1. Co-Incubation for four hours 60
3.3.2. Co-Incubation for eight hours 66
3.3.3. Gene analysis for co-incubations 79
3.3.3.1. Interleukins 80
3.3.3.2. ICAMs 81
3.3.3.3. TNFSFs 82
3.3.3.4. CXCLs 83
3.3.3.5. NFκBs and RELs 84
3.3.3.6. EPOR 85
3.4. Fluorescence-Activated Cell Sorting of HMVEC-L 86
4. Discussion 87
4.1. Enrichment of infected erythrocytes over HULEC-5a 87
4.1.1. *Var* genes 87
4.1.2. *Rifin* genes 88
4.1.3. *Stevor* genes 88
4.2. Enrichment of infected erythrocytes over HMVEC-L 88
4.3. Co-Incubation of iRBCs and HMVEC-L 89
4.3.1. Co-Incubation for four hours 89
4.3.2. Co-Incubation for eight hours 90
4.3.3. Gene analysis for co-incubations 91
4.3.3.1. Interleukins 91
4.3.3.2. ICAMs 91
4.3.3.3. TNFSFs 92
4.3.3.4. CXCLs 93
4.3.3.5. NFκBs and RELs 93
4.3.3.6. EPOR 94
4.4. FACS of HMVEC-L 94
4.5. Conclusion 96
5. Summary 97
6. Zusammenfassung 98
7. Abbreviations 99
8. Lists of Tables and Figures 102
8.1. List of Figures 102
8.2. List of Tables 103
9. References 104
10. Supplements 116
11. Acknowledgements 117
12. Curriculum Vitae 118
13. Declaration on Oath 119

Aim of this Study

P. falciparum is the most relevant pathogen of malaria and can cause severe malaria and death. *P. falciparum* infected erythrocytes induce a broad variety of physical symptoms which can include lung involvement and pulmonary manifestations. The understanding of the underlying process is relevant to address the clinical impact of pulmonary oedema, ALI, and ARDS.
Previous studies have shown that *P. falciparum* performs a *var* gene switch to escape the immune response and to support binding to endothelial receptors. The cytoadhesion is mediated by different receptors, as many studies implicate, and it consequently leads to sequestration, inflammation, and finally disease burden.

The aim of this study was to add to the knowledge about the described process specifically in lung tissue by a multi-step approach:

1. Identification of the expressed *var* genes of *P. falciparum* after selection and enrichment over two lung endothelial cell lines (HULEC-5a and HMVEC-L),
2. Analysis of the transcriptome of lung primary cells (HMVEC-L) after co-incubation with iRBCs and detection of upregulated and downregulated genes.
3. Examination of the receptors on lung primary cells (HMVEC-L) via FACS after TNF stimulation.

1. Introduction

1.1. Malaria disease

The infectious disease malaria was first mentioned in human records from 2700 BC and, until today, has a major impact on the global health situation (Carter, 2002).

Until the 19th century the parasitic origin of the fever disease was unknown. Therefore, the name malaria resulted from the Italian “mal’aria” meaning “spoiled air” due to the idea that the malady was rising from swamps. In 1880, the responsible parasite *Plasmodium falciparum* (*P.falciparum*) was discovered by Charles Louis Laveran and, later in 1897, the corresponding mosquito vector Anopheles was identified by Ronald Ross (Cox, 2010; Ross, 1897).

Thereafter and continuing until today, an intense research followed, trying to understand and to cure or even prevent the disease.

Countries in tropical and subtropical areas are mainly affected by malaria (Fig 1.1). In 2022, the World Health Organisation (WHO) reported an estimated 249 million cases with 608.000 deaths from malaria globally. Although these incidence rates declined since 2010, the burden is still immense on developing countries and further efforts are necessary (Fig. 1.1). Pregnant women and children under the age of five suffer mostly of severe malaria, the latter accounted for 76% of all malaria deaths worldwide in 2018 (WHO, 2023).

Malaria is transmitted to its human host by a bite of a female Anopheles mosquito and the simultaneous transmission of Plasmodium parasites, which belong to the family of apicomplexan parasites. There are five Plasmodium species known to infect humans*: P. falciparum*, *P. vivax*, *P. ovale*, *P. malariae* and *P. knowlesi*, whereby their global distribution and their severity widely differs. The predominant parasite species is *P. falciparum*, which is also the species most likely to cause severe malaria and death (WHO, 2023).

The symptoms caused by malaria depend on the patient immune system and the level of severity of the infection. It can range from an asymptomatic patient to a case of severe malaria (SM) with major complications such as cerebral malaria (CM), respiratory failure, acute renal failure, severe anaemia and acute respiratory distress syndrome (ARDS). Between these two poles, patients have to deal with an uncomplicated malaria (UM) with a flu-like syndrome including symptoms like fever, malaise, anorexia, lassitude, dizziness, headache, backache,

myalgia, nausea, vomiting and a sense of chilliness (Bartoloni & Zammarchi, 2012; Nayak et al., 2011).

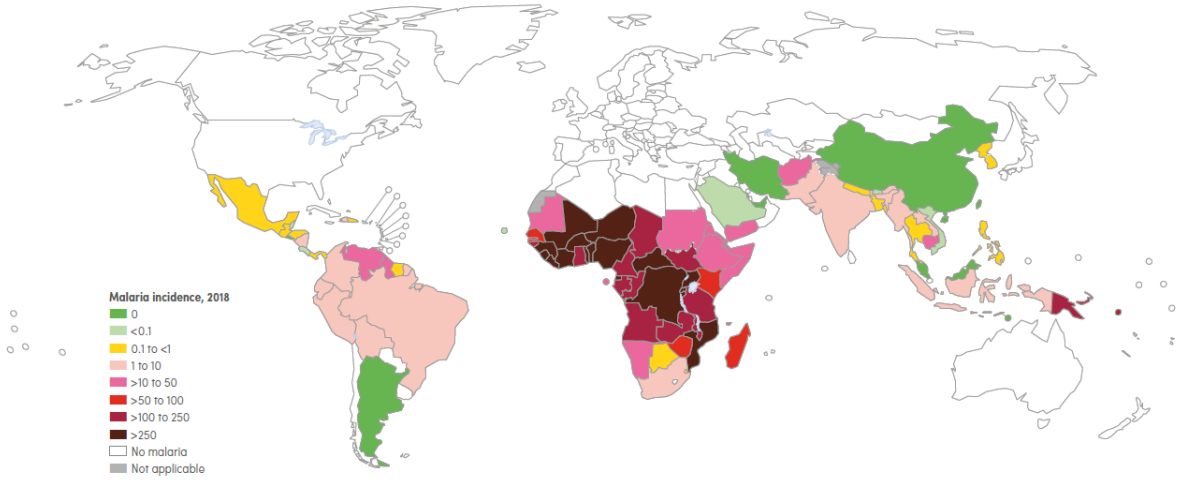

Figure 1.1 Map of malaria case incidence rate (cases per 1000 population at risk) by country, 2018. In 2018 WHO reported 228 million cases and 405.000 deaths from malaria worldwide (WHO, 2019).

1.1.1. Clinical picture of *P. falciparum* infection

P. falciparum parasite is transmitted to the human host by the bite of an infected female Anopheles mosquito. The incubation period ranges from 9 to 30 days. The first symptoms are non-specific and resemble a flu-like syndrome. These symptoms include malaise, myalgia, backache in the lumbar and sacroiliac region, anorexia, dizziness, nausea, vomiting, and lassitude (Warrell & Gilles, 2017). Fever is the cardinal symptom of malaria and the fever in *P. falciparum* malaria is usually irregular without a distinct periodicity as in *P. vivax*, *P. ovale* and *P. malariae* malaria.

In laboratory examinations, there is little or no anaemia at first, the erythrocytes are normochromic and normocytic, the reticulocyte and white cell count are normal and thrombocytopenia is possible and common. The serum transaminases, lactic dehydrogenase and bilirubin are elevated, prothrombin and partial tromboplastin time may be prolonged. C-reactive protein and procalcitonin are probably increased and hyponatremia is possible. Urine analysis shows albuminuria and urobilinogen.

In an examination of the peripheral blood, for example via thick blood smear, many infected red blood cells (iRBCs) with early trophozoites in their typical small ring shape can be recognized (Ahiboh et al., 2008; Bartoloni & Zammarchi, 2012).

This described picture of an uncomplicated malaria case could deteriorate rapidly to severe malaria and serious complications could develop at any stage. Therefore, a fast diagnosis and an adequate treatment are essential for a good prognosis. Normally, patients respond well and rapidly to treatment. Fever and most symptoms should resolve within three days. If erythrocytic forms of the parasites persist, a recrudescence and another clinical manifestation are possible (Bartoloni & Zammarchi, 2012; Farrar et al., 2013).

Malaria is a complex disease and thus the range of symptoms described varies between children and adults (Fig 1.2). Adult patients have a higher mortality rate and a higher probability for multiorgan system involvement. Adults with severe malaria have a mortality rate of 18.5%, whereas children with severe malaria have a mortality rate of 9.7% (Dondorp et al., 2010; South East Asian Artesunate Malaria Trial (SEAQUAMAT) group, 2005; Wassmer et al., 2015) . It should be noted that about 1-2% of malaria infections lead to severe malaria (Marsh, 1992; Reinsch, 2018).

In adults, the major organs affected in a case of severe malaria are the brain with cerebral malaria, the lungs with ARDS, the liver with jaundice and the kidneys with an acute renal failure.

In children, the symptoms CM, severe anemia and acidosis are dominating, while ARDS and renal failure are uncommon. This discovery suggests that children and adults experience different pathophysiological disease mechanisms to which the underlying molecular mechanisms are still unclear (Wassmer et al., 2015).

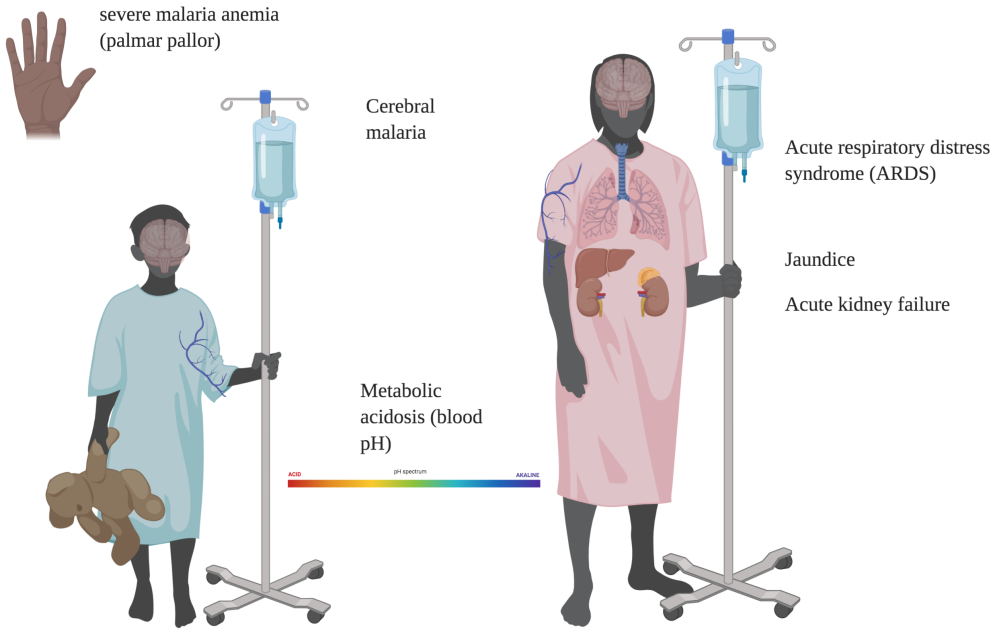

Figure 1.2 The major clinical complications associated with adult severe malaria and paediatric severe malaria. The major clinical complications in children are metabolic acidosis, severe anaemia and CM. In adults, CM is often accompanied by multi-organ system complications with metabolic acidosis, jaundice, ARDS and acute kidney failure (modified after Wassmer et. al, 2015).

1.1.2. Prophylaxis

To reduce the number of imported malaria cases into non-endemic regions a chemoprophylaxis is required. In Germany, 88% of imported malaria patients did not take a prophylaxis.

The go to drug for prophylaxis, Mefloquin, is no longer prescribed in Germany due to the association with irreversible neuropsychiatric side effects.

Instead, the combination of Atocaquon and Proguanil is used to prevent infection and should be taken from one to two days before entering until seven days after leaving a high-risk endemic area (Vinnemeier & Rolling, 2018).

It should be noted that there is no infection without a mosquito bite beforehand, so it is advised to take the appropriate precautions (Hatz, 2004; Labbé et al., 2001).

1.1.3. Treatment

Malaria still means a significant threat to global health despite decades of research and progress. As long as there is no successful vaccine, the management of clinical malaria cases aims to prevent worsening, to reduce mortality, and to limit the spreading of the infection as well as the distribution of *Plasmodium* resistant strains. Researchers are looking for a drug that fights the replication of blood erythrocytic asexual forms, primarily schizonts, and liver hypnozoites. In addition, in endemic areas the ideal drug should also be potent to challenge the sexual form of gametocytes to limit the transmission via the vector mosquitoes.

For centuries, single drug regimens with quinine selective therapeutical value were recommended and included the drugs pamaquine (1924), chloroquine (1934), proguanil (1944), pyrimethamine (1952), primaquine (1956), sulphonamides (1960), mefloquine (1971), and halofantrine (1989).

In the early 1960s this regimen was first challenged due to the discovery and spread of *P. falciparum* with reduced sensitivity to all existing antimalarial drugs in South-East Asia and Colombia (Castelli et al., 2012; Tse et al., 2019).

At the end of the 20th century, the anti-parasite efficacy of artemisinin and its derivates were discovered and artemisinin based combination treatments (ACT) were successfully tested to become the new and potent standard of care for complicated and uncomplicated malaria (Castelli et al., 2012).

The chance of a genetic resistance mutation to happen depends on the number of replicating parasites and the drug concentration they are exposed to. Thus, the idea was to combine a rapidly acting potent drug with a highly concentrated, long-acting partner drug aiming to ensure both the fast reduction of parasite number and to limit the selective potential of a low drug concentration. Unfortunately, parallel to the history of chloroquine and possibly due to misuse of ACT, there have been reported resistances to artemisinin derivatives. It remains crucial to avoid monotherapy at all costs in order to slow down the rise of resistances until there is a vaccine or another equally potent drug as artemisinin derivates (Castelli et al., 2012; Labbé et al., 2001; Tse et al., 2019).

According to the current WHO *falciparum* malaria treatment guidelines artemisinin derivates are the drugs of choice. In a case of UM, patients are treated with artemether/lumefantrin (Riamet ®, Coartem®), atovaquon/proguanil (Malarone®) or dihydroartemisinin/piperaquin (Eurartesmin®). In more severe cases, patients need intensive care as well as a supportive therapy to reduce the fever and to avoid hypoglycaemia. The guidelines recommend the

intravenous administration of artesunate for 72 hours, followed by oral therapy of atovaquon/proguanil or artemether/lumefantrin (WHO, 2015).

1.1.4. Vaccine

The research to develop a potent vaccination against malaria has been long and strenuous and is still ongoing. The difficulty lies in the complex life cycle of Plasmodia with a mosquito vector, a human host and pre-erythrocytic, erythrocytic and mosquito stages. It is expected that probable vaccine candidates may only be effective in a certain species at a defined stage. To make matters worse, Plasmodium has shown skills and ways to escape immune responses and hence avoid vaccine-induced immunity (Wang et al., 2009).

Researchers are still hopeful to discover a vaccine, since in nature an acquired immunity through repeated infection has been described (Hviid, 2007).

Up to now, research mostly focused on subunit vaccine approaches, which probably will not eliminate malaria but could prove useful in combination with existing control strategies to improve global health (Arama & Troye-Blomberg, 2014; Wang et al., 2009).

These subunit vaccine approaches target different stages in the *Plasmodium* life cycle:

First, transmission-blocking vaccines (TBVs) aim to directly prevent the parasite development in the mosquito midgut by targeting antigens on gametes, zygotes, and ookinetes. TBV would only prevent the spread of infection without offering direct protection upon the individual and hence has a difficult reputation as well as financing problems (Arama & Troye-Blomberg, 2014; Carter et al., 2000).

Second, pre-erythrocytic vaccines target the parasites at their sporozoite stage or liver-stage to consequently prevent malaria in the human host. They can be further classified into subunit vaccines and whole cell vaccines (Metzger et al., 2020).

Subunit vaccines do not contain live components of the pathogen, but antigenic parts to elicit a protective immune response. The effectivity of the immune response and the formation of an immunological memory depends on the precise quality of the vaccine (Christensen, 2016). The subunit vaccine RTS,S/AS01 consists of two dominant epitopes ‘R’ (repeat region of circumsporozoite protein CSP) and ‘T’ (T-cell-epitop of CSP), one fused and one free hepatitis B surface antigen (‘S,S’), and is combined with a liposomal adjuvant (AS01). RTS,S/AS01, today called Mosquirix^{TM}, started its phase 5 trial in April 2019 to further examine the phase 3 trial results of high tolerability and safety with moderate effectiveness and fast decline of

effectiveness (Müller et al., 2015). In 2021, WHO approved RTS,S/AS01 as the first malaria vaccine for widespread use in the immunization of children in high-risk regions (El-Moamly & El-Sweify, 2023).

Whole cell vaccines contain complete *P. falciparum* sporozoites (PfSPZ). To avoid a life threatening malaria infection, those living vaccine sporozoites can be attenuated by different methods like chemical attenuation, genetic attenuation, attenuation by radiation and attenuation by chemoprophylaxis (Ishizuka et al. 2016; Mueller et al. 2005; Purcell et al. 2008; Rénia et al. 2013). The protection against *P.falciparum* malaria by pre-erythrocytic whole cell vaccines is surprisingly high in controlled human malaria infections (CHMI), but further verification and field tests in endemic areas are required (Epstein et al., 2017; Olotu et al., 2018; Sissoko et al., 2017).

Third, blood stage vaccines aim to attack the parasites in their erythrocytic forms especially as merozoites. So far, research has mostly shown only moderate efficacy, but studies with subunit vaccines against the merozoite surface protein 1 (MSP1), the invasion protein RH5, and the camouflage protein SE36 are still ongoing and results are pending (Beeson et al., 2016; Jäschke et al., 2017; Payne et al., 2017; Theisen et al., 2017; Tougan et al., 2018).

Fourth, multi-stage vaccines attempt to combine and attack all mentioned *P. falciparum* stages. The Multi-Stage Malaria Vaccine Consortium (MMVC) launched a program in Oxford in 2018 with international cooperation to develop a vaccine with 75% lasting efficacy by 2023 which combines four stages by four proteins: the pre-erythrocytic R 21, a pre-erythrocytic protein of the liver stage, the blood stage protein RH5, and the ookinetes protein Pfs 25. (Boes et al., 2015). The developed R21 malaria vaccine showed good to high efficiency depending on time of application while being cost effective and safe. In 2023, WHO recommends the R21/Matrix-M vaccine for malaria prevention. Both accepted malaria vaccines, RTS,S and R21, show great prospect in fighting malaria together (Genton, 2023).

Fifth and last are placenta vaccines aiming to prevent pregnancy-associated malaria and to protect the especially endangered patient groups of pregnant women and new-borns (Fried & Duffy, 2017). The designed vaccine PAMVAC (pregnancy associated malaria vaccine) has proven to be safe and immunogenic and a randomized, double-blind clinical trial is currently running to verify its efficacy (Fried & Duffy, 2015; Mordmüller et al., 2019).

1.2. Life cycle of *P. falciparum*

1.2.1. Overview

The normal course of malaria includes a cyclical infection of the two crucial hosts, humans and female Anopheles mosquitos (Fig. 1.3). The cycle in the human host starts when an Anopheles mosquito bites a human and injects parasites in the sporozoite form (Sidjanski & Vanderberg, 1997). The sporozoites move to the liver where they invade hepatocytes and start to produce thousands of exoerythrocytic merozoites over the course of eight to ten days (Mota et al., 2001; Prudêncio et al., 2006). After that, the merozoites travel in vesicle-like components, called merosomes, through the liver and the liver sinusoids. Merozoites are finally released into the blood stream, where they continue to invade erythrocytes and grow into trophozoites and into mature schizonts (Portugal et al., 2011; Sturm et al., 2006). The mature schizonts rupture releasing merozoites that can reinvade red blood cells (Petter & Duffy, 2015). During one intraerythrocytic cycle, which takes about 48 hours, one schizont can form up to 32 new merozoites. Some of the asexual blood stage parasites differentiate into sexual erythrocytic stages called gametocytes. When gametocytes are taken up by another feeding mosquito, they can then mature into male (microgametocytes) and female (macrogametocytes) gametes in the mosquito's gut. The following amplification in the second host, the Anopheles mosquito, is known as the sporogonic cycle. In the mosquito's stomach, the microgametes penetrate the macrogametes in order to give rise to zygotes. The fertilized zygotes then become motile and elongated into ookinetes which continue to invade the mosquito's midgut wall where they develop into oocysts. The oocysts enlarge until they rupture and consequently release sporozoites that migrate to the salivary glands of the mosquito (Matuschewski, 2006; Shute, 1945). Finally, the inoculation of the new generation of sporozoites into a new human host completes the malaria life cycle and perpetuates the survival of the parasite (Cowman et al., 2012; Cowman & Crabb, 2006).

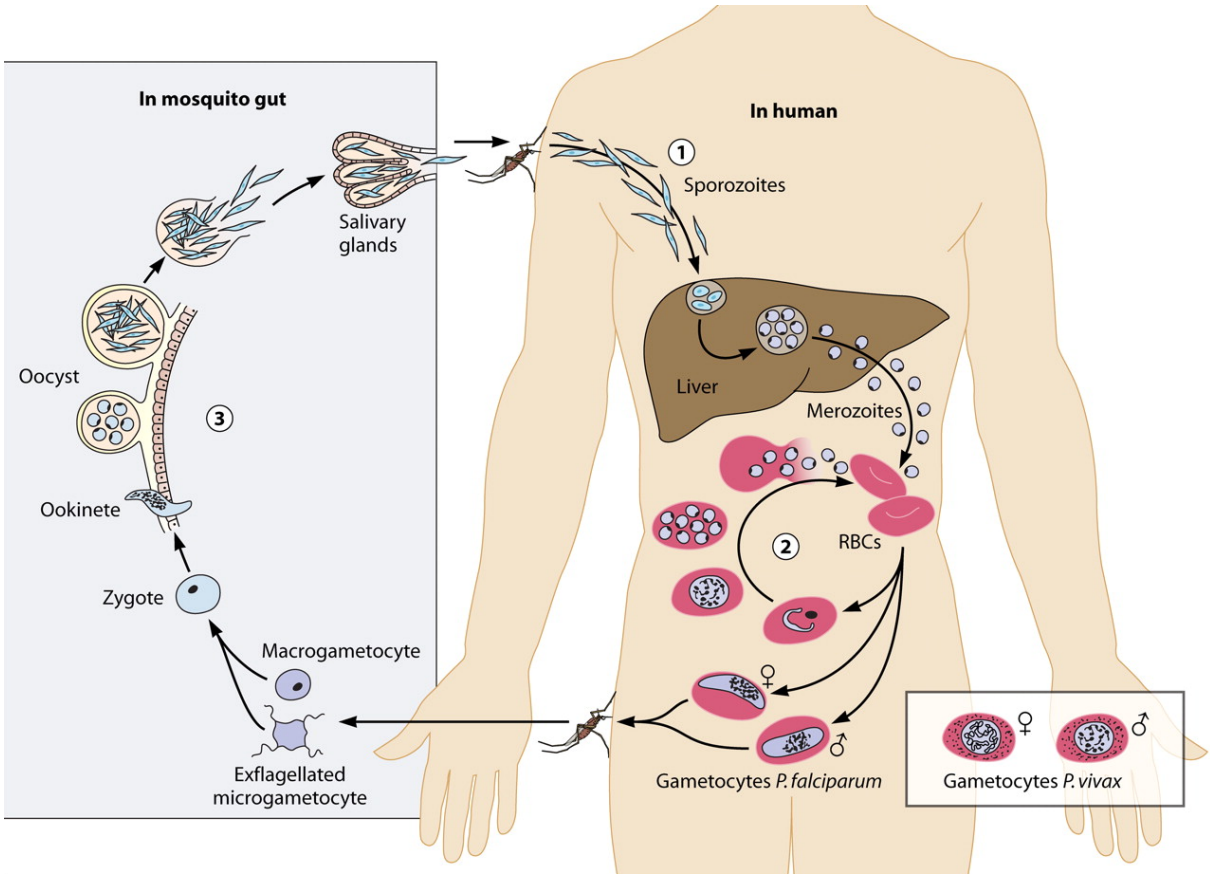

Figure 1.3 P. falciparum life cycle. An Anopheles mosquito injects Plasmodium sporozoites into the host dermis. The sporozoites reach the blood vessels and continue to the liver. They invade a hepatocyte. Inside the hepatocyte, asexual replication and development take place. The formed merozoites are released into the bloodstream. The merozoites infect red blood cells. Asexual replication takes place. Occasionally, replication cycles take the sexual pathway and originate female and male gametocytes. When taking a blood meal, a mosquito ingests gametocytes into its midgut. In the mosquito midgut, the gametes are fertilized. Ookinetes and oocysts are formed. The oocyst releases sporozoites. The sporozoites travel to the mosquito's salivary gland. They are released during the next blood meal (Bousema & Drakeley, 2011).

1.2.2. Asexual stages

1.2.2.1. Merozoite stage

The merozoite stage represents an important phase since it is a period during which the parasites survive extracellular and with exposition to the immune system of the host. Merozoites are polar ovoid cells approximately 1µm long with an apical complex that is providing the parasite with specialized secretory organelles such as rhoptries, micronemes and dense granules (Fig. 1.4) (Aikawa et al., 1981; Wright & Rayner, 2014). These organelles release their content in a specific order during and right after the invasion process. These released ligands interact with

corresponding erythrocyte surface receptors in order to form an electron-dense thickening of the erythrocyte membrane at the link of erythrocyte-merozoite contact. The junction then passes around the merozoite surface in a belt-like structure by means of an actin-myosin motor which is located at the merozoite's inner membrane complex (IMC). Finally, the moving junction shuts behind the merozoite like an iris diaphragm, the merozoite is enclosed inside the erythrocyte in a parasitophorous vacuole, and the process of invasion is completed. This complex mechanism happens in less than two minutes according to recent studies. The possible explanation for this speed is the need to evade an immunological attack while being extracellular (Wright & Rayner, 2014).

This defense mechanism is supported by an array of invasion-associated proteins. The most well-studied ones have been systematized in the following functional classes: MSPs (merozoite surface proteins), *Pf*EBAs (*P. falciparum* erythrocyte binding antigens) and *Pf*RHs (*P .falciparum* reticulocyte binding protein homologues) (Wright & Rayner, 2014).

MSPs are suspected to play a role during the initial phases of invasion. Hence, they are exposed to the host and to its antibodies early-on. To escape this immune response, MSPs are often highly polymorphic and their genes are under balancing selection pressure. This leads to a parallel circulation of multiple variants of the same gene within one group. Confronted with these diversity-creating mechanisms even a primed immune system is unable to effectively stop the invasion of all merozoites in their short period of being extracellular (Wright & Rayner, 2014).

*Pf*RHs and *Pf*EBAs are considered to be active later during invasion and they are thought to help the invasion process by offering alternative invasion pathways and thus generating functional redundancy to outsmart the host's immune response (Wright & Rayner, 2014).

As mentioned before, merozoites contain an apical complex with secretory organelles, more precisely with rhoptries, micronemes, and dense granules (Fig. 1.4) (Bannister et al., 2000).

Rhoptries are a pair of electron-dense, membrane-bound, pear shaped and deducted structures filled with rhoptries proteins. They are suspected to play a major role in the formation of the parasitophorous vacuole membrane (PVM).

Micronemes, on the other hand, are smaller than rhoptries and stretched between the rhoptry duct and the apical cytoplasm of the merozoite. They are suspected to disappear during invasion by releasing their content by membrane fusion into the rhoptry duct (Preiser et al., 2000).

Dense granules are spheroidal membranous vesicles with densely granular interiors lying free within the cytoplasm between the rhoptries and the merozoite nucleus. When the erythrocyte is invaded, the dense granules move to the merozoite surface and release their contents via

exocytosis into the PVM. An important contained protein is RESA (ring infected erythrocyte surface protein) which is suspected to associate with spectrin in the cytosol and thus inhibiting further invasion by intensifying the cell membrane's rigidity (Bannister et al., 2000; Preiser et al., 2000).

The parasitophorous membrane is supposed to mediate between the parasite and the host cell. The parasite spans a complex interconnected network of tubovesicular membranes (TVM) between the PVM and the erythrocyte cytosol with the purpose of a transport network that ensures the efficient movement of nutrients (Lauer et al., 1997).

1.2.2.2. Ring stage

When the process of invasion is completed, the parasite changes shape from the ovoid form into the thin discoidal, flat disc form of the trophozoite stage (Grüring et al., 2011). The cells have a surrounding broad band of cytoplasm with all the organelles while the centre is thin and only with few structures (Fig 1.4). The name "ring stage" derives from this thickened parameter and the position of the nucleus when stained with Giemsa and observed under light microscopy (Bannister et al., 2000). The parasite starts to feed on its host cell and digests it from the inside out through a small ring on the surface called the cytostome (Slomianny, 1990). By this technique it pulls in about 75% of the host haemoglobin and the haem derivative is then converted into inert brown haemozoin crystals (Abu Bakar et al., 2010; Hanssen et al., 2010). These haemozoin crystals accumulate in the pigment vacuole, first in multiple smaller vacuoles and later in one fused large vacuole. The parasite continues to grow and the PVM keeps extending until it again changes shape, now from the ring shape to a more rounded or irregular trophozoite (Bannister et al., 2000). The duration of the ring stage is about 20 hours and the ring stage parasites are to be found in the peripheral blood circulation as they are not yet fully able to adhere to the endothelial cells of target organs (Spielmann et al., 2006).

1.2.2.3. Trophozoite stage

In comparison to the ring stage, the trophozoite stage comprises parasites with a larger endoplasmic reticulum (ER) and more free ribosomes in order to have an increased protein synthesis (Bannister et al., 2000). In addition, the surface of the trophozoite expands and forms

irregular bulges and tubular hollows (Fig 1.4). On the surface of the infected erythrocytes (IE) electron dense knob like structures become visible and act as important attachment points in cytoadherence. These knobs are mainly formed by parasite-encoded knob-associated histidine-rich protein (KAHRP) and *P. falciparum* erythrocyte membrane protein 1 (*Pf*EMP1) (Oh et al., 2000). In electron microscopy, trophozoites often reserve their ring-like shape or appear amoeboid and the cytoplasm is denser than in young ring stage (Bannister et al., 2000; Coatney et al., 1971). Their might be a transition from multiple smaller foci of haemozoin to one single haemozoin complex which suggests the switch from multiple small food vacuoles (FVs) to a single FV. Following, the parasite continues in the `schizont stage` to complete the asexual life cycle (Grüring et al., 2011).

1.2.2.4. Schizont stage

In theory, a schizont is an intraerythrocytic parasite that is experiencing or has experienced repetitive nuclear division. During the schizont stage, the number of knobs on the surface of IEs increases and the surface appears more irregular due to the cytoskeletal distortion (Fig 1.4). 10-15 hours before rupture, the FV moves from the periphery to a central position. Two to three hours before rupture, the parasite fills most of the host cell. The parasite creates a series of centres of merozoite formation. In each centre, the different elements of merozoites are assembled in a concretely ordered sequence of steps. It starts with the apical organelles and ends with the appearance of mitotic spindles (Bannister et al., 2000). Finally, the host cell ruptures and up to 32 daughter merozoites are released into the blood stream ready to invade new erythrocytes and to complete the asexual life cycle (Grüring et al., 2011).

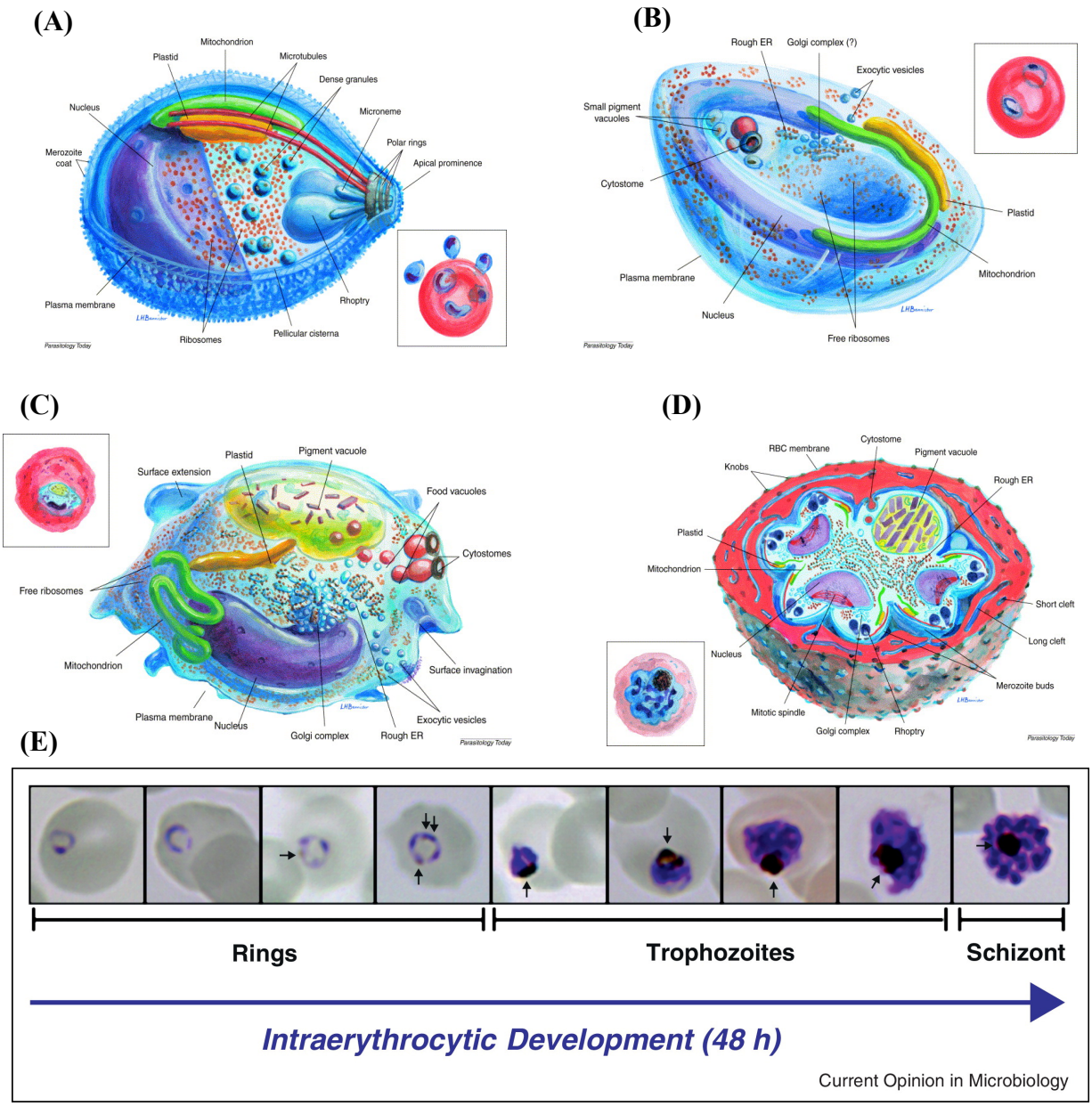

Figure 1.4 The P. falciparum blood stages. (**A)** A *P. falciparum* merozoite. The internal structure is shown. Inset on the right: relative sizes of merozoites and the RBC. **(B)** A *P. falciparum* early ring stage in a cup-like form. RBC and PVM are not shown. Inset on the right: Ring stage as seen in a Giemsa-stained film by light microscopy. **(C)** A *P. falciparum* in the trophozoite stage. Increase in protein synthesis apparatus, increased feeding (multiple cytosomes), growth of pigment vacuole. Inset on the left: Relative sizes of trophozoite and RBC as seen by light microscopy. **(D)** A *P. falciparum* schizont. The schizont infected the surrounding RBC. The merozoites are budding from the surface of the schizont. The apex of each merozoite contains the apical organelles. Mitochondria and plastids are migrating into the buds. Inset on the left: relative size of RBC and schizont. (E) Intraerythrocytic development of the *P. falciparum* stages (Bannister et. al, 2000; Klonis et. al, 2013).

1.2.3. Sexual stage

As mentioned before, there are also merozoites that are bound to differentiate into a male or female gametocyte. These merozoites invade red blood cells and instead of entering the described asexual life cycle, they perform the sexual replication and differentiate into a gametocyte after 10-12 days (Eksi et al., 2012; Hawking et al., 1971). The formed gametocytes from one schizont are all either male or female (Guttery et al., 2012). The morphology during maturation is described in five stages by Field and Shute (Fig 1.5):

In stage I, the shape is first indistinguishable from small round trophozoites and later changes to a larger round shape. The erythrocyte plasmalemma is 'knobless' while the asexual infected erythrocytes are knobbed.

In stage II, the gametocyte elongates and becomes D-shaped due to the formation of a subpellicular membrane and microtubule complex.

In stage III, the gametocyte still appears D-shaped and the slightly distorted erythrocyte shows a pink/blue distinction of male/female. The male nucleus is notably bigger while the female contains more ribosomes, ER, and mitochondria.

In stage IV, the parasite appears elongated and thin with the male's pigment more scattered compared to the female's dense pigment. The formed membrane and microtubule complex now surrounds the gametocyte.

In stage V, the parasite is sausage shaped with rounded extremities and analogue to stage IV, male and female gametocytes differ in pigment colour as well as density. The subpellicular microtubules are lost by depolymerisation. The male gametocyte, called microgametocyte, reduces the ribosomal density and has a large nucleus while the female gametocyte, called macrogametocyte, has many mitochondria, ribosomes, osmophilic bodies, and a smaller nucleus (Talman et al., 2004).

The developed gametocytes can then be taken up by a mosquito's feeding and enter the sporogonic cycle in an Anopheles mosquito (Sidjanski & Vanderberg, 1997).

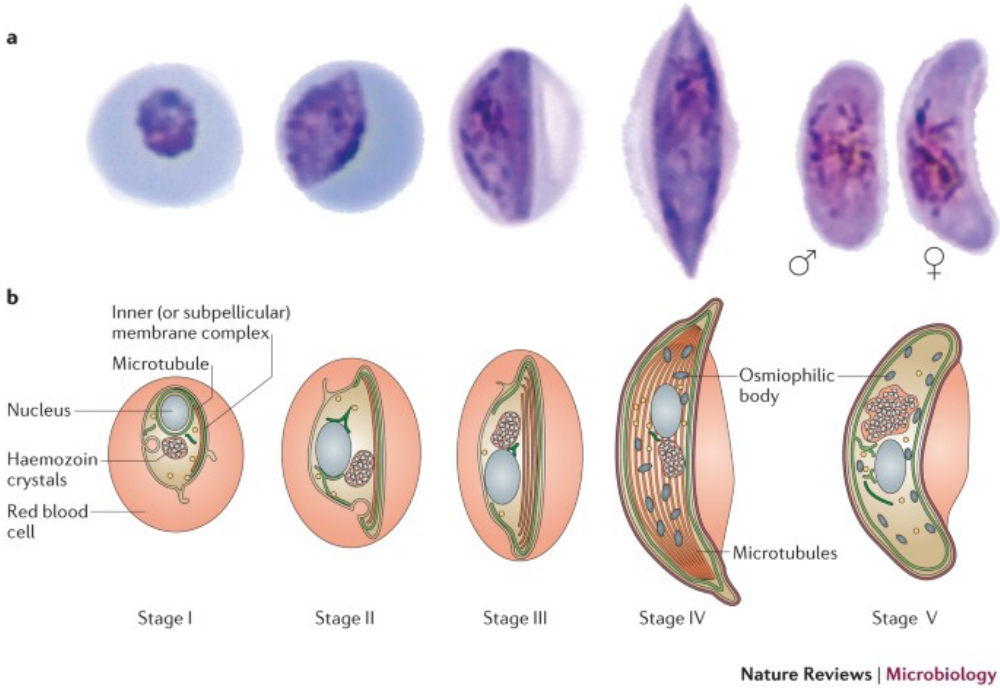

Figure 1.5 Stages I - V of sexual development in P. falciparum parasites (Josling &Llinás, 2015). Stage I: small, round shape. Stage II: elongated, D-shaped, formation of subpellicular membrane. Stage III: D-shaped, colour change of male/female, male nucleus bigger than female. Stage IV: elongated and thin, membrane and microtubule complex surround gametocyte. Stage V: sausage shaped, male/female differ in colour and density.

1.2.4. Mosquito stage

Only sexual blood-stage parasites can effectively infect the mosquito and initiate the sporogonic cycle. After the ingestion by a mosquito, the male and female gametocytes encounter a lower temperature, a different pH and the existence of canthurenic acid. These factors lead to their maturation into gametes in the mosquito mid-gut. Next, the male gametocytes perform three rounds of DNA replication to form an octoploid nucleus and assemble eight flagella. The sexually competent male gametes are then released during exflagellation and fuse with the female gametes to form a diploid zygote. The zygote develops into an ookinete and passes through the mid-gut epithelial cell wall to form an oocyste which then ruptures and releases sporozoites. The sporozoites travel to the mosquito's salivary glands, where they are ready for the mosquito's next blood meal to simultaneously switch to the next human host (Josling & Llinás, 2015; Ngwa et al., 2013).

1.3. Pathogenesis of *P. falciparum*

The pathogenic mechanisms leading to malaria and potentially to life threatening symptoms of severe malaria are not finally explored. Current theories suggest, that in variable relevance depending on syndrome and stage, the impacts of parasite sequestration, inflammation and vascular endothelial dysfunction lead to the known clinical picture of malaria (Cunnington et al., 2013). Before *P. falciparum* infected erythrocytes can sequester to the corresponding endothelia, they cytoadhere via *Pf*EMP1 mediated binding mechanisms. This makes cytoadhesion another key virulence determinant (Smith et al., 2013).

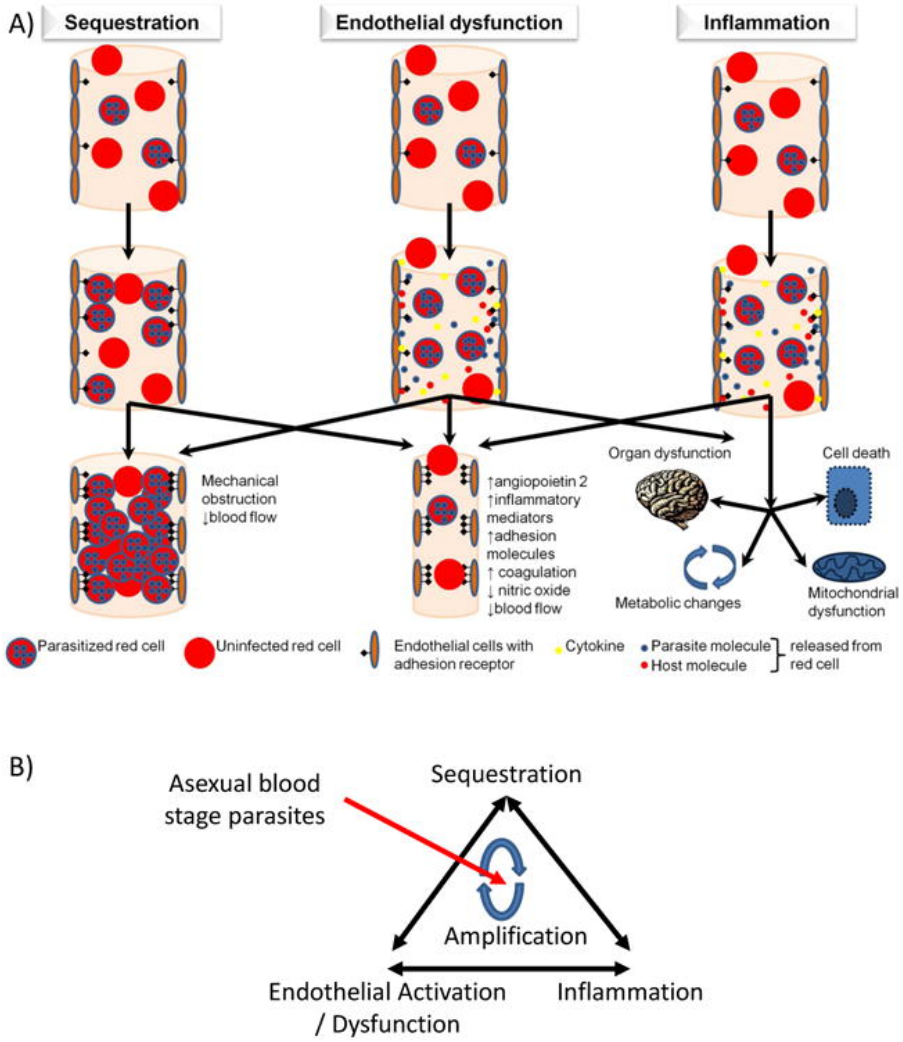

Figure 1.6 The pathogenesis of severe malaria. **(A)** Sequestration, endothelial dysfunction and inflammation are believed to jointly cause the pathogenesis of severe malaria. The sequestration of cytoadherent iRBCs on small blood vessels might induce the mechanical obstruction of blood flow. The iRBCs and host cells release molecules which can cause vascular endothelial activation and dysfunction leading to harmed blood flow and activation of clotting. The released molecules have direct inflammatory effects on target organs. **(B)** Those pathogenic mechanisms are expected to interdependent and amplify each other with rising parasite biomass (Cunnington et. al, 2013)

1.3.1. Cytoadhesion

Cytoadherence describes the mechanism when mature infected red blood cells in erythrocytic stages evade from the splenic clearance by binding to endothelial cells. In the relatively hypoxic tissue environment, parasite growth is promoted (Alister et al., 2012).

Mature iRBCs are rarely discovered circulating in the peripheral blood. *P. falciparum* modify the surface of their host erythrocytes by exporting specific proteins making them more rigid and inflexible. When being less flexible, RBCs have problems circulating through the microvasculature and their adhesion to endothelial cells is facilitated (Dondorp et al., 2004).

The process of cytoadhesion is controlled by precise interactions between members of the *Pf*EMP1 family and receptors on the surface of endothelial cells (Rowe et al., 2009).

The *P. falciparum* erythrocyte membrane protein 1 is encoded by about 60 different *var* genes. They are introduced further in chapter 1.3.5.

The well explored matching endothelial receptors are CD36, endothelial protein C receptor (EPCR), intracellular adhesion molecule 1 (ICAM-1), and P-selectin, while many others are little understood and their function in malaria disease remains unclear (Smith et al., 2013; Yipp et al., 2007).

The CD36 receptor is expressed on microvascular endothelia, monocytes, macrophages, dendritic cells and platelets. The receptor binding does mediate IE sequestration and supports non-opsonic IE phagocytosis. The binding between infected erythrocytes and CD36 is generally associated with cases of uncomplicated malaria and might support the sequestration to rather non-pathogenic tissues such as adipose tissue as well as skeletal muscles instead of vital organs (McCormick et al., 1997; Rowe et al., 2009).

The EPCR is expressed on endothelial cells as well as leukocytes and the corresponding protein C-EPCR signalling pathway has anti-inflammatory, anti-thrombotic effects to secure endothelial cells and to keep vascular integrity. The binding to EPCR is associated with cases of severe malaria and brain involvement is more likely (Avril et al., 2012; Smith et al., 2013; Turner et al., 2013).

ICAM-1 is a member of the immunoglobulin superfamily and is expressed on endothelial cells as well as leukocytes. When infected erythrocytes bind to ICAM-1 it leads to rolling and static adhesion. It has been suggested that ICAM-1 and CD36 act in synergy to intensify static adhesion (Chakravorty & Craig, 2005; McCormick et al., 1997). The pathophysiological significance of ICAM-1 is unclear (Rowe et al., 2009).

P-selectin is a glycoprotein, expressed on endothelial cells and activated platelets. It is crucial for the trafficking of leukocytes and it supports rolling of infected erythrocytes on endothelial cells. P-selectin interacts with *Pf*EMP1 by not yet identified binding dominants and the role of P-selectin in severe malaria is still to be determined (Rowe et al., 2009; Senczuk et al., 2001). Other potentially relevant and discussed receptors are thrombospondin (TSP), platelet endothelial cell adhesion molecule 1 (PECAM1), E-selectin, vascular cell adhesion molecule 1 (VCAM1) and heparin sulphate (Rowe et al., 2009).

1.3.2. Sequestration

Red blood cells infected by mature asexual stages of *P. falciparum* sequester in the microvasculature. They are able to mechanically obstruct blood flow by the sheer number of sequestering parasitized red blood cells (Cunnington et al., 2013). The tendency for sequestration might explain the possible lethality of *P. falciparum* malaria: iRBCs can sequester and obstruct small blood vessels in the brain and then lead to clinical manifestations of coma and death (Idro et al., 2005). The sequestration lowers the blood flow in all affected tissues and oxygen delivery is decreased. Thus, a shift from aerobic to anaerobic glucose metabolism, the production of lactic acid and a drop in the blood pH are caused. The human body aims to control this metabolic acidosis by increasing the respiratory excretion of carbon dioxide and showing symptoms of respiratory distress (Cunnington et al., 2013; Hanson et al., 2012). Sequestration together with the effect of cytoadhesion constitute a parasite survival advantage by avoiding splenic clearance, easing asexual replication, prolonging the infectious state and promoting the survival of sexual, transmissible stages (Buffet et al., 2011; Fonager et al., 2012, p. 36).

1.3.3. Vascular endothelial dysfunction

In its normal functioning state, the vascular endothelium helps to regulate the microvascular blood flow, represses the coagulation cascade and acts as a barrier to substances within the circulation. In malaria, this normal function is disturbed by inflammatory cytokines and haemoglobin, glycosylphosphatidylinositol and histones released from iRBCs. This activation process causes abnormal perfusion, coagulation and vascular leak. Studies demonstrated the activation of clotting in the small blood vessels and the interference with the barrier function,

which could possibly allow a direct interplay between cytokines or toxins with the host tissues (Cunnington et al., 2013; Hanson et al., 2012; Kim et al., 2011).

1.3.4. Inflammation

Multiple studies have shown elevated concentrations of inflammatory mediators in severe malaria compared to uncomplicated malaria. Leukocytes release cytokines and other inflammatory mediators, having both, direct effects on target organs as well as indirect effects through the activation of vascular endothelium, metabolic derangement and mitochondrial dysfunction. The actual individual impact of inflammation on severe malaria is not explored and overlapping impacts with other factors are expected (Cunnington et al., 2013).

1.3.5. *Pf*EMP1 and *var* genes

As mentioned before in chapter 1.3.1, the interactions between iRBCs and endothelial cells are mediated by receptors on the endothelial cells and *Pf*EMP1 on the erythrocytes. *Pf*EMP1 is encoded by *var* genes which belong to the family of variant surface antigens (VSAs). The other members of VSAs are *rifin*, *stevor* and *PfMC-2TM* (Fig 1.6)(Dzikowski & Deitsch, 2006).

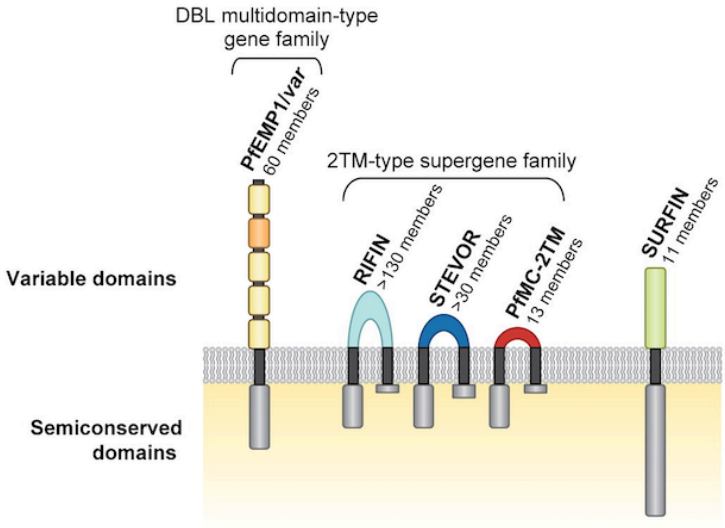

Figure 1.7 Gene families coding for molecules associated with the surface of iRBCs (Scherf et al., 2008). DBL multidomain-type gene family: PfEMP1; 2TM-type supergene family: *rifin, stevor, Pf*MC-2TM; *surfin*.

VSAs are part of the many ways by which the parasites evade the human immune system. They offer the ability to change some of their surface antigens. This process is called antigenic variation (Scherf et al., 2008).

Var genes are allocated in clusters across most of the 14 chromosomes and expressed in a mutually exclusive fashion. The 60 *var* genes are divided into three main groups based on conserved sequences upstream of the coding region (Fig 1.7). Group A *var* genes are confined to subtelomeric regions. I*n vivo* gene expression studies connected group A *var* genes to the pathogenesis of severe malaria. Group B *var* genes can be found within chromosomes and at the subtelomere. Group C *var* genes are only identified in internal chromosome regions. Parasites can perform an antigenic switch between *var* genes to evade the host immune system and to elevate their virulence factor (Claessens et al., 2014; Guizetti & Scherf, 2013). The

Var gene switching leads to the expression of only one *Pf*EMP1 on the surface of the IEs. The expression is controlled by the processes of silencing, activation, poising and switching: The *var* genes are all silenced except for one activated *var* gene in the ring stage. This active *var* gene is repressed in later stages of the cycle but remains in a poised state for transcription. The parasite is able to switch the expressed and active *var* gene by a not yet explained method (Scherf et al., 2008). The 60 *var* genes and their distribution in groups A, B, C are presented in table 1.1.

From notable interest is *var*04, also called *var*2CSA. It is known to enable the binding of iRBCs, which express *Pf*EMP1 coded by *var*04, to Chrondroitin sulfate A (CSA) on the surface of the syncytiotrophoblast. By this mechanism, CSA functions as a receptor for the sequestration of Plasmodium falciparum in the placenta during pregnancy. Therefore, the gene switch to *var*2CSA is not only an important virulence factor for the development of placental malaria but also a potential target for therapy or vaccine research (Reeder et al., 1999; Rieger et al., 2015).

Table 1.1 IT4 PfEMP1 variants **(predicted extracellular protein structure)***(Rask et al., 2010)*:

Gene name	UPS	NTS	Extracellular Domain Structure (Predicted)	ATS
IT4_var08	A1	A6	DBLα1.7 CIDRγ3 DBLβ3 DBLδ4 CIDRγ1 DBLζ6 DBLε9	A1
IT4_var35	A2	A1	DBLα1.1 CIDRα1.2 DBLβ11 DBLγ1 DBLε1 DBLγ8 DBLζ1 DBLε5	
IT4_var03	A3	A6	DBLα1.3 DBLε8	Var3
IT4_var02	A3	A6	DBLα1.5 CIDRδ1 DBLβ3 DBLγ12 DBLδ5 CIDRβ3 DBLβ9	A5
IT4_var07	A3	A6	DBLα1.7 CIDRα1.4 DBLβ1 CIDRβ3 DBLγ10 DBLδ1 CIDRβ1	A4
IT4_var18	A3	A3	DBLα1.2 CIDRα1.6 DBLβ3 DBLγ16 DBLγ2 DBLδ1 CIDRβ1	A6
IT4_var64	A3	A5	DBLα1.5 CIDRδ1 DBLβ7 DBLγ11 DBLγ11	A4
IT4_var22	A3	A2	DBLα1.4 CIDRα1.7 DBLβ3 DBLγ10 DBLγ11 DBLδ1 CIDRβ1	A3
IT4_var60		A7	DBLα1.8 CIDRβ2 DBLγ7 DBLζ5 DBLε11 DBLε12	A1
IT4_var09		A8	DBLα1.6 CIDRγ3 DBLγ15 DBLε1 DBLδ1 CIDRβ1	
IT4_var14	B1	B3	DBLα0.23 CIDRα5 DBLβ5 DBLδ1 CIDRγ2 DBLγ3 DBLζ4	
IT4_var46	B1	B3	DBLα0.10 CIDRα2.2 DBLδ1 CIDRγ4 DBLε2 DBLζ3 DBLε3	B19
IT4_var10	B1	B3	DBLα0.5 CIDRα2.6 DBLβ10 DBLδ1	
IT4_var67	B1	B3	DBLα0.10 CIDRα2.2 DBLε2 DBLζ3 DBLε12	B5
IT4_var13	B1	B3	DBLα0.3 CIDRα5 DBLβ5 DBLδ9 CIDRγ9 DBLγ11 DBLζ4	B5
IT4_var19	B1	B3	DBLα2 CIDRα1.1 DBLβ12 DBLγ6 DBLδ1 CIDRβ1 DBLγ9	B3
IT4_var32a		B3	DBLα0.23 CIDRα3.2 DBLγ6 DBLδ1 CIDRβ1	B16
IT4_var32b	B1	B3	DBLα2 CIDRα1.1 DBLβ12 DBLγ6 DBLδ1 CIDRβ1	B15
IT4_var06	B1	B3	DBLα2 CIDRα1.1 DBLβ12 DBLγ6 DBLδ1 CIDRβ4	B15
IT4_var41	B1	B3	DBLα0.4 CIDRα5 DBLβ5 DBLγ5 DBLδ1 CIDRβ1	
IT4_var16	B1	B3	DBLα0.4 CIDRα5 DBLβ5 DBLγ16 DBLδ1 CIDRβ6	B18
IT4_var31	B1	B3	DBLα0.18 CIDRα4 DBLβ3 DBLγ9	
IT4_var44	B1	B3	DBLα0.16 CIDRα3.4 DBLβ13 DBLδ1 CIDRβ6	B2
IT4_var11	B1	B3	DBLα0.3 CIDRα2.4 DBLβ10 DBLδ1 CIDRβ1	B1
IT4_var12		B3	DBLα0.18 CIDRα6 DBLβ4 DBLδ1 CIDRβ1	B2
IT4_var17	B1	B3	DBLα0.11 CIDRα2.4 DBLβ8 DBLδ1 CIDRγ4 DBLγ10	B18
IT4_var29	B1	B3	DBLα0.3 CIDRα3.2 DBLδ1 CIDRγ5	B20
IT4_var24	B1	B3	DBLα0.10 CIDRα2.2 DBLδ1 CIDRγ5	B1
IT4_var45	B1	B3	DBLα0.5 CIDRα2.9 DBLδ1 CIDRβ1	B1
IT4_var33	B1	B3	DBLα0.11 CIDRα2.4 DBLδ1 CIDRβ5	B15
IT4_var25	B1	B3	DBLα0.11 CIDRα2.4 DBLδ1 CIDRβ1	B8
IT4_var61	B1	B3	DBLα0.9 CIDRα2.7 DBLδ1 CIDRβ1	B6
IT4_var54	B1	B3	DBLα0.1 CIDRα3.1 DBLδ1 CIDRβ1	B1
IT4_var63	B1	B3	DBLα0.7 CIDRα3.4 DBLδ1 CIDRβ1	B5
IT4_var26	B1	B3	DBLα0.23 CIDRα3.3 DBLδ1 CIDRβ1	B1
IT4_var40	B1	B3	DBLα0.12 CIDRα2.11	
IT4_var20	B2	B3	DBLα2 CIDRα1.1 DBLβ12 DBLγ6 DBLδ1 CIDRβ1	B16
IT4_var27	B2	B3	DBLα0.6 CIDRα3.1 DBLβ5 DBLγ5 DBLδ1 CIDRβ1	B2
IT4_var58	B3	B3	DBLα0.1 CIDRα3.1 DBLδ1 CIDRβ5	
IT4_var59	B3	B3	DBLα0.1 CIDRα3.1 DBLδ1 CIDRβ1	B14
IT4_var21		B3	DBLα0.1 CIDRα3.1 DBLδ1 CIDRβ1	B14
IT4_var15	B7	B3	DBLα0.8 CIDRα3.5 DBLβ8 DBLδ1 CIDRβ1	B13
IT4_var01	C1	B6	DBLα0.18 CIDRα6 DBLβ5 DBLγ10 DBLδ2 CIDRγ6	

IT4_var51	C1	B3	DBLα0.17	CIDRα3.1	DBLδ1	CIDRγ12					B5
IT4_var66	C1	B3	DBLα0.19	CIDRα2.10	DBLδ1	CIDRβ1					
IT4_var23	C1	B3	DBLα0.1	CIDRα3.1	DBLδ1	CIDRγ10					B10
IT4_var05	C1	B3	DBLα0.5	CIDRα2.3	DBLδ1	CIDRβ1					B1
IT4_var34	C1	B3	DBLα0.1	CIDRα3.1	DBLδ1	CIDRβ4					B12
IT4_var47	C1	B3	DBLα0.1	CIDRα3.3	DBLδ1	CIDRβ1					B4
IT4_var62	C1	B3	DBLα0.1	CIDRα3.1	DBLδ8	CIDRβ2					B11
IT4_var68	C1	B3	DBLα0.1	CIDRα3.2							
IT4_var28	C2	B2	DBLα0.4	CIDRα3.1	DBLδ1	CIDRβ5					B6
IT4_var30			DBLα0.13	CIDRα2.10	DBLδ1	CIDRβ1					B5
IT4_var36			DBLα0.8	CIDRα5	DBLδ1	CIDRβ1					B6
IT4_var39		B3	DBLα0.5	CIDRα2.5	DBLδ1	CIDRβ6					B9
IT4_var04	E	pam	DBLpam1	DBLpam2	CIDRPpam	DBLpam3	DBLεpam4	DBLεpam5	DBLε10		pam1
IT4_var65			CIDRβ1								B10

1.4. Lungs during *P. falciparum* infection

The role of lung involvement in malaria has been observed for a long time but still its pathogenesis and management is not comprehensively resolved. In its most severe form, patients present with pulmonary oedema because of intravascular fluid loss due to increased alveolar capillary permeability.

1.4.1. Pulmonary manifestations

At first malaria patients usually show acute breathlessness. In a longitudinal study, cough was frequent in patients with uncomplicated malaria as well as in patients with severe malaria (Maguire et al., 2005). The small airways may be obstructed, the alveolar ventilation may be impaired, the gas transfer may be lowered and the pulmonary phagocytic activity may be intensified (Anstey et al., 2002). This can quickly deteriorate to respiratory failure, either at disease presentation or after treatment, when parasitemia is decreasing and clinical improvement is expected but instead the cytokine balance shifts to favouring lung inflammation (Taylor et al., 2006). In a prospective case study of severe malaria in adult patients, pulmonary oedema was diagnosed in 9-21% (Aursudkij et al., 1998; Mohanty et al., 2003). Interestingly pregnant women are especially at risk of developing pulmonary oedema and experiencing acute lung injury (ALI) and acute respiratory distress syndrome. Pulmonary oedema might develop

after delivery of the placenta. Especially so, when the woman is anaemic or fluid-overloaded (Looareesuwan et al., 1985; World Health Organization, 2000). ALI or ARDS in paediatric malaria on the other hand seems to be comparatively low (Taylor et al., 2006).
It is crucial to detect, diagnose and manage a case of malaria-induced ALI/ARDS early. It must be treated with effective drugs and patients should be managed in an intensive care unit. The respiratory comprise might require mechanical ventilation and since ALI/ARDS can also be related to a coincidental bacterial sepsis, the use of broad spectrum antibiotic should be taken into consideration. Unfortunately, even despite excellent management, the prognosis of severe malaria with ARDS is bad and unsatisfactory (Taylor et al., 2006).

1.4.2. Acute lung injury / acute respiratory distress syndrome

The definitions of ALI and ARDS have been standardized and they depend on the criteria of onset, oxygenation, posteroanterior (PA) chest x-ray and pulmonary artery wedge pressure as outlined in table 1.2.

Table 1.2 Diagnosing criteria of ALI and ARDS:

Criteria	**ALI** (Acute lung injury)	**ARDS** (acute respiratory distress syndrome)
Timing	Acute onset	Acute onset
Oxygenation	$PaO_2/FiO_2 \leq 300$ mmHg	$PaO_2/FiO_2 \leq 200$ mmHg
PA chest x-ray	Bilateral infiltrates	Bilateral infiltrates
Pulmonary artery wedge pressure	≤ 18mmHg or no clinical evidence of left atrial hypertension	≤ 18mmHg or no clinical evidence of left atrial hypertension

In malaria-associated ALI/ARDS, the human host reacts to the parasite infection with a complex inflammatory response in the lung. This includes pro- and anti-inflammatory cytokines, neutrophil activation, macrophage activation, ischemic hypoxia and red cell sequestration in the lung (Anstey et al., 2002; N. P. Day et al., 1999). Following, the permeability of the alveolar capillary membrane progresses and in the exudative phase protein-

rich fluids leak into the lung. The ventilation perfusion ratio becomes a ventilation perfusion mismatch when the blood circulates through already collapsed alveoli and oedematous lung tissue without participating in the gas exchange. The lung function is compromised (Charoenpan et al., 1990; Lewis & Martin, 2004; Taylor et al., 2006).

1.4.3. Lung endothelia in *P. falciparum* malaria

A post-mortem lung sections study of patients with malaria associated ARDS (MA-ARDS) detected a high level of von Willebrand factor (VWF) and angiopoietin-2 (ANG-2) in the oedematous alveoli. Both are markers for the activation of lung endothelium. At the same time VWF was decreased in the endothelial lining of blood vessels and intravascularly increased which may represent endothelial activation and Weibel-Palade body release, the storage for VWF and p-selectin (Pham et al., 2019).

Another post-mortem histopathological, immunohistochemical and electron microscopic study investigated the role of the protein C system, the EPCR and thrombomodulin (TM) in the pathogenesis of malaria-associated ARDS and its relation to hemozoin and pro-inflammatory cytokines-induced pneumocyte injury. The severity of ARDS was connected to the level of hemozoin in the lungs and the internal alveolar haemorrhage. Interestingly, a loss of EPCR and TM was noticed and appeared to depend on the level of hemozoin, iRBCs and white blood cell accumulation in the lung. This process of dysregulation of the coagulation system and the subsequent apoptotic pathway could be an important player in the pathogenesis of MA-ARDS (Angchaisuksiri, 2014; Maknitikul et al., 2017; Moxon et al., 2013). Research usually focuses on the role of endothelial cells in the development of ARDS. Although the endothelial impact should not be underestimated, the role of epithelial cells and their injury should also be investigated. The loss of type II pneumocytes and their integrity impairs the alveolar fluid transport, reduces surfactant production and may lead to whole alveoli collapse (Fanelli & Ranieri, 2015; Maknitikul et al., 2017; van den Brand et al., 2014). Additionally, it was shown that interleukin-13, interleukin-31 and hemozoin induced penumocytic cell injury and apoptosis (Ayimba et al., 2011). In real-time PCR, the up-regulation of caspase recruitment domain family member 9 (CARD-9) expression, a regulator of the apoptotic pathway through the nuclear factor (NF)-κB signalling, was detected. It is likely that CARD-9 is involved in the pulmonary apoptotic activity in severe malaria as proven to be in the brain and liver. These factors lead to a blockade of the pulmonary resolution and a disruption of the blood gas barrier.

The present fluids accumulate in the alveolar space and hyaline membranes are formed (Maknitikul et al., 2017).

2. Materials and Methods

2.1. Materials

2.1.1. Technical devices

Table 2.1 Technical devices:

Type	Details	Supplier
Bioanalyzer System	Agilent 2100	Agilent Technologies
Centrifuge	5415 D, 5810R	Eppendorf, Hamburg
	Rotor JA-10, Rotor JA-12	Beckmann, Coulter, Krefeld
	Rotina 48 centrifuge	Hettich Technology, Tuttlingen
Counting chamber	BD FACSAria™	BD Biosciences, USA
Freezing container	Mr. Frosty®	Thermo Scientific, Langenselbold
	Nitrogen Container	Thermo Fisher Scientific, USA
Heating block	Thermomixer compact	Eppendorf, Hamburg
Incubator with CO2	Function Line	Heraeus Instruments, Hanau
Ice machine	EF 156 easy fit	Scotsmann, USA
Microscope	EVOS XL, EVOS FL Auto	Thermo Fisher Scientific, USA
	Axioscope M1	Zeiss, Jena
	Cx31	Olympus, Hamburg
Photometer	NanoDrop 2000	Thermo Scientific, Langenselbold
pH-Meter	CG840	Sartorius AG, Göttingen
Pipetting aid	2/20/200/1000 µl	Gilson, USA
	S1 pipetting aid	Thermo Scientific, Langenselbold
Pumps	Ibidi Pump System 10902	Ibidi, Martinsried
Scales	SPO 51	Scaltec, Göttingen
	Sartorius BP210S	Sartorius AG, Göttingen
Sterile bench	Class II BSC	ESCO Labculture®, Singapore
Vortex mixer	VF2	Janke & Kunkel IKA, Staufen
Water bath	SW 20	Julabo, Seelbach

2.1.2. Software

Table 2.2 Software:

Software	Supplier
FlowJo, 10.4.2	LLC,
MySamples, 2.0	Mydata
Prism, 6.0	GraphPad

2.1.3. Labware and disposables

Table 2.3 Labware and disposables:

Labware	Supplier
Adhesive qPCR seal (95.1999) 100 pieces	Sarstedt, Nümbrecht
Cryotubes	Sarstedt, Nümbrecht
Falcon™ 15mL conical centrifuge tube	Sarstedt, Nümbrecht
Falcon™ 50mL conical centrifuge tube	Sarstedt, Nümbrecht
Glass coverslips	R. Langenbrinck, Emmendingen
Gas mixture: 1% O_2, 5% CO_2, 94%N_2	Air liquid, Düsseldorf
Hydrophobic filters, o.45 µm, sterile	Thermo Fisher, Scientific, USA
Microscope slide	Thermo Fisher Scientific, USA
Millipore Stericup™ Sterile Vacuum Filter	Merck, Darmstadt
Parafilm	Bemis, USA
Pasteurpipette	Brand, Wertheim
Petri dish 92x16mm with cams	Sarstedt, Nümbrecht
Pipette tips without filter 1-10/20-200/100-1000 µL	Sarstedt, Nümbrecht
Pipette tips with filter 1-10/20-200/100-1000 µL	Sarstedt, Nümbrecht
Safe-lock tube PCR clean 0.5/1.5/2 mL (RNA free)	Eppendorf, Hamburg
Sterile FACS tubes (PP, 5mL)	Falcon, USA
Tissue culture flask 250 ml (T75-658175)	Greiner Bio-One, Frickenhausen
Tissue culture flask 50 ml (T25-690175)	Greiner Bio-One, Frickenhausen
384 LightCycler plate (721.985.202) 100 pieces	Sarstedt, Nümbrecht

2.1.4. Kits

Table 2.4 Kits:

Kit	Supplier
Qiamp DNA Mini	QIAGEN GmbH, Hilden
PureLink RNA Mini Kit	Thermo Fisher Scientific, USA
Ribo-ZeroTM Magnetic Gold Kit (Human/Mouse/Rat)	Illumina, USA
RNeasy MinElute Cleanup Kit	QIAGEN GmbH, Hilden
ScriptSeqTM v2 RNA-Seq Library Preparation Kit	Illumina, USA
SYBR Green PCR Master Mix	Thermo Fisher Scientific, USA
TURBO DNase Kit	Life Technologies, Darmstadt

2.1.5. Chemical and biological reagents

Table 2.5 Chemical and biological reagents:

Chemicals	Supplier
Accutase (500-720U/mL)	GE Healthcare, Sweden
Biocoll Separating Solution	Biochrom, Berlin
Bovine Serum Albumine (BSA)	Biomol, Hamburg
Cryo solution (Cryo-SFM); for PC	Provitro AG, Berlin
dNTP's 10mM each 100 rxn 100µL	ThermoFischer
DPBS	PAN, Biotech, Aidenbach
D-Glucose	Merck, Darmstadt
D-Sorbitol	Merck, Darmstadt
Ethanol	Carl Roth, Karlsruhe
Gentamycin 40 mg/mL	Ratiopharm, Ulm
Giemsa solution (500mL)	Merck, Darmstadt
HCl	Merck, Darmstadt
Hoechst 33342	Sigma-Aldrich, USA
Human Blood O^+	UKE, Hamburg
Human Serum A^+	Interstate blood bank, Inc., USA

Hypoxanthine (9636-5G)	Sigma-Aldrich, USA
Immersion oil	Zeiss, Jena
Methanol	Carl Roth, Karlsruhe
NaCl	Carl Roth, Karlsruhe
NaOH	Carl Roth, Karlsruhe
Penicillin-Streptomycin	Life Technologies, USA
QuantiTect SYBR Green 400rxn	Qiagen, Hilden
RNase AWAY Spray Bottle	Carl Roth, Karlsruhe
RNase OUT 125rxn 125µL	ThermoFischer, Karlsruhe
RPMI + L-Glutamin; +25mM HEPES; -$NaHCO_3$	AppliChem, Darmstadt
TRIzol reagent	Life Technologies, USA

2.1.6. stock solutions, buffers and mediums

Table 2.6 RPMI-HS:

RPMI-HS **Plasmodium complete growth medium with human serum**	**1 L**
RPMI 1640; dissolved in 800mL dH_2O	16.4 g
Hypoxanthine; dissolved in 50mL dH_2O	0.05 g
Heat inactivated human serum A^+	100 mL
7.5% $NaHCO_3$	30 mL
Gentamicin 40mg/mL	500 µL
Add dH_2O to total volume	
Set pH with NaOH	7.4
Sterile filtration (0.22 µm)	
Store at 4°C for maximum 4 weeks	

Table 2.7 5% D-Sorbitol:

5% D-Sorbitol **Synchronization solution**	**1 L**
D-Sorbitol	50g
Add dH_2O to total volume	
Sterile filtration (0.22 µm)	
Store at 4°C	

Table 2.8 Binding medium:

Binding medium **Static binding assay**	**1 L**
RMPI 1640	16.4 g
Glucose; H_2O-free	20 g
Add dH_2O to total volume	
Set pH with NaOH	7.4
Sterile filtration (0.22 µm)	
Store at 4°C for maximum 4 weeks	

Table 2.9 Malaria freezing solution:

Malaria Freezing Solution (MFS) **Cryogenic conserved stocks**	**1 L**
D-Sorbitol	3 g
NaCl	0.65 g
Add dH_2O to total volume	
Sterile filtration (0.22 µm)	
Glycerol; autoclaved	28 mL
Sterile filtration (0.22 µm)	
Store at 4°C	

Table 2.10 Malaria thawing solution:

Malaria Thawing Solution (MTS) **Re-culturing of cryogenic conserved stocks**	**1 L**
NaCl	35 g
Add dH_2O to total volume	
Sterile filtration (0.22 µm)	
Store at 4°C	

Table 2.11 10% Giemsa stain:

10% Giemsa stain **Plasmodium blood smear staining of static binding assay**	**100 mL**
Giemsa solution	10 mL
Add dH_2O to total volume	90 mL
Store at room temperature for maximum 2 to 4 days	

Blood **Sterile, human erythrocyte concentrate, blood group 0^+**

2.1.7. HULEC-5a cell culture

Table 2.12 HULEC-5a cell culture:

Culture medium	
Base medium MCDB131	500 mL
Epidermal Growth Factor	
Hydrocortisone	
Glutamine	
Fetal Bovine Serum	50 mL

2.1.8. Lung primary cell culture

Table 2.13 Lung primary cells culture medium:

Lung primary cells culture medium	
Microvascular endothelial cell growth medium, basal	500mL
Microvascular endothelial cell growth Supplement-Mix, FCS **Antibiotics**	

Table 2.14 Lung primary cells cryo solution:

Lung primary cells cryo solution, Cryo-SFM	
Cryogenic conserved stocks	**30 mL**
Cryo-SFM	

2.1.9. *P. falciparum* isolates

In the performed experiments, the *Plasmodium falciparum* strain FCR3/IT4 was used.
The strain was obtained from a patient in Fajara-Gambia, West Africa in 1976 and it was directly and continuously cultured using the Petri dish candle jar technique (Jensen and Trager, 1978). The isolate was supplied by Mo Klinkert from BNITM, Hamburg.

2.2. Methods

2.2.1. Cell biological methods

2.2.1.1. HULEC-5a culture methods

The immortalized human lung microvascular endothelial cell line 5a (HULEC-5a) was provided by the American Type Culture Collection in Manassas, Virginia (ATCC®CRL-3244™).

Culture

The adherent HULEC-5a lung endothelial cells were cultured in T25 or T75 culture flasks with either 5 mL or 15 mL of complete growth medium. The flasks were permanently incubated at 37°C with 5% CO_2. The confluency and the overall vitality of the cells were controlled daily with an inverted fluorescence microscope. The culture medium was changed at least every third day.

Splitting

In order to split the adherently growing cells, first the culture medium was removed and then the cells were washed with 37°C prewarmed phosphate puffered sulfate (PBS). To separate the cells from the bottom of the flask, 300 to 700 µL, depending on the flask size, of 37°C prewarmed accutase were added and the flask was carefully tilted to wet the whole bottom area. Following, the flask was incubated for 5 min at 37°C and 5% CO_2. The successful detachment of all lung endothelial cells was controlled with an inverse light microscope. If successful, the enzymatic activity of accutase was inhibited by the addition of complete HULEC-5a growth medium and the cells were splitted as required and cultivated as mentioned above (chapter 2.2.1.1).

Thawing

The cryogenic tubes containing the frozen HULEC-5a cells were thawed and incubated for 2min in a 37°C water bath. The thawed cells were then transferred to a 15 mL reaction tube and 10 mL of 37°C prewarmed complete growth medium were added. The suspension was spun down at 300 x g for 2 min and the supernatant was removed. Finally, the cell pellet was resuspended with complete growth medium and the cells were cultured in a flask a mentioned above.

Freezing

After the process of detaching the adherent cells by the addition of accutase as mentioned above in chapter 2.2.1.1, 5 mL of complete growth medium were added and the reaction tube was centrifuged at 300 x g for 2 min. The supernatant was removed and the pellet was resuspended with HULEC-5a freezing solution (about 3 mL for a T25 flask). The cell suspension was transferred to cryogenic tubes in corresponding aliquots and frozen to -80°C using a Mr. Frosty™ freezing container to ensure a safe and controlled freezing process. For long-term storage, it is possible to transfer the tubes to the gas phase of a liquid nitrogen tank at -172°C.

2.2.1.2. Lungs primary cell culture methods

The human microvascular endothelial lung cell line (HMVEC-L) was provided by Provitro AG in Berlin.

Culturing

The adherent lung endothelial primary cells (PC) were cultured in T25 or T75 culture flasks with either 5 mL or 15 mL of complete growth medium. The flasks were permanently incubated at 37°C with 5% CO_2. The confluency and the overall vitality of the cells were controlled on a daily basis with an inverted fluorescence microscope and photos of the growth progress were taken (Fig 2.1.). The culture medium was changed at least every third day.

Splitting

In order to split the adherently growing PC, first the culture medium was removed and then the cells were washed with 37°C prewarmed PBS. To separate the cells from the bottom of the flask, 300 to 700 µL, depending on the flask size, of 37°C prewarmed accutase were added and the flask was carefully tilted to wet the whole bottom area. Following, the flask was incubated for 5 min at 37°C and 5% CO_2. The successful detachment of all lung endothelial primary cells was controlled with an inverse light microscope. If successful, the enzymatic activity of accutase was inhibited by the addition of complete lung primary cell growth medium and the cells were splitted as required and cultivated as mentioned above (chapter 3.2.1.2).

Thawing

The cryogenic tubes containing the frozen lung endothelial primary cells were thawed and incubated for 2min in a 37°C water bath. The thawed cells were then transferred to a 15 mL reaction tube and 10 mL of 37°C prewarmed PC complete growth medium were added. The suspension was spun down at 300 x g for 2 min and the supernatant was removed. Finally, the cell pellet was suspended with complete growth medium and the cells were cultured in a flask a mentioned above.

Freezing

After the process of detaching the adherent cells by the addition of accutase as mentioned above in chapter 3.2.1.2, 5 mL of PC complete growth medium were added and the reaction tube was centrifuged at 300 x g for two minutes. The supernatant was removed and the pellet was resuspended with lung primary cells cryo solution (about 3 mL for a T25 flask). The cell suspension was transferred to cryogenic tubes in corresponding aliquots and frozen to -80°C using a Mr. Frosty™ freezing container to ensure a safe and controlled freezing process. For long-term storage, it is possible to transfer the tubes to the gas phase of a liquid nitrogen tank at -172°C.

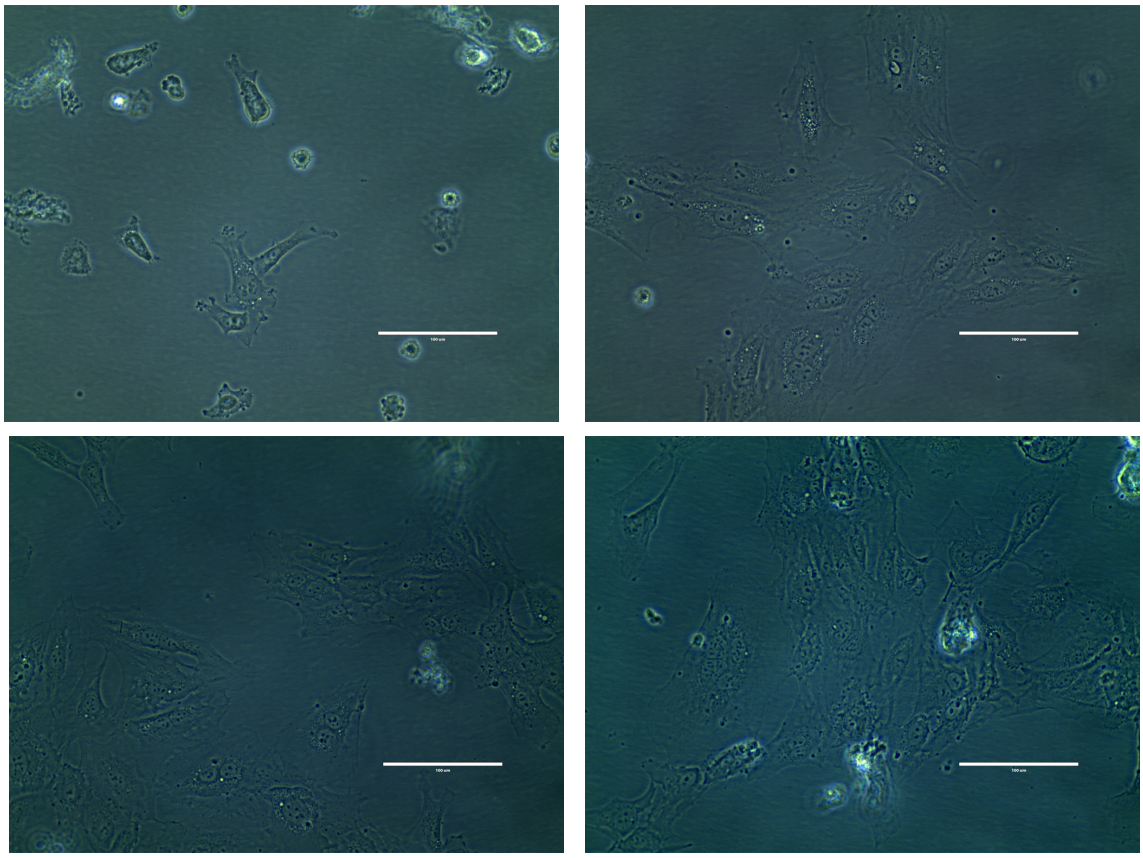

Figure 2.1 Lung endothelial primary cells growing in culture in T25 or T75 flasks. Daily controls performed with inverted fluorescence microscope to check for vitality and confluency.

2.2.1.3. P. falciparum culture methods

Culturing

The used IT4 strain was cultured following the standard culture methods (Trager and Jensen, 1997). The *P. falciparum* parasites were cultivated in a 10 mL Petri-dish with cams at a 5% haematocrit, which was adjusted with blood of blood group 0^+ and in 10% human serum (A^+). The Petri-dishes were incubated at 37°C with a gas composition of 1% O_2, 5% CO_2 and 94% N_2. The medium was changed daily and the parasitemia was balanced between 0.1% and 10% depending on the changing requirements.

Thawing

The cryogenic conserved isolates were thawed in a water bath at 37°C for about 2min. The content of the cryotube was then transferred to a 15 mL reaction tube and an equal amount of 37°C prewarmed malaria thawing solution (MTS) was added. After centrifugation at 300 x g for 2 minutes, the supernatant was removed and the cell pellet was washed 2 more times with 1 mL malaria thawing solution until the supernatant was clear. Finally, the erythrocyte pellet was resuspended in 10 mL RPMI + HS (roswell park memorial institute 1640 + human serum) medium and cultured according to standard procedures as described in the section above.

Freezing

The aim is to have permanent cryogenic conserved stocks of *P. falciparum*. Therefore, the synchronized culture with at least 1% rings (the more the better) was centrifuged for 5 min at 800 x g and the supernatant was removed. The remaining cell pellet was resuspended in four times the pellet volume of malaria freezing solution (MFS). The suspension was divided into 1.5 mL aliquots in cryogenic tubes and immediately frozen to -80°C by usage of Mr. Frosty™ freezing containers to ensure a controlled and slow freezing process. After 24 to 48 hours, the cryotubes were removed from the freezing containers and stored in their designated location. For long-term storage, the cryogenic tubes were transferred from -80°C storage to the gas phase of a liquid nitrogen tank at -173°C.

Giemsa staining

To estimate the percentage of parasitemia in the corresponding culture, 10 µL of sedimented cell culture were used to make thin blood smears on glass slides. The slides were air dried, fixed with methanol for 30 seconds and then immersed in 10% Giemsa staining solution for at least 10 minutes. After, the slides were rinsed with clear water, air dried and examined by light microscopy at 100x magnification using immersion oil.

Parasitemia

When examining the Giemsa stained slides by light microscopy as described above, two populations were counted. First, all the erythrocytes in one quarter were counted. This number was multiplied by four to determine the number of all erythrocytes in one visual field. Second, all the IEs in one quarter were counted and that number was also multiplied by four. The parasitemia of the culture is determined by the following calculation:

$$\frac{IEs}{all\ erythrocytes} \times 100 = Parasitemia\ in\ \%$$

Splitting

The parasitemia of the *P. falciparum* cell culture was kept between 0.1% and 10% depending on the changing requirements. High parasitemia was reduced by dilution with RPMI + HS medium and addition of non-infected erythrocytes.

Synchronization

Aiming for a highly synchronized ring stage parasite culture, the culture was grown until the ring stage parasitemia was at least 5%. The IE culture was centrifuged for 5 min at 800 x g and the supernatant was removed. The remaining erythrocyte pellet was then resuspended in a 6-fold volume of 5% D-sorbitol solution and incubated for 5 to 7 minutes at 37°C with gentle shaking every 2 min.
In contact with D-sorbitol solution, the infected erythrocytes with adult staged parasites like trophozoites and schizonts are lysed due to the excessive uptake of D-sorbitol solution through an increased permeable membrane system and the following osmotic burst.
After five to seven minutes of incubation, the culture was centrifuged again for five minutes at 800 x g and the supernatant was discarded. The pellet was washed with culture medium and centrifuged again at the parameters mentioned above. Finally, the erythrocyte pellet was resuspended in 10 mL medium and further cultivated as described in chapter 2.2.1.3 (*culturing)*.
For a well synchronized culture, either this procedure or the process of knob enrichment mentioned in the section below was performed once a week.

Knob enrichment

To isolate IE with knobs from a mixed cell culture the usage of 1% gelatine was required. Erythrocytes with knobs on their surface tend to detach from erythrocytes without knobs by contact with gelatine.
First, the cell culture was centrifuged for two minutes at 800 x g and the supernatant was discarded. Next, one time the volume of the remaining cell pellet of RPMI medium and 2-fold of prewarmed 1% gelatine were added. It is important to mix the solution carefully to avoid bubbles. The mixture was incubated at 37°C for 15 to 20 min. After incubation, the supernatant, which now contained the IE with knobs, is obtained and transferred to a new tube. To remove the lysed cells and the gelatine from the knob enriched IE, the cells were washed with 5 mL medium by centrifugation at 800 x g for 2 minutes. The supernatant was removed and the remaining cell pellet cultured as usual.

2.2.1.4. Selection and enrichment of P. falciparum

In order to obtain a homogenous culture of *P. falciparum* IE that is capable of binding to a specific human endothelial receptor, it is required to perform an enrichment of the parasite populations via panning assays.
In preparation for the enrichment the confluency of the HULEC-5a cells or the HMVEC-L cells in the flasks was raised to at least 80% on the day of the panning procedure. On the day before enrichment, the IE were synchronized with 5% Sorbitol as described in chapter 3.2.1.3. The parasitemia was controlled at 5% or more trophozoites on the day of enrichment.

On the day of the enrichment via panning assay, the medium from the HULEC-5a or HMVEC-L flask was removed and the lung endothelial cells were washed and incubated for 15 min at 37°C and 5% CO2 with prewarmed binding medium. The culture of *Pf* IE was first knob enriched as described in 2.2.1.3. The culture was then spun down in a tube for 5 min at 800 x g. The supernatant was removed and the cell pellet was resuspended with 6 mL of prewarmed binding medium. To initiate the enrichment process, the binding medium was removed from the HULEC-5a or HMVEC-L flask and the *P. falciparum* culture was added by pipetting. Afterwards, the flask with lung endothelial cells and infected erythrocytes was incubated for 90 minutes at 37°C with gentle circular shaking every 15min. After incubation, the supernatant

and the unbound IE were carefully removed by washing the flask for five to seven times with prewarmed binding medium. Thereupon, the now firmly bound IE were controlled under an inverted light microscope and control photos were taken. As a final step, the culture flask was filled with 15 mL of completed culture medium (RPMI+HS) and 300 to 500 µL of uninfected blood. The culture flask was then incubated for about 20 to 26h in a vacuum container at 37°C with a gas mixture of 1% O_2, 5% CO_2 and 94% N_2.

2.2.1.5. Harvest of P. falciparum culture after selection

A density gradient centrifugation with Biocoll separating solution allows the separation of different cell types according to their different densities. The used medium Biocoll contains the hydrophilic polymer polysuccrose with a molecular weight of about 400 kDa. The polysuccrose can be used to create aqueous solutions with a density of up to 1.1 g/mL. The average density of endothelial cells ranges from about 1.060 to 1.045 g/mL, whereas erythrocytes have an average density of 1.1 g/mL. So, when spun down, the infected erythrocytes migrate down through the Biocoll separation solution while the HULEC-5a cells remain on top of the Biocoll solution.

To execute the Biocoll density gradient centrifugation the culture was first transferred from the T25 flask to a 15 mL reaction tube and the old medium was removed by centrifugation at 800 x g for 5 min. The cell pellet was then resuspended in 7 mL of prewarmed RPMI+HS medium. Another reaction tube with 7 mL of Biocoll solution was prepared and the resuspended cell culture was carefully layered on top of the Biocoll solution. A mixture of the two liquids should be avoided. Afterwards, the gradient was centrifuged for 20 min at 1300 x g with the centrifugal break turned off. After the spin down process, the supernatant was removed and the cell pellet was washed with 8 mL of prewarmed RPMI+HS medium by centrifugation at 800 x g for 5min. Finally, the pellet was resuspended following the established protocol (see chapter 2.2.1.2) and the haematocrit was adjusted according to the requirements.

2.2.1.6. Harvest using TRIzol reagent

The harvest of *P. falciparum* infected erythrocytes can be done with a highly synchronized and highly ring staged parasitized culture. It should only be done directly after a round of

enrichment if there is a sufficient amount of ring staged parasitized IE. The hereby used chemical is called guanidinium-thiocyanate-phenol-chloroform-extraction although it is better known with its brand name TRIzol. TRIzol leads to the disruption of cells as well as cell compartments and to the inactivation of RNases and other enzymes. During this process, the RNA integrity stays intact and dissolves within the phenol phase of the chemical.
In order to harvest the cells for RNA isolation, the parasite culture was transferred to a centrifuge tube and then spun down at 1000 x g for 5 min. The supernatant was removed and the cell pellet was quickly resuspended in a 10fold volume of 37°C prewarmed TRIzol reagent. The solution was shaken rigorously to ensure the successful disruption of the cells and then the tube was incubated for 5 min in a 37°C water bath. Finally, the sample tube can either be used immediately for an RNA isolation or stored at -80°C for long term storage.

2.2.1.7. Co-incubation of iRBCs with HMVEC-L

The HMVEC-L were seeded in T25 flasks on the day before the determined experiment day. On the day of the co-incubation, at least 70% of cell confluence was required. After selection of the knobby parasites with 1% gelatine (2.2.1.3.), about 2mL of pellet of iRBCs was resuspended in 3mL serum free RPMI and then transferred into the T-25 flask containing the HMVEC-L. The flask was incubated at 37°C with 5% CO2 and slightly swayed every 15 minutes. After 2 hours of the described protocol, the medium was aspirated and the cells were washed five to seven times. The cells were then examined under the EVOS XL microscope to confirm the successful binding of iRBCs to HMVEC-L. When successful, the protocol of co-incubation was continued for a total amount of four or eight hours. After these time frames, the medium was aspirated. The cells were washed, detached and collected in a collection tube. The collected cells were centrifuged at 800 x *g* for 2 minutes. The supernatant was discarded and the pellet was treated with 10 times the volume of TRIzol. This mix was stored at -80°C until RNA isolation.

2.2.2. Molecular biology methods

2.2.2.1. RNA isolation of P. falciparum and lung endothelial cells

This protocol of RNA isolation was performed on iRBCs after enrichment over HULEC-5a and HMVEC-L.

The harvested TRIzol lysates from step 2.2.1.5. and 2.2.1.7. were divided in multiple 1.5 mL RNase free safe lock tubes à 1 mL lysate each. Then 200 µL of chloroform was added to each tube. The tube was closed and shaken for 15 seconds. It followed an incubation time of two to three minutes at room temperatures. When completed, the tubes were centrifuged for 30 minutes at 12000 x *g* and 4 °C. After centrifugation, the upper aqueous phase containing the desired RNA (~ 400 µL) was aspirated and transferred into a new 15 mL RNase free falcon. The falcon was placed over ice and an equal volume (~ 400 µL) of ethanol was added. The PureLink® RNA Mini Kit was used and the proposed protocol was followed for RNA extraction: 700 µL of the RNA sample was transferred over the supplied spin column and centrifuged for 15 seconds at 13000 x *g* and at room temperature. This described step was repeated multiple times until all the sample volume was processed. Next, 700 µL of washing buffer I was added and centrifuged for 15 seconds at 13000 x *g* at room temperature. Then the column was transferred to a new washing tube and washed two times with 700 µL each of washing buffer II (centrifugation as mentioned before). To completely dry the column, it was centrifuged for one minute at 13000 x *g* at room temperature. The column was transferred into the recovery tube. The RNA was eluted two times by adding 25 µL of RNase free water and the column was centrifuged again at 13000 x *g* at room temperature. Next, the tube, containing the RNA, was quickly placed over ice. The concentration of RNA as well as the contamination with DNA or proteins was measured using the NanoDrops. For RNA A260/280 ratio ~2,0 was accepted. This performed step is further described in chapter 2.2.2.2. Finally, the RNA was stored at -80 °C until further steps were performed.

2.2.2.2. Measurement of RNA concentration via NanoDrops

A Thermo Scientific, Langenselbold NanoDrops was used to perform measurement of isolated RNA concentration. This device allows photometric analysis and evaluation of purity. An absorption ratio of 260 nm/280 nm and a value of ~ 2 indicate a pure RNA solution. A value of less than 1,8 suggest a contamination with proteins or DNA.

2.2.2.3. Synthesis of cDNA from plasmodia RNA

Step 2.2.2.1 of RNA isolation was followed by the synthesis of complementary DNA (cDNA). It was made sure that, with every sample, only 1 µg of RNA was used per 20 µL cDNA sample. 1 µL of Random Primer (3 µg/µL) and 1 µL of dNTPs (10mM) were added to the RNA sample in a 0,5 mL reaction tube. The reaction tube was transferred first to a thermocycler for 5 min at 65 °C and second on ice for one minute. Next, 4 µL 5x FS buffer, 1 µL 0,1 M DTT (Invitrogen, Superscript III Reverse Transcriptase), 1 µL SS III RT, and 1 µL RNase OUT (Invitrogen, RNase OUT) were added to the tube. The sample was transferred to the thermocycler and the cDNAHex program was started: 5 min at 20 °C, 60 min at 50 °C, and 15 min at 70 °C. Finally, the cDNA was diluted in the ratio 1:4 in RNase free water. In step 2.2.2.5 a volume of 1 µL on the diluted sample was used for real time qPCR.

2.2.2.4. Fluorescence activated cell sorting

Cells can be sorted by different characteristics with the help of flow cytometry using the technique of fluorescence activated cell sorting (FACS). Highly specific antibodies linked to fluorescent markers are used for the sorting process.
First, the cells were prepared in a specific way: The cells were washed with DPBS and afterwards detached with accutase. The detached cells were resuspended in 1mL FACS buffer (1xPBS + 2% iFCs). Next, the average number of cells per ml were calculated with the counting chamber and approximately 2x10^4 cells were placed in each tube. Then, the cells were diluted with 1mL FACS buffer and the mix was centrifuged for 5min at 1200x *g* at 4°C in order to discard the supernatant. This step was repeated one time. The labelled antibody was added and the mix was incubated for 15 minutes on ice. Again, the mix was washed with

1mL FACS buffer and the supernatant was discarded to be ready for the fluorescence-activated-cell-sorting.
The cells were suspended in a liquid stream and then inserted in a laser beam in a single file. The interaction with the laser light is evaluated by an electronic light detector as light scatter and fluorescence intensity. In the present work, FACS was used to quantify the existing ICAM-1, CD-36 and CSA receptors present on HMVEC-L. The cells are separated by these receptor groups with the help of antibodies that mark the specifically expressed surface antigens.
The FACS data are collected by a computer to display how many cells of each colour, depending on the expressed surface antigens, were sorted.

2.2.2.5. Real-time quantitative polymerase chain reaction

After RNA isolation and cDNA synthesis, the preparations for real-time quantitative polymerase chain reaction (RT qPCR) were performed. The method of RT qPCR enables both, the duplication of nucleic acids and the quantification of the extracted DNA. This quantification is made possible by measuring the fluorescence of the used SYBR Green. The forward and reverse primer stocks are diluted with distilled water in a 1:50 ratio. The used primer pairs are outlined in table 2.15. A Master Mix, containing 5 µL SYBR Green and 1,5 µL distilled water per reaction, was prepared. The Master Mix was set up in a 384 wells plate with 2,5 µL of 0,5 µM *forward* primer and 2,5 µL of 0,5 µM *reverse* primer per reaction. The wells were completed by adding either 1 µL of cDNA or 1 µL of distilled water as a negative control. Consequently, complying to this protocol, the volume should be 10 µL per reaction. The qPCR was performed with the LightCycler 480 with the following set up outlined in table 2.16.

Table 2.15 Oligonucleotides used for RT qPCR:

Gen	Gen ID	Forward Primer	Reverse Primer
aldolase	PFIT_1446000	TGT ACC ACC AGC CTT ACC AG	TTC CTT GCC ATG TGT TCA AT
sbp1	PFIT_0501400	TTA GCC GAC GAA CCA ACA CA	TTC GGT TGT CTC TGG TAC TGC A
Arginyl-tRNA	PFIT_1218300	TTC AAA ACA CGA AGT GGA ACA AC	AAT TCT CTG CAG CAA GTC GC
KAHRP		CCA TCA TCA CCA CCA TCA TC	GGT CTT GCT TCC CTG AAT AC
***Pf*EMP3**		AAT CAG CAG GTC ATC CAT TT	GGT TGG TGG TTC ATG TTC T
IT4_var01	PFIT_0616500	GCC CAC CTA GGA ACA TAT AAA C	TCA CCG TCA GTA CGA CTA TC
IT4_var02	PFIT_bin08900	GGG AAA GAC AAC GAC AAA GA	ACG AGG AGG TGT CGA TTT A
IT4_var03	PFIT_bin02700	AAG GTG AAT GTG GGG CAT GT	AGA TCT TTG CCG CGT ACG AT
IT4_var04	PFIT_1200200	GGT AAA GGA GGC GAG AAA C	CCC ATA ACT CTC CAA CAC ATA A
IT4_var05	PFIT_1240400	CAA CTG GTG GTG GTC AAA	GTG TCC CAT GTT CCT TCT AC
IT4_var07	PFIT_1300100	AAC GGC AAC AAG GAG AAG	GTG GTG GTG GTT TCG TAT TA
IT4_var08	PFIT_1150900	AAC TTT CAC TCG CAC CCG AT	CGG GGG AGG TAA GCT TTG TT
IT4_var09	PFIT_0411400	AGA TAC AGG AGT GGG CGA GT	GGA TTT GGG TTT GGC ACC AC
IT4_var13	PFIT_0800100	AAA CCG TAA GCC ACA AGA G	GTA CAT GCT CCA CCG TTA TT
IT4_var14	PFIT_bin07000	CAA GTG GTG AAG GAC ATG AA	CCA CCA CAA TCA TCA CTA CC
IT4_var16	PFIT_bin09100	CCA ATC GTA ATC CTG CTC AA	CTT ACC TGT TCT CCA CCT TTC
IT4_var18	PFIT_bin10900	GCC AAA ACA CGC AGC ACT AA	TAC ACC CCG CAC ACT TCT TC
IT4_var22	PFIT_bin01000	GTG ATG AAG CCA AGT CCC CA	TTT GAT AGT GCA GGA GGC CG
IT4_var23	PFIT_0411000	AGG AGG CAG AGG AAC TAA A	CCA CAG GTA GGA ACA ACA C
IT4_var27	PFIT_0411500	GAG GAT GAC GAG GAG GAT TA	CAG ACG TAT TTC CAC CTT CTT
IT4_var28	PFIT_0711000	TTC GTG ACG CCG ATA GT	GTC GAA ACC ACC AAG GTA TAG
IT4_var29	PFIT_bin02100	TGT CAA ACT CGA CGA ACA TAG	TCA AGG TAT CGG AAG TAG GG
IT4_var32B	PFIT_bin00900	CTG TCC CGA TGG TGT AGT TG	TGG AGT AGG CGT CTC ATA TT
IT4_var41	PFIT_0900100	CCA ATC GTA ATC CTG CTC AA	CTT ACC TGT TCT CCA CCT TTC
IT4_var47	PFIT_1241100	GCG GAA CAG TAA CAA CGT CC	GGG TTC GGG TTC TTC ATC GT
IT4_var60		GGC ACA TTA TCA AAC GCC CG	CTC TGT TCG CTG TCC ACC AA
IT4_var64	PFIT_0710900	AAT CCC TGC GGT ACT GGT GG	TCT GCC ACA TCT TTC ACG CT
IT4_var65	PFIT_0811500	GGC ACT GAA GAG AAC ACT AC	CTT TAT CGG CGG GTT GTT
IT4_var66	PFIT_0710800	CTG GTG TTA GTG GTG GTA ATA G	CAA CCT CAC CCT GTA CAT TC
IT4_var68	PFIT_0710600	CGC AAC CCT GCA GAT ATT	CGA CCA CTT CCC GAT TAT TT

Table 2.16 Program qPCR LightCycler 480:

Temperature	Time	Cycle
95 °C	15 min	1
95 °C	15 secs	40
55 °C	15 secs	40
65 °C – 95 °C	1 min	40
65 °C	5 min	1

2.2.2.6. Next generation sequencing

Next generation sequencing is a technique to figure out the precise order of nucleotides in a given molecule of DNA or RNA. Its predecessor, the Sanger sequencing, was developed in 1975 by Edward Sanger. The Sanger method works via chain termination and it enabled the completion of the Human Genome Project. With the commercial availability of NGS in 2005, a cheaper, faster and more reliable standard was established. NGS works via massive parallel processing of spatially separated, clonally amplified DNA templates or single DNA molecules in a flow cell.

The mRNA samples were sequenced using Nextseq Illumina NGS in the BNITM-NGS core facility. The data analysis was completed by Dr. Stephan Lorenzen (BNITM). The reads were trimmed and filtered with Trimmomatic. They were then aligned to IT4 genome data which is available at PlasmoDB with RSEM and Bowtie2software. The P-values were corrected to $P_{adjusted}$ with the Holm's method.

3. Results

The present work aims to analyse the influence of cytoadhesion of *P. falciparum* infected erythrocytes on human lung endothelial cells as outlined in chapter 1.

The work included simultaneous experiments with the HULEC-5a cell line and the lung primary cell line (HMVEC-L).

First, *P. falciparum* infected erythrocytes were enriched for six rounds over HULEC-5a in 3.1.1. and the corresponding RNA was analysed with NGS in 3.1.2.

Likewise, iRBCs were enriched for four rounds over lung primary cells in 3.2.1.

Second, the over lung primary cells enriched IEs were co-incubated with the corresponding endothelial cells for four hours and four eight hours. This co-incubation with lung PCs is described in chapter 3.3.

Third, the lung primary cells and their receptors were examined via FACS in chapter 3.4 after TNF stimulation.

The co-incubated enriched IEs are displayed as iRBCs-4hrs (co-incubation for 4 hours) and iRBCs-8hrs (co-incubation for 8 hours). The control co-incubations with red blood cells are displayed as RBCscontrol-4hrs (co-incubation for 4 hours) and RBCscontrol-8hrs (co-incubation for 8 hours).

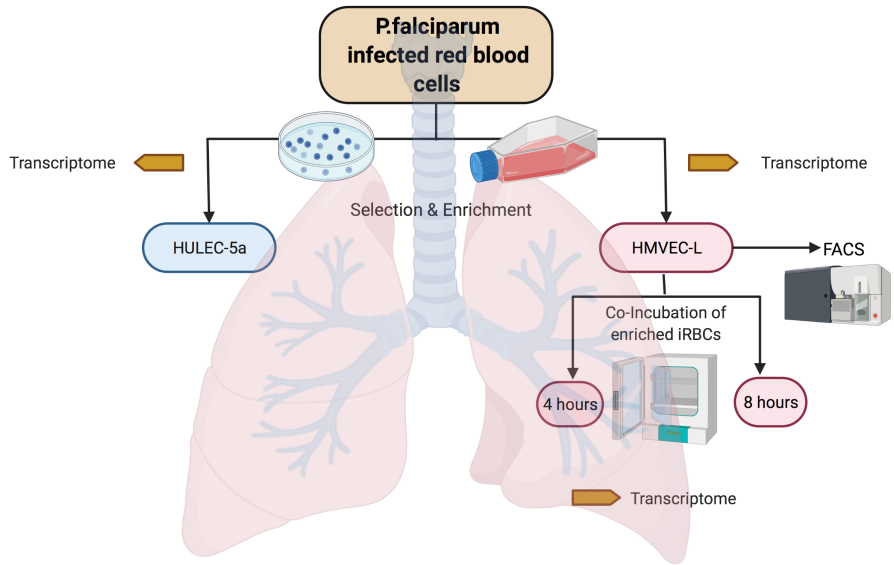

***Figure 3.1 Plan of performed experiments*:** a) Selection and enrichment of *P. falciparum* infected erythrocytes over HULEC-5[a] and HMVEC-L, analysis of transcriptome. B) Co-incubation of HMVEC-L with enriched iRBCs for four and eight hours, transcriptome analysis of HMVEC. C) FACS of TNF stimulated HMVEC-L.

3.1. Enrichment of infected erythrocytes over lung endothelial cells (HULEC-5a)

3.1.1. Selection and enrichment via panning assay

A culture of infected erythrocytes was controlled at a parasitemia of around 10% and then the selection and enrichment was performed over HULEC-5a cells as described in chapter 2.2.1.4. The binding IEs were documented in photos with the EVOS XL microscope (Fig. 3.2). The selected binding IEs were taken in culture again. This process was repeated for a total of six enrichment rounds. The change in the binding pattern of the IEs to the endothelial cells was assessed.

In the first round of enrichment, 23 binding IEs /mm^2 were counted.

In the second round of enrichment, 180 binding IEs /mm^2 were counted.

In the third round, 63 binding IEs /mm^2 were counted.

In the fourth round, 145 binding IEs /mm^2 were counted.

In the fifth round, 244 binding IEs/mm^2 were counted.

In the sixth round, 267 binding IEs/mm^2 were counted.

Excluding the second round of enrichment, the trend with each round was to a higher number of binding IEs.

For each round of enrichment, a part of the early-ring stage IEs was resuspended in TRIzol and the RNA was isolated as described in chapters 2.2.1.6. and 2.2.2.1. The RNA samples were stored at -80 °C until further investigation.

The IEs of the enrichment round number five were analysed in NGS to identify the coding *var* genes. The corresponding results are documented in chapter 3.1.2.

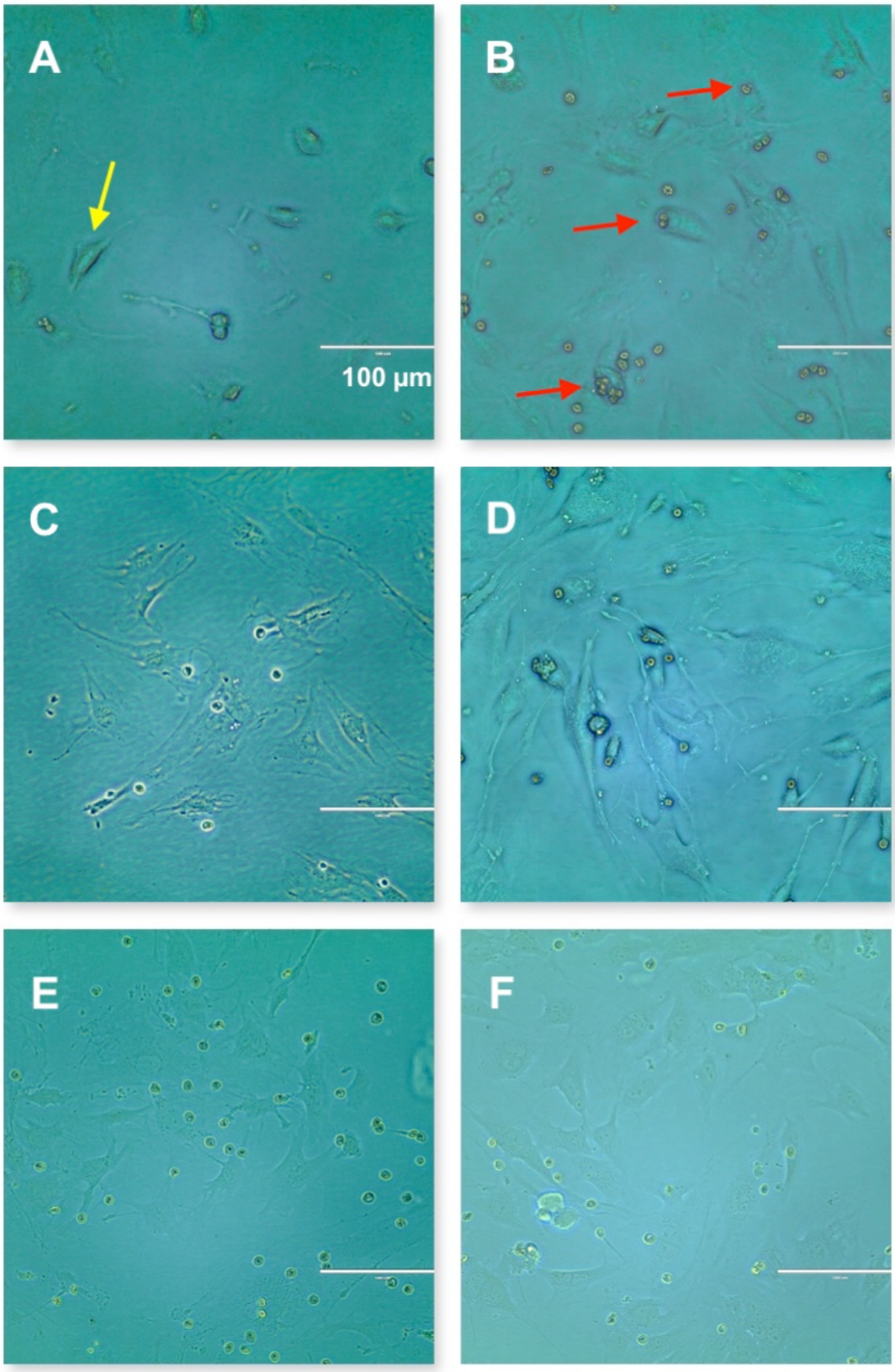

Figure 3.2 Selection and Enrichment of IT4 infected erythrocytes over HULEC-5a lung endothelial cells. Recorded with EVOS XL microscope. Endothelial cells (yellow arrow in **A**) *P. falciparum* IEs were co-incubated for 1.5 hours. After several washing steps, the cytoadhered erythrocytes remained (red arrow in **B**). **A** binding erythrocytes after 1st round of enrichment, **B** after 2nd round, **C** after 3rd round, **D** after 4th round, **E** after 5th round and **F** after 6th round of enrichment.

3.1.2. Next generation sequencing of HULEC-5a enriched infected erythrocytes

The IEs from round five of enrichment were collected in their early-ring stage and resuspended with TRIzol. The RNA was isolated and the samples were sent for a NGS analysis. As a control, samples of a starting culture were analysed via NGS as well. The analysis was done with the help of Dr. Stephan Lorenzen, BNITM. The sequencing was executed with the Nextseq Illumina NGS. The whole transcriptome was analysed. The results for *var*, *rifin* and *stevor* multigene families are displayed in the next subsections. The three analysed samples of the control starting culture are combined in the value 'baseMeanControl'. The four sent samples of enriched over HULEC-5a cultures are combined in the 'baseMeanEnriched'. The ratio of 'baseMeanControl' and 'baseMeanEnriched' is the so called 'foldChange'. The p-values were corrected ($p_{adjusted}$) by the Holm's method. This helps to reduce the chance of getting false positive results.

3.1.2.1. Var genes

In total fifty *var* genes have been investigated for their expression levels (Figure 3.3). Only two *var* genes are expressed at a significant value (Table 3.1):

- *Var*04 was expressed about 173 times higher in the enriched culture compared to the starting culture. *Var*04, often known as *var*2csa, belongs to upstream sequences groups E (UPs E).
- *Var66*, on the other hand, was expressed about 20 times less in the enriched culture compared to the control starting culture. Var66 belongs to UPs C.

Table 3.1 Significantly expressed var genes after five enrichment rounds of IT4 culture over HULEC-5a:

gene ID	*var* gene	baseMeanControl	baseMeanEnriched	foldChange	UPS
PfIT_120006100	IT4_var04	67,63290103	11739,72701	173,3970374	E
PfIT_040025500	IT4_var66	27967,37035	1611,592806	0,057617371	C

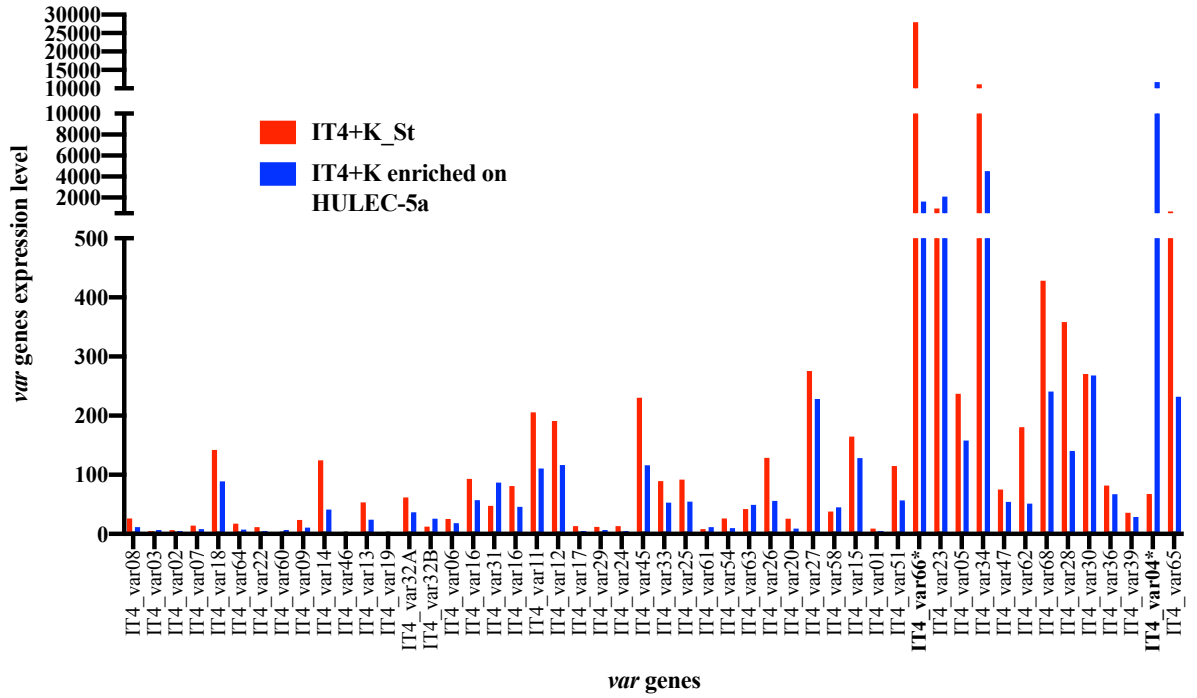

Figure 3.3 var genes expression levels of IT4 culture enriched over HULEC-5a and control IT4 starting culture. Expression levels analysed via NGS. The mean expression levels are compared. P-values were adjusted using Holm's method. *: significant

3.1.2.2. Rifin genes

With the NGS analysis, 139 *rifin* genes were investigated for their expression levels in the control starting culture and in the enriched over HULEC-5a culture (Figure 3.4). Seven *rifin* genes were expressed at a significant value:

- PfIT_040017200, a protein coding *rifin* pseudogene, was expressed about 5 times higher in the enriched culture compared to the control starting culture.
- PfIT_040025700, a protein coding *rifin* pseudogene, was expressed about 5 times less in the enriched culture.
- PfIT_050038100 was expressed about 4 times higher.
- PfIT_080037300 was expressed about 4-fold more, as well.
- PfIT_090005500 was expressed about 10 times less.
- PfIT_120005900 was about 185 times overexpressed in the enriched culture.
- PfIT_120060200 was about 208 times higher expressed in the enriched culture compared to the starting culture.

Table 3.2 Significantly expressed rifin genes after five enrichment rounds of IT4 culture over HULEC-5a:

gene ID	name	baseMean Control	baseMean Enriched	foldChange	p-value
PfIT_040017200	*rifin*, protein coding pseudogene	4,591354374	23,95878932	5,190162065	0,010133451
PfIT_040025700	*rifin*, protein coding pseudogene	211,8304796	47,0695238	0,221386364	0,001412093
PfIT_050038100	*rifin*, protein coding	2,712020691	11,22077129	4,14458915	0,049872237
PfIT_080037300	*rifin*, protein coding	33,47492792	131,6483751	3,929654406	0,035074942
PfIT_090005500	*rifin*, protein coding	14,28464902	1,390969847	0,097524668	0,037734604
PfIT_120005900	*rifin*, protein coding	0	40,00527031	185,2144429	3,01E-06
PfIT_120060200	*rifin*, protein coding	0,467259937	87,28843756	208,409985	0,004397079

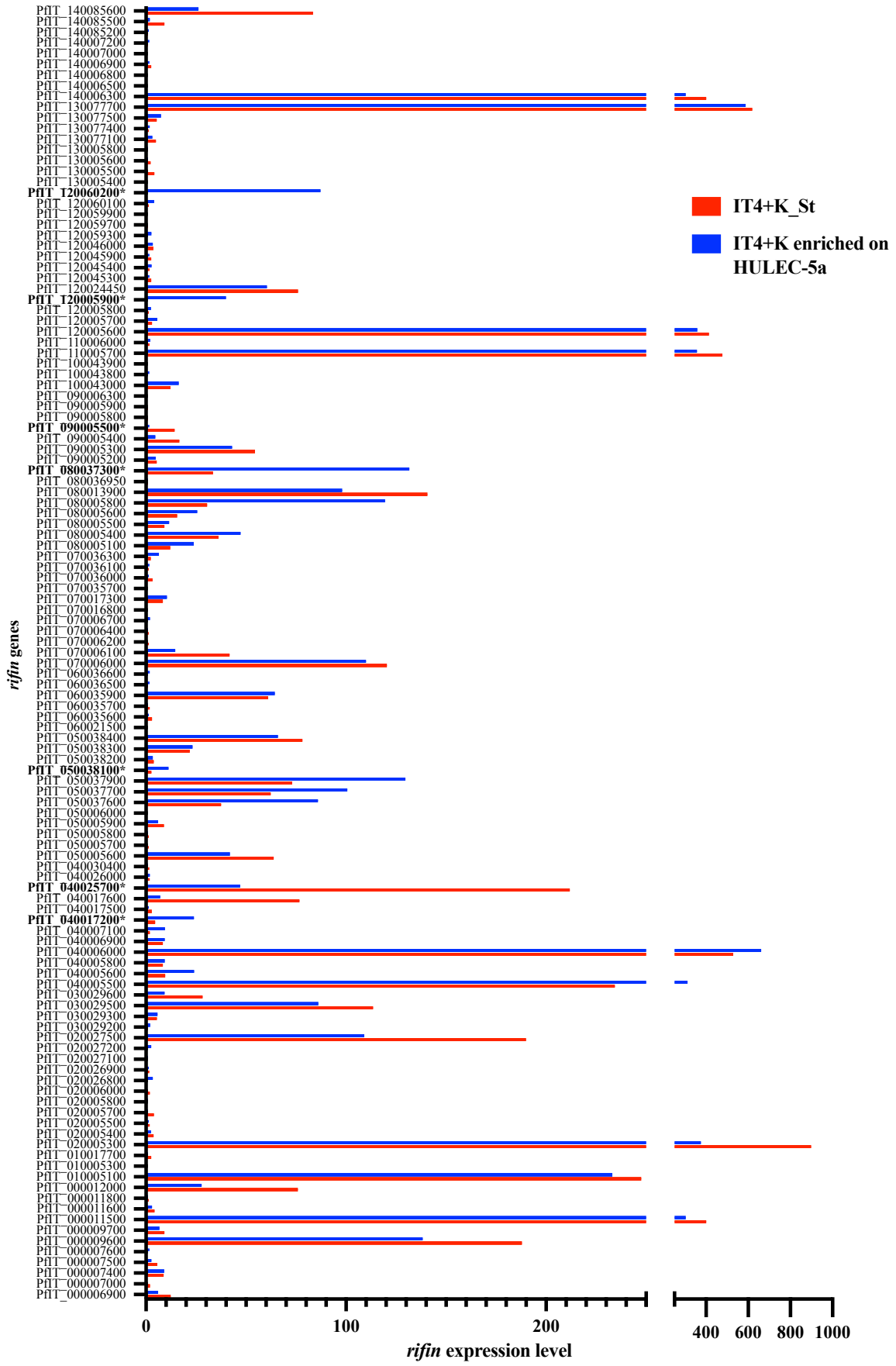

Figure 3.4 rifin genes expression levels of IT4 culture enriched over HULEC-5a and control IT4 starting culture. Expression levels analysed via NGS. The mean expression levels are compared. P-values were adjusted using Holm's method. *: significant

3.1.2.3. Stevor genes

The NGS analysed 37 *stevor* genes for their different expression levels in the control starting culture and in the enriched over HULEC-5a culture (Figure 3.5) One *stevor* gene was expressed at a significant value (Table 3.3.): PfIT_040007000 was expressed about 27 times higher in the enriched culture.

Table 3.3 Significantly expressed stevor genes after five enrichment rounds of IT4 culture over HULEC-5[a]:

Gene ID	name	baseMean Control	baseMean Enriched	foldChange	p-value
PfIT_040007000	*stevor*, protein coding	0	5,790188432	26,64911711	0,020289843

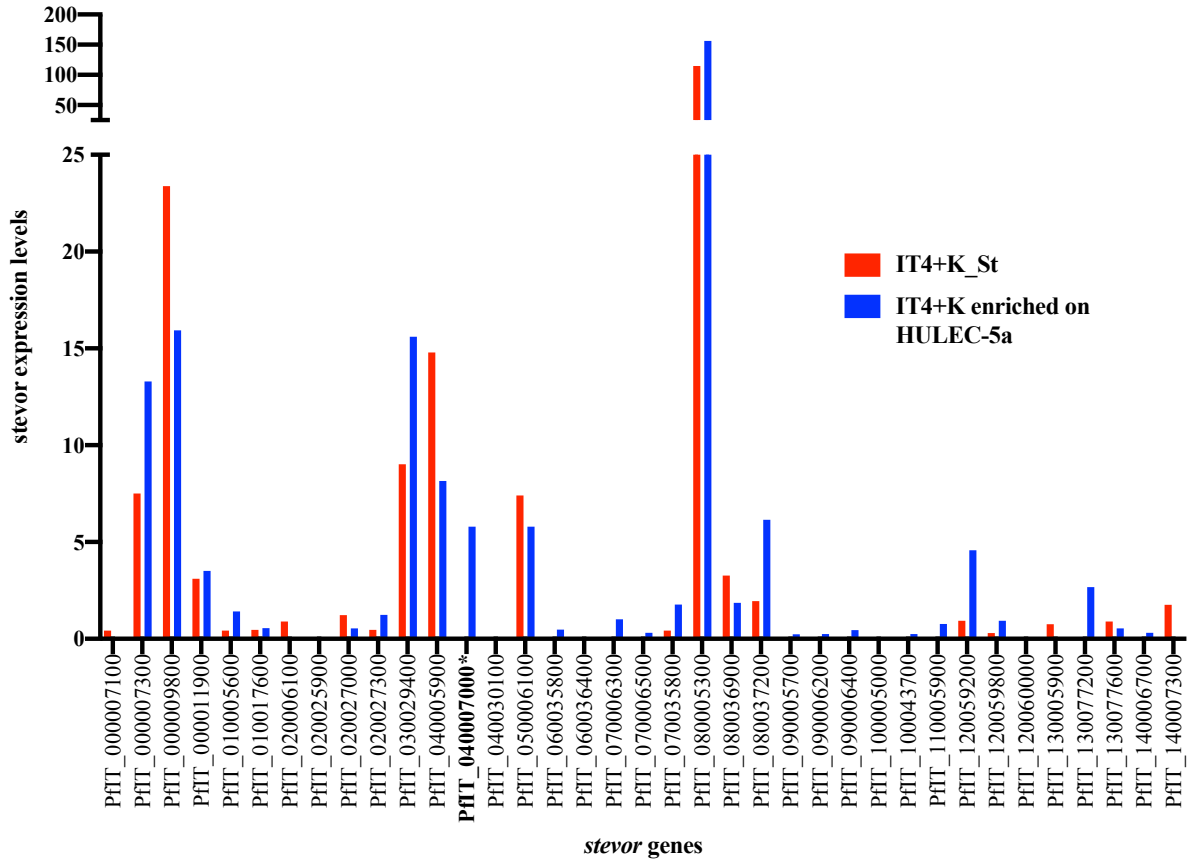

Figure 3.5 stevor genes expression levels of IT4 culture enriched over HULEC-5a and control IT4 starting culture. Expression levels analysed via NGS. The mean expression levels are compared. P-values were adjusted using Holm's method. *: significant

3.2. Enrichment of infected erythrocytes over lung primary cells

3.2.1. Selection and enrichment via panning assay

Parallel to chapter 3.1.1., the enrichment and selection was also performed over lung endothelial primary cells. Four rounds of enrichment were completed and the binding of IEs to lung primary cells was documented with the EVOS XL microscope (Figure 4.6.). For each round of enrichment, the binding pattern was analysed by counting the bound IEs:
In the first round of enrichment, 156 binding IEs/mm^2 were counted.
In the second round, 58 binding IEs/mm^2 were counted.
In the third round, 186 binding IEs/mm^2 were counted.
In the fourth and final round, 552 binding IEs/mm^2 were counted.
Excluding the second round of enrichment, the trend with each round was to a higher number of binding IEs.
For enrichment rounds number one, three and four, a part of the ring stage IEs was resuspended in TRIzol and the RNA was isolated as described in chapters 2.2.1.6 and 2.2.2.1. The RNA samples were stored at -80 °C until further investigation.
Unfortunately, the hereby collected RNA was not analysed due to workflow reasons.
Hanifeh Torabi, a colleague from the BNITM performed enrichment of infected erythrocytes over lung primary cells following the same protocol and the collected RNA was analysed. The gained results will be discussed in 4.2.

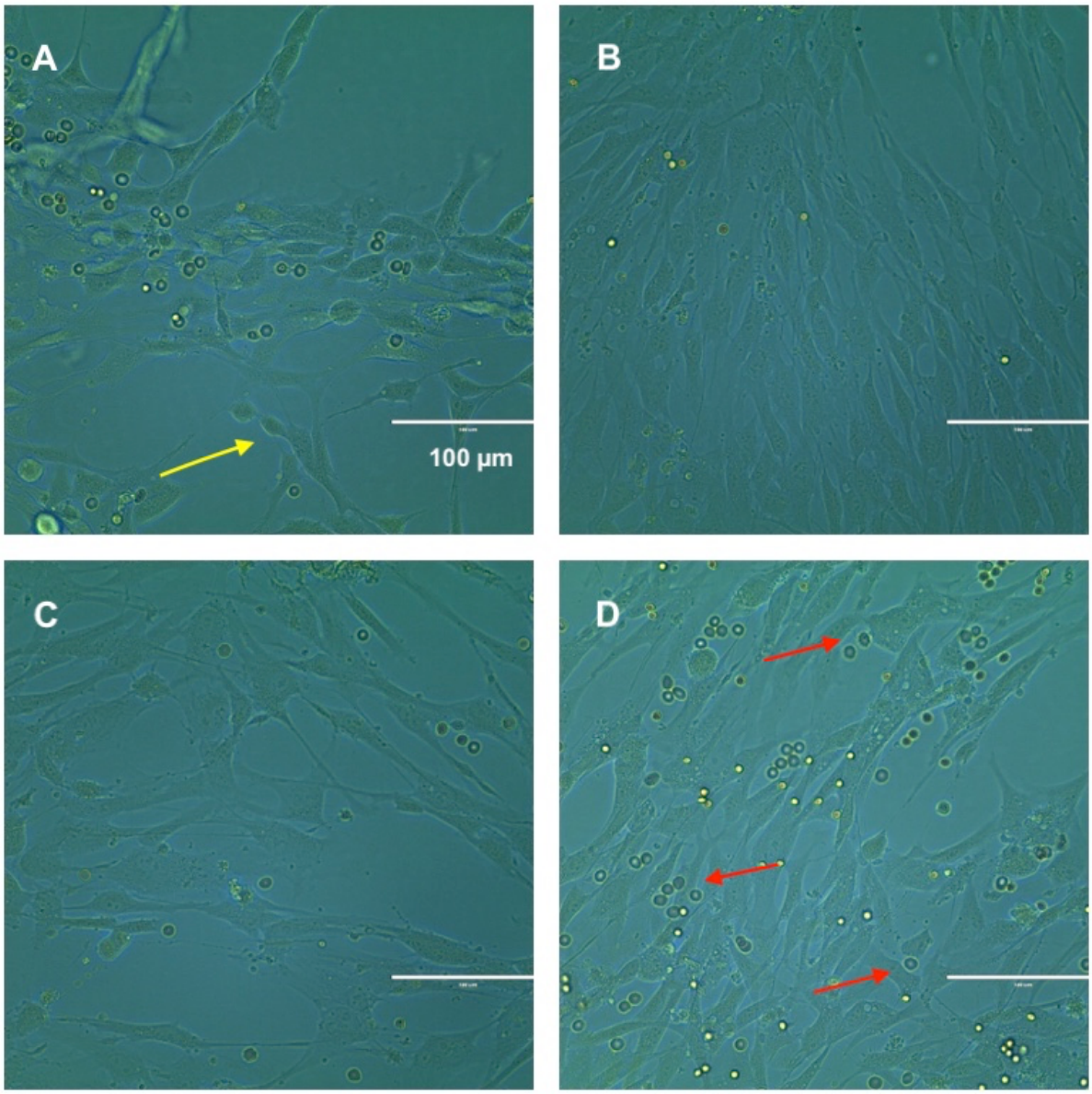

Figure 3.6 Selection and Enrichment of IT4 infected erythrocytes over HMVEC-L lung endothelial primary cells. Recorded with EVOS XL microscope. Endothelial cells (yellow arrow in **A**) and *P. falciparum* IEs were co-incubated for 1.5 hours. After several washing steps, the cytoadhered erythrocytes remained (red arrows in **D**). **A** Binding erythrocytes after 1st round of enrichment, **B** after 2nd round, **C** after 3rd round and **D** after 4th round of enrichment.

3.3. Co-Incubation of enriched iRBCs and lung primary cells (HMVEC-L)

As provided for in the work flow, after enrichment of iRBCs over HMVEC-L (chapter 3.2.), the enriched IEs were co-incubated with the HMVEC-L. The co-incubation was performed for four hours and for eight hours. The results were compared to a control co-incubation with uninfected RBCs. The control co-incubations were likewise executed for four hours and for eight hours.
The co-incubation followed the protocol as outlined in chapter 2.2.1.7. The lung primary cells were collected and resuspended with TRIzol. The RNA was isolated and the samples were sent for a transcriptome analysis (2.2.2.1.).
The control co-incubations are combined in a base mean value. The co-incubations of four hours and the co-incubations of eight hours with infected erythrocytes are combined in their corresponding base mean values. The ratio of a 'normalized gene expression in control' and a 'normalized gene expression in co-incubation' (four hours or eight hours) is the 'foldChange'. The p-values were corrected ($p_{adjusted}$) by the Holm's method in order to reduce the chance of getting false positive results.

3.3.1. Co-Incubation for four hours

The co-incubation of enriched IEs and lung PCs was executed for four hours. The whole transcriptome of co-incubated lung PCs was analysed and 48 genes were significantly differently expressed. 12 genes were overexpressed and 36 genes were underexpressed.
The following figure 3.7 shows the 12 significantly overexpressed genes after a 4 hours co-incubation with iRBCs and lung PCs:

- POSTN (Periostin)
- HMOX1 (Heme oxygenase 1 gene)
- FST (Follistatin)
- CACNA2D1(Calcium voltage-gated channel auxiliary subunit alpha2delta 1)
- MTIX (Metaxin 1)
- EGR1 (Early growth response protein 1)
- LOC613037 (nuclear pore complex interacting protein pseudogene)
- COL5A3 (Collagen type V alpha 3 chain)
- SEPT5-GP1BB (septin5 – glycoprotein 1b)

- DENND2C (DENN domain containing 2C)
- ALS2CR12 (amyotrophic lateral sclerosis 2 chromosome region, candidate 12)
- SMN2 (survival of motor neuron 2)

The figure contains the mean values of normalized gene expression and its standard deviations for the respective three samples of controls and iRBCs.

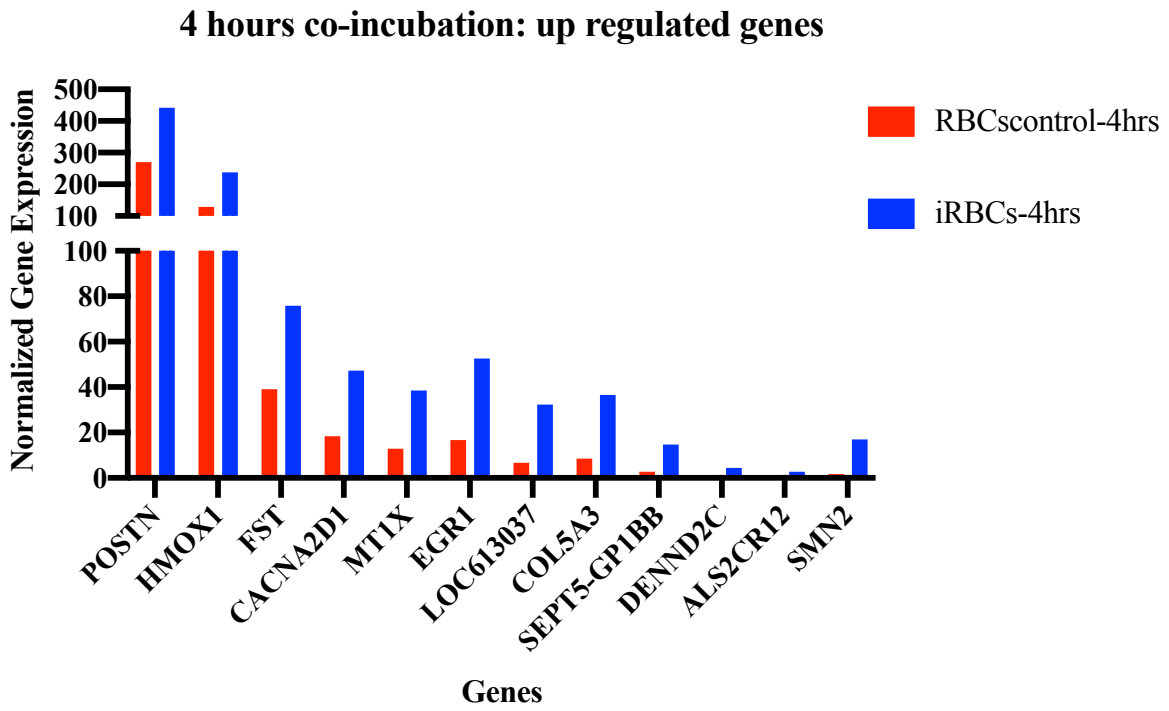

Figure 3.7 4 hours co-incubation: up regulated genes. Expression levels of 4 hours co-incubation of iRBCs and control RBCs analysed via NGS. The mean expression levels are compared. P-values were adjusted using Holm's method. *: significant

The following table 3.4 displays the exact normalized expression levels, the corresponding fold change and its p-value:

Table 3.4 Up regulated genes in 4 hours co-incubation:

Genes	normalized expression in control	normalized expression in 4hrs co-incubation	fold change	p-value
POSTN	269,8775602	442,2491527	1,621753153	0,036891353
HMOX1	128,7277682	238,2435079	1,884312974	0,021876933
FST	39,05937052	75,88299296	1,961620557	0,021987543
CACNA2D1	18,42617077	47,20977156	2,209900681	0,049265022
MT1X	12,83817748	38,51602105	2,553260738	0,044163898
EGR1	16,62276213	52,64790317	3,093567545	0,009957512
LOC613037	6,710924545	32,32291216	3,67588375	0,018485912

COL5A3	8,54811162	36,59016124	4,031165886	0,01468613
SEPT5-GP1BB	2,776216072	14,762311	4,505626463	0,036754402
DENND2C	0,349251982	4,443305885	7,645774398	0,049615603
ALS2CR12	0	2,69310326	21,1570337	0,0478262
SMN2	1,498734595	17,02696409	40,08913579	0,025277007

The following figure 3.8 shows the 36 significantly under expressed genes after a 4 hours co-incubation with iRBCs and lung PCs. It shows the mean values of normalized gene expression and its standard deviations for the respective three samples.

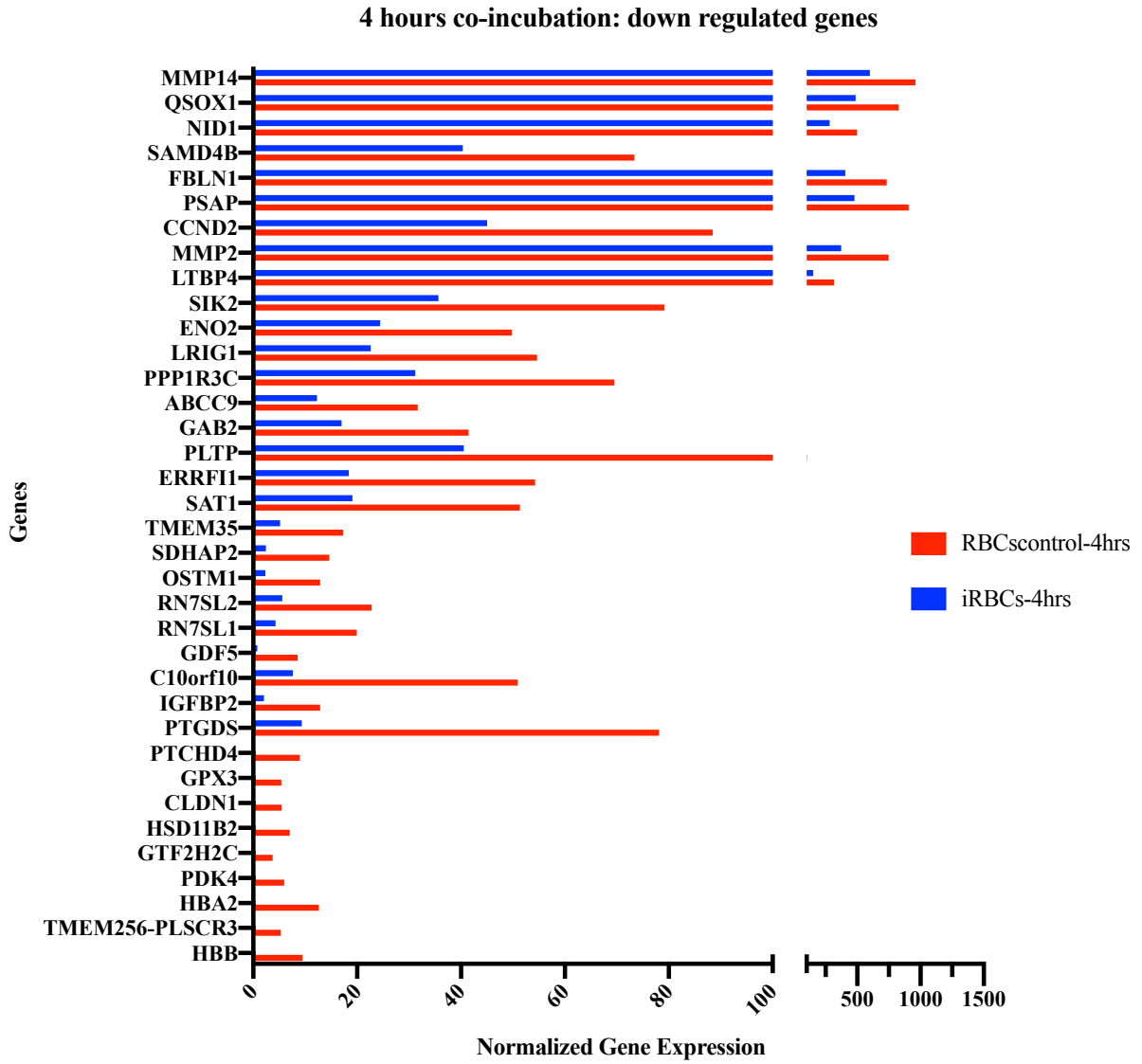

Figure 3.8 4 hours co-incubation: down regulated genes. Expression levels of 4 hours co-incubation of iRBCs and control RBCs analysed via NGS. The mean expression levels are compared. P-values were adjusted using Holm's method. *: significant

The table 3.5 displays the exact normalized expression levels, the corresponding fold change and its p-value of the down regulated genes after a 4 hours co-incubation.

Table 3.5 Down regulated genes in 4 hours co-incubation:

Genes	Normalized expression in control	Normalized expression in 4hrs co-incubation	fold change	P-value
HBB	9,501645928	0	0,032231075	0,002340034
TMEM256-PLSCR3	5,328404674	0	0,048912317	0,012310099
HBA2	12,62232445	0,30334952	0,058630161	0,003018646
PDK4	5,944107093	0,103884219	0,069230922	0,028904737
GTF2H2C	3,730346922	0	0,071549131	0,048697834
HSD11B2	7,046914764	0,103454755	0,071961753	0,027315816
CLDN1	5,434829331	0,103853477	0,076212351	0,04310786
GPX3	5,402765107	0,1033918	0,0819164	0,033348907
PTCHD4	8,97305399	0,308943562	0,084790906	0,009945974
PTGDS	78,12450157	9,337350884	0,131049662	0,037752272
IGFBP2	12,8800812	2,081231209	0,160387097	0,03336904
C10orf10	50,94014482	7,618841048	0,161283734	0,028709021
GDF5	8,55507272	0,725385055	0,162619295	0,042428272
RN7SL1	19,92574886	4,306550377	0,222898587	0,022283615
RN7SL2	22,82664332	5,570143041	0,226032465	0,011139889
OSTM1	12,86941942	2,356227817	0,234496048	0,038198984
SDHAP2	14,65190004	2,45903283	0,251418076	0,041010906
TMEM35	17,33677055	5,169530058	0,276962483	0,047288423
SAT1	51,34072424	19,08978975	0,372530066	0,034732091
ERRFI1	54,2544773	18,39224007	0,378516154	0,030421707
PLTP	102,978204	40,54093962	0,399095231	0,017984097
GAB2	41,48185719	17,02501529	0,415325758	0,043040264
ABCC9	31,68586136	12,29481751	0,432629383	0,047593511
PPP1R3C	69,54490444	31,21132136	0,443830249	0,028705721
LRIG1	54,6503776	22,62542272	0,449076052	0,042792944
ENO2	49,79596226	24,45313549	0,459174233	0,048491923
SIK2	79,12434241	35,65506064	0,487435182	0,040130291
LTBP4	319,0023931	152,5836654	0,491253536	0,025366638
MMP2	749,1559481	372,3997102	0,500259999	0,019011037
CCND2	88,45305516	45,02487343	0,50436176	0,049739124
PSAP	906,4144731	478,4809601	0,529902765	0,017665096
FBLN1	733,9310413	404,9346062	0,558918264	0,033056433
SAMD4B	73,3836959	40,36368595	0,569691827	0,0468433
NID1	499,2203104	282,2590018	0,57854715	0,045887172
QSOX1	828,5272615	487,9976166	0,594716498	0,032051035
MMP14	959,223637	600,7845952	0,625989454	0,04235228

In the next step, the 46 significantly differently expressed genes were checked for groups and functions. Two upregulated genes are responsible for interleukin signalling: HMOX1 and EGR1. The subsequent figure 3.9 shows the normalized gene expression of HMOX1 and EGR1.

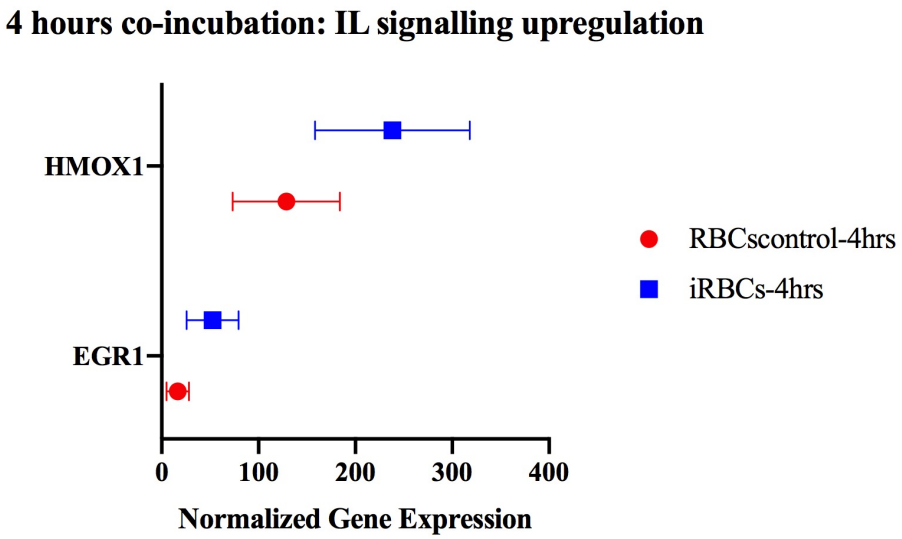

Figure 3.9 4 hours co-incubation: analysis of up regulated genes – IL signalling. Expression levels of 4 hours co-incubation of iRBCs and control RBCs analysed via NGS. The mean expression levels are compared. P-values were adjusted using Holm's method. *: significant

The table 3.6 displays the exactly analysed values of the normalized expression levels, the fold change and the p-value for HMOX1 and EGR1.

Table 3.6 Upregulated genes in 4 hours co-incubation involved in IL signalling:

Gene	Normalized expression in control	normalized expression in 4 hrs co-incubation	Fold change	p-value
HMOX1	128,7277682	238,2435079	1,884312974	0,021876933
EGR1	16,62276213	52,64790317	3,093567545	0,009957512

Furthermore, six of the 36 detected downregulated genes are involved in the organisation of the extracellular matrix:

- LTBP4 (latent-transforming growth factor beta-binding protein 4),
- FBLN1 (fibulin-1),
- MMP2 (matrix metalloproteinase-2),
- MMP14 (matrix metalloproteinase-14),

- NID1 (nidogen-1), and
- GDF5 (growth differentiation factor 5).

The graph below (figure 3.10) contains the six downregulated genes. It shows the mean values of normalized gene expression and its standard deviations for the three samples.

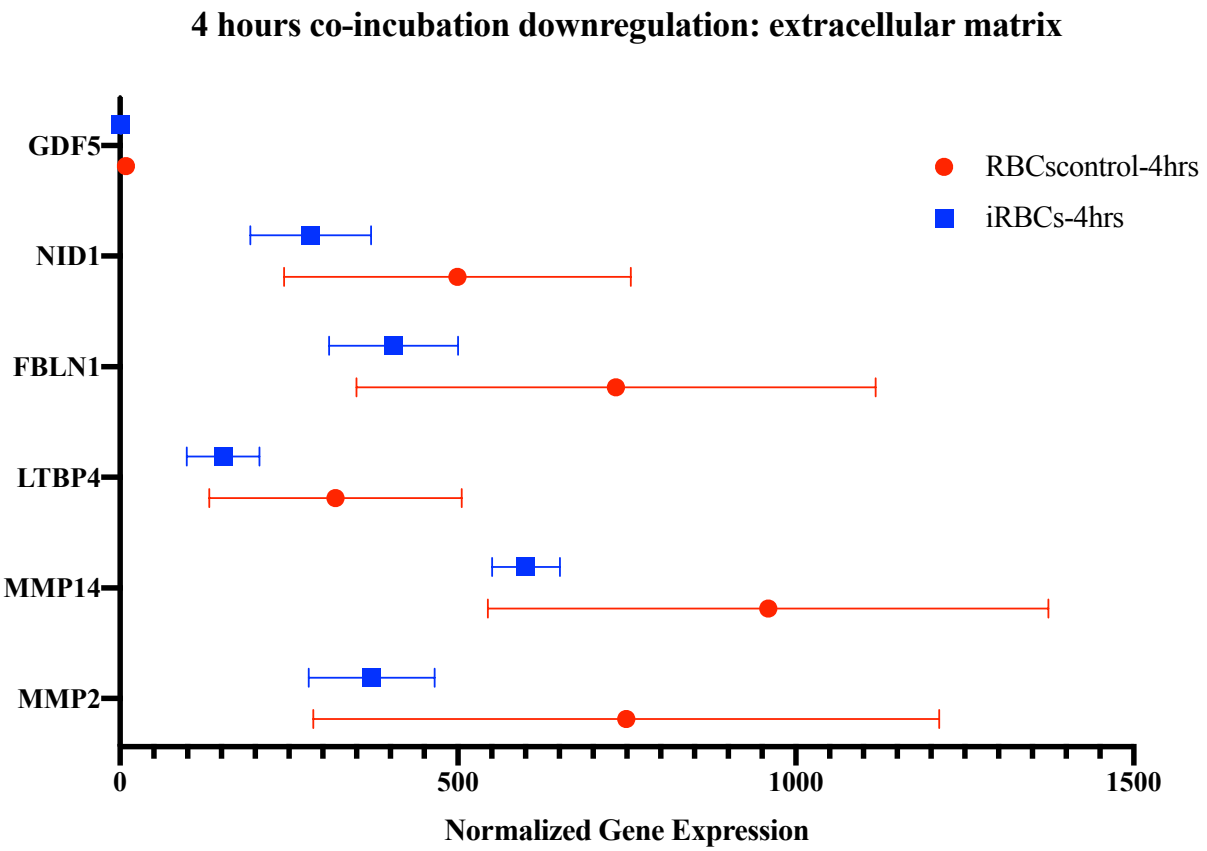

***Figure 3.10 4 hours co-incubation: analysis of down regulated genes –Extracellular matrix*:** Expression levels of 4 hours co-incubation of iRBCs and control RBCs analysed via NGS. The mean expression levels are compared. P-values were adjusted using Holm's method. *: significant

The following table 3.7 displays the exactly analysed values of the normalized expression levels, the fold change and the p-value for MMP2, MMP14, LTBP4, FBLN1, NID1, and GDF5.

Table 3.7 Downregulated genes in 4 hours co-incubation involved in extracellular matrix:

Gene	Normalized expression in control	normalized expression in 4 hrs co-incubation	Fold change	p-value
MMP2	749,1559481	372,3997102	0,500259999	0,019011037
MMP14	959,223637	600,7845952	0,625989454	0,04235228

LTBP4	319,0023931	152,5836654	0,491253536	0,025366638
FBLN1	733,9310413	404,9346062	0,558918264	0,033056433
NID1	499,2203104	282,2590018	0,57854715	0,045887172
GDF5	8,55507272	0,725385055	0,162619295	0,042428272

3.3.2. Co-Incubation for eight hours

In line with the four hours co-incubation, an eight hours co-incubation of enriched IEs and lung PCs was performed as well. The protocol described in chapter 2.2.1.7. was followed. Again, the whole transcriptome of the co-incubated lung PCs was analysed and the results were compared to the controls. In total, 462 genes were significantly differently expressed. 232 genes were upregulated and 230 genes were downregulated compared to the performed controls.
The following figures 3.11 to 3.16 display the normalized expression levels of the 232 upregulated and 230 downregulated genes.

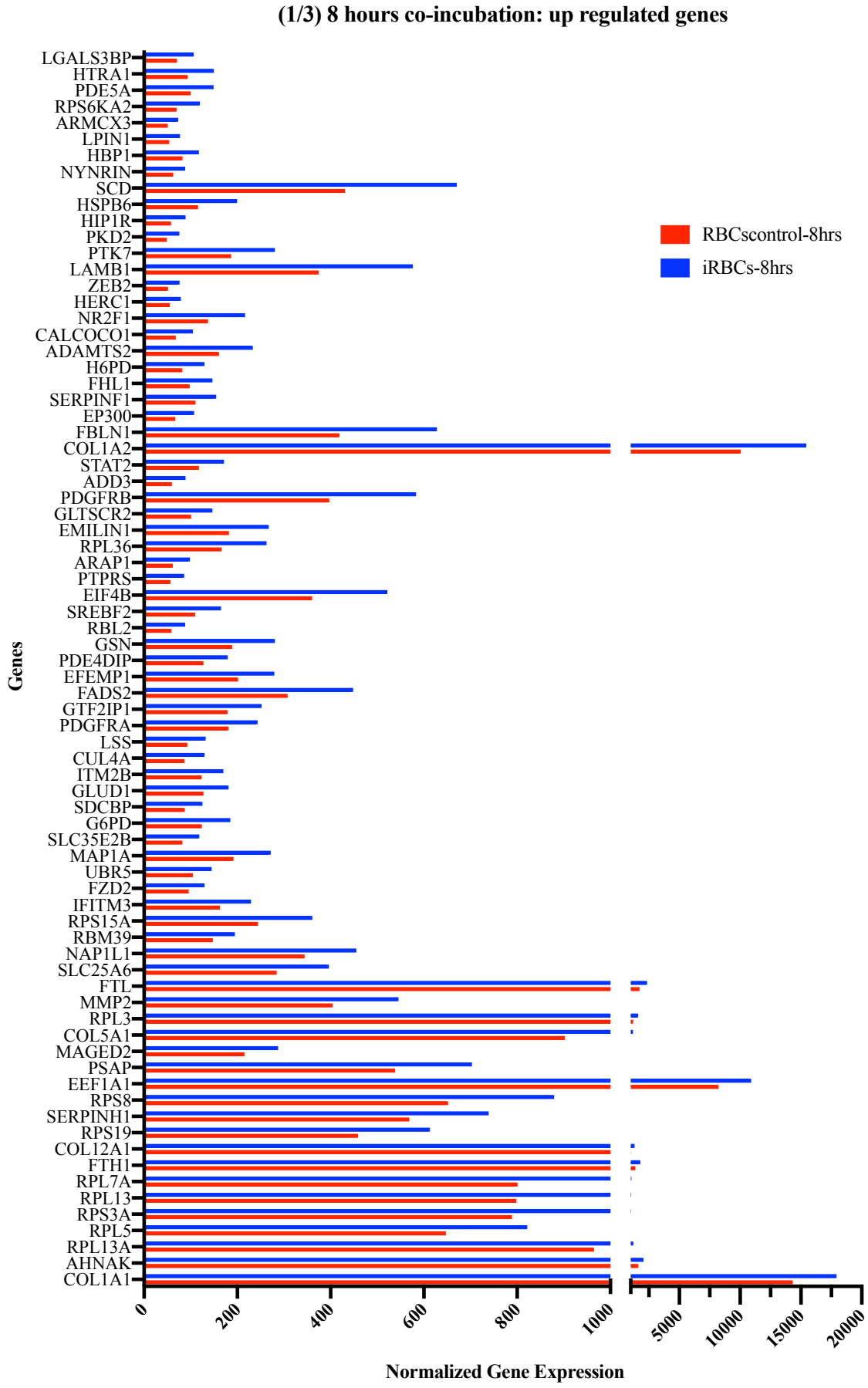

Figure 3.11 normalized gene expression of up regulated genes after 8 hours co-incubation (1/3)

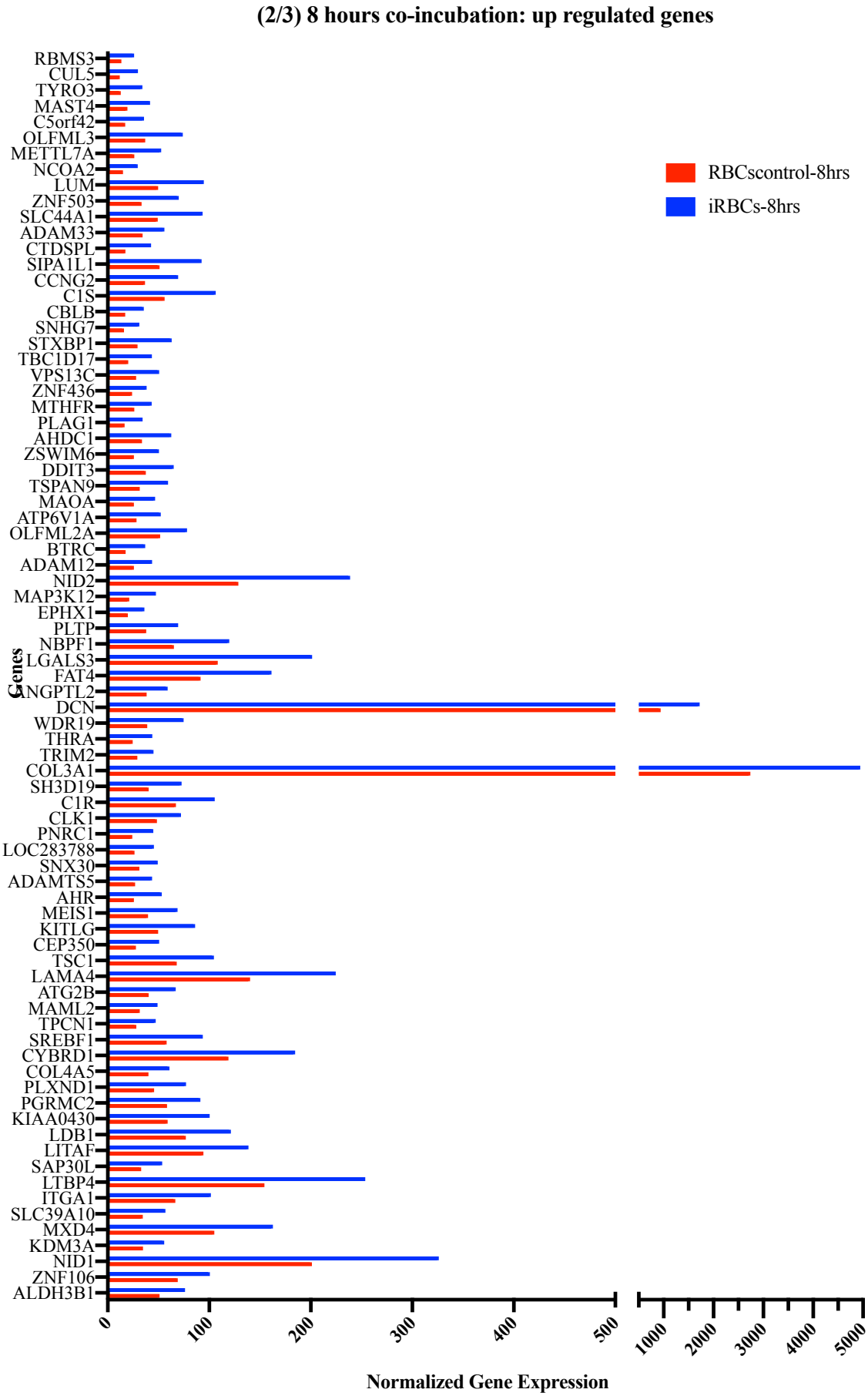

Figure 3.12 normalized gene expression of up regulated genes after 8 hours co-incubation (2/3)

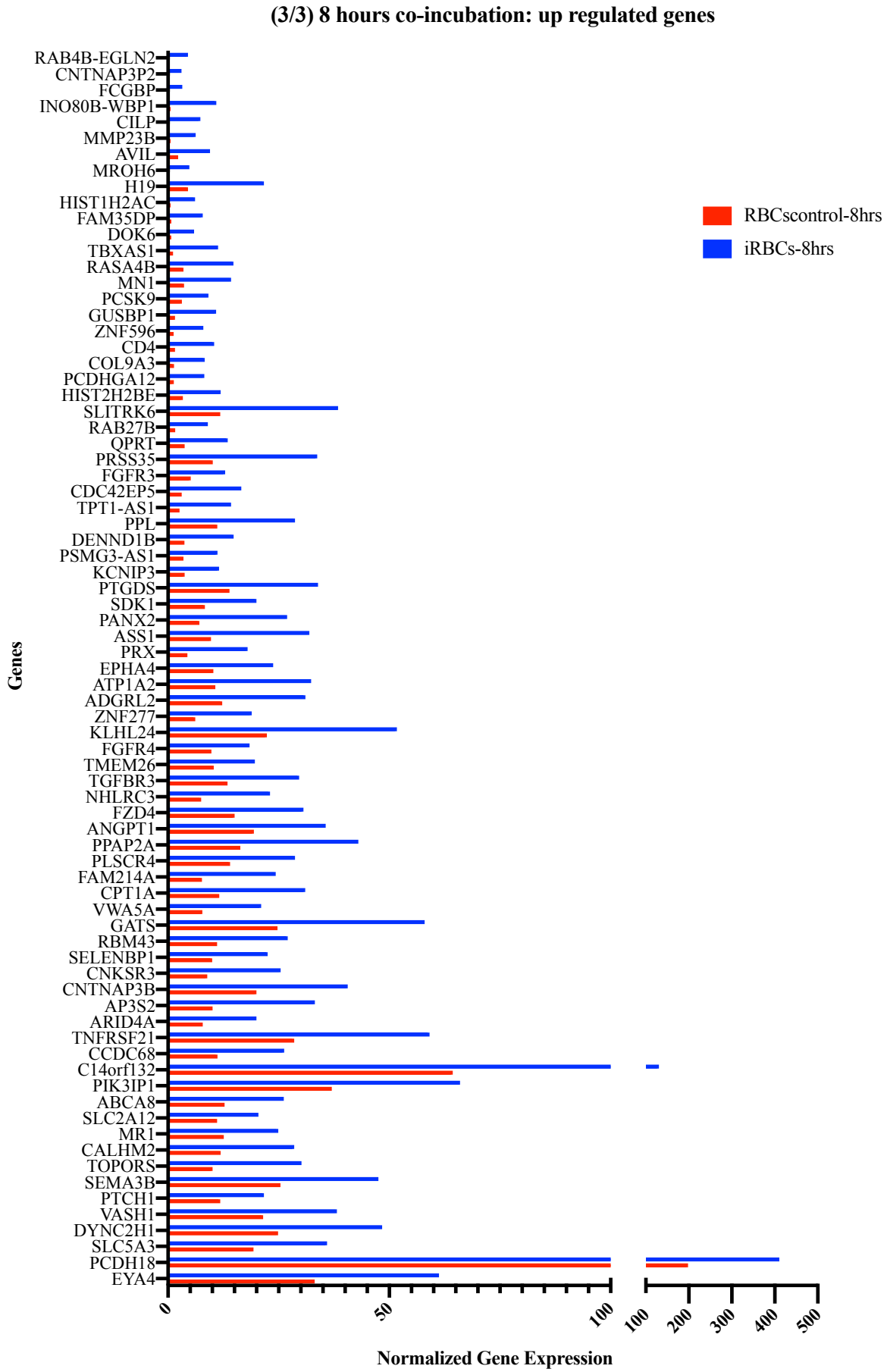

Figure 3.13 normalized gene expression of up regulated genes after 8 hours co-incubation (3/3)

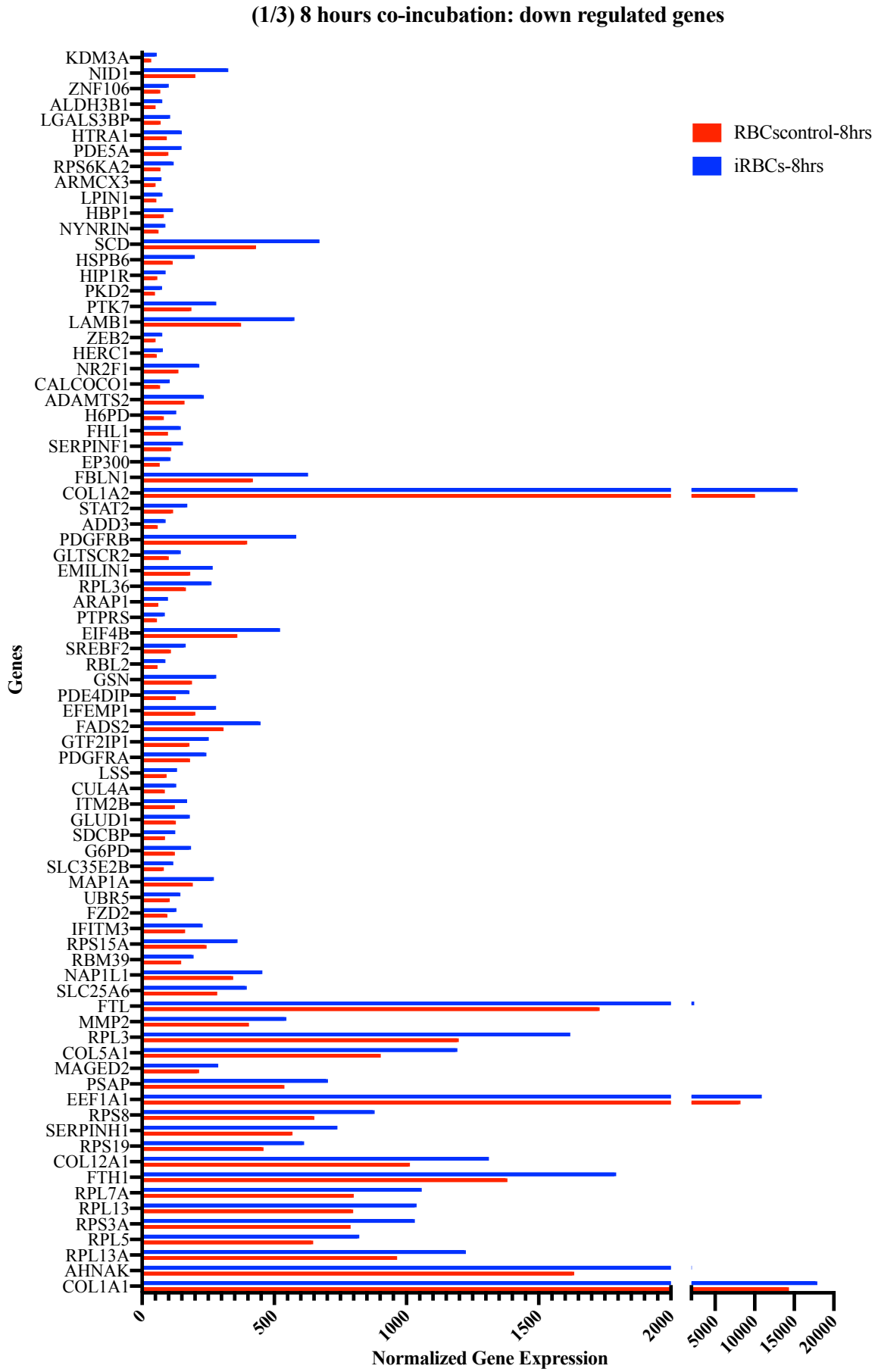

Figure 3.14 normalized gene expression of down regulated genes after 8 hours co-incubation (1/3)

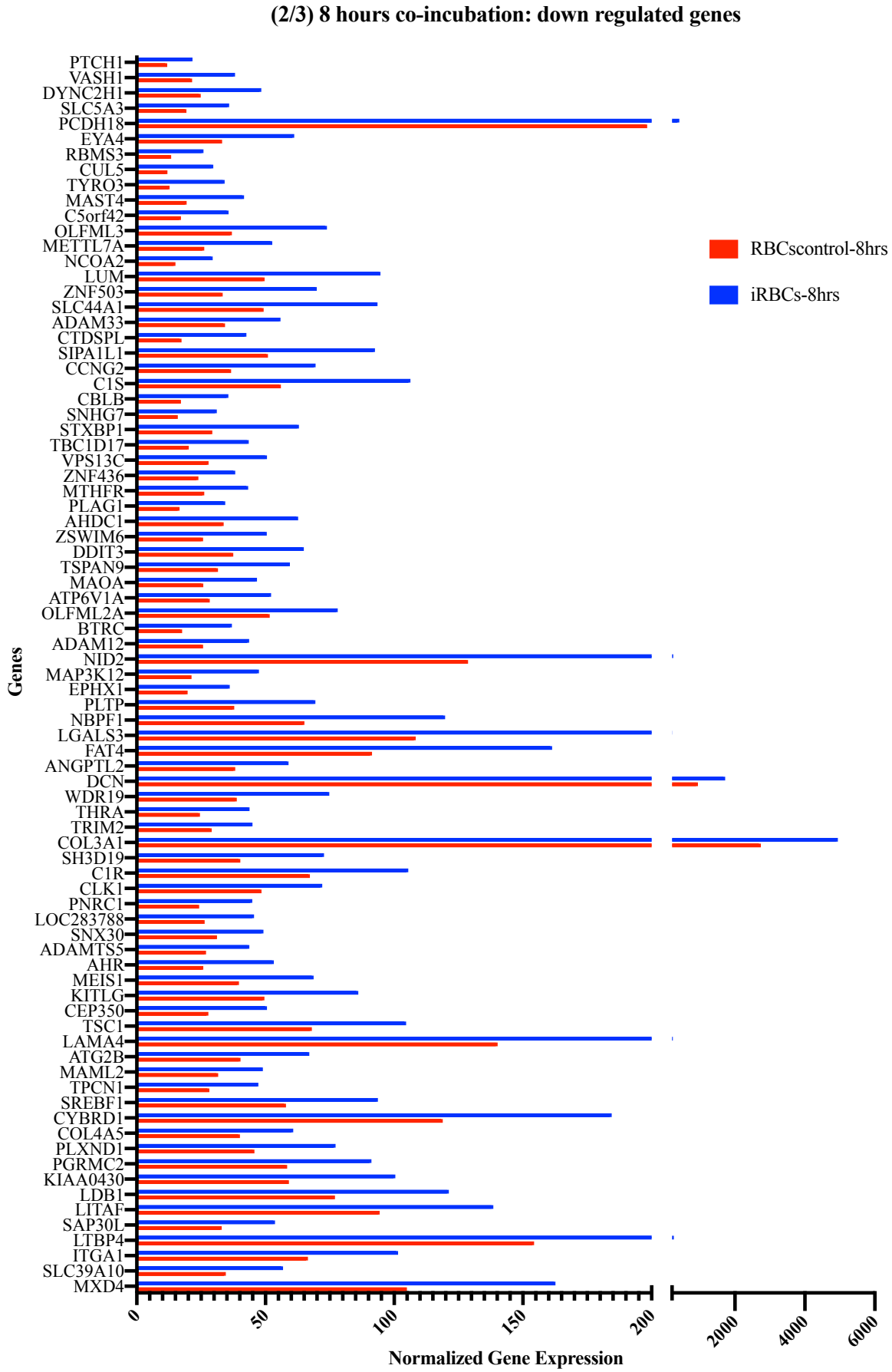

Figure 3.15 normalized gene expression of down regulated genes after 8 hours co-incubation (2/3)

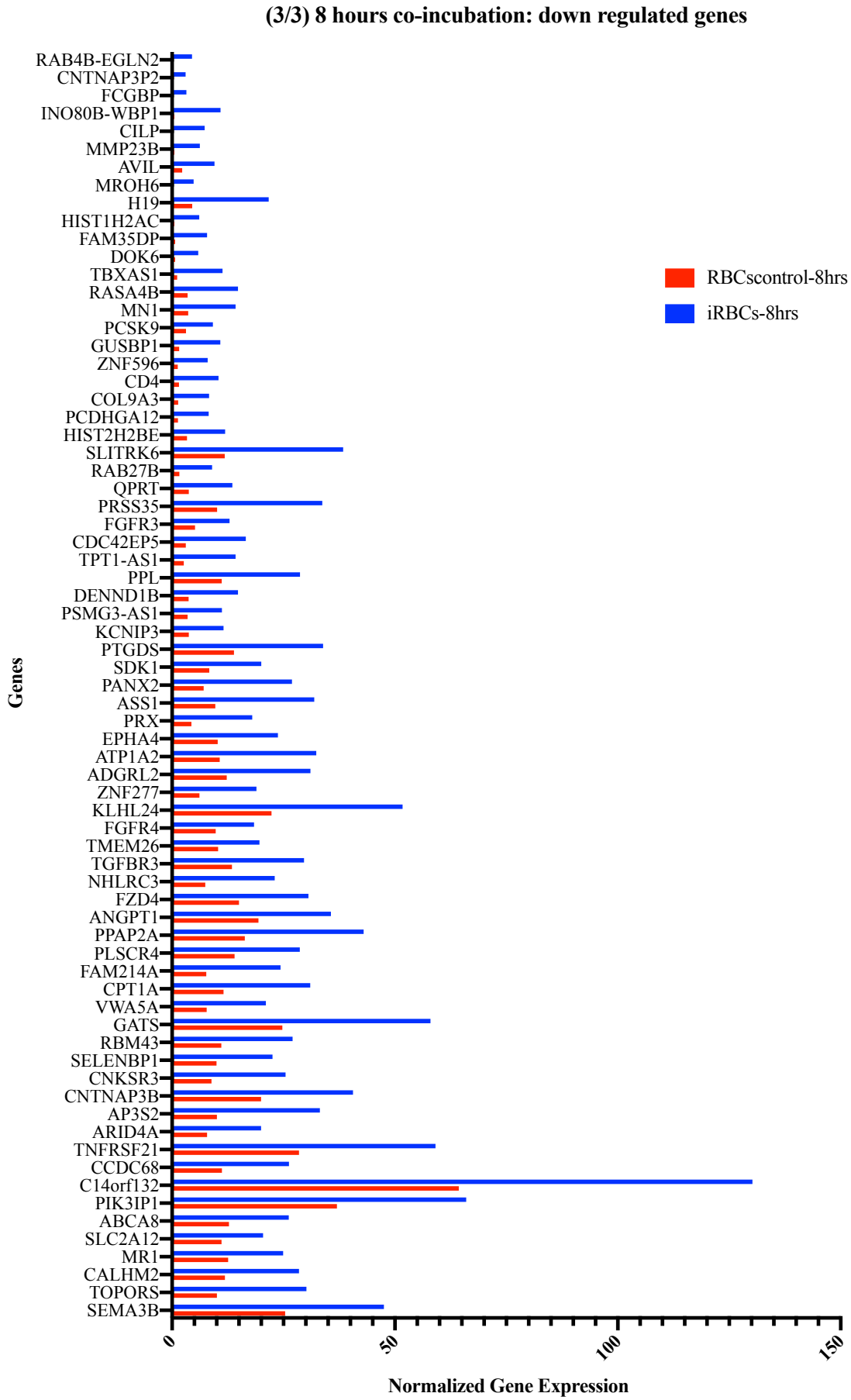

Figure 3.16 normalized gene expression of down regulated genes after 8 hours co-incubation (3/3)

The 462 genes were checked for groups and functions. Seven of the upregulated genes are involved in the interleukin signalling:

- MMP2 (matrix-metalloproteinase 2),
- MAOA (monoamine oxidase A),
- COL1A2 (collagen type I alpha 2 chain),
- BTRC (beta-transducin repeat containing E3 ubiquitin protein ligase),
- STAT2 (signal transducer and activator of transcription 2),
- CD4 (cluster of differentiation 4), and
- RPS6KA2 (ribosomal protein S6 kinase A2)

The subsequent figure 3.17 contains the normalized expression levels of the seven upregulated genes involved in IL signalling measured after an 8 hours co-incubation.

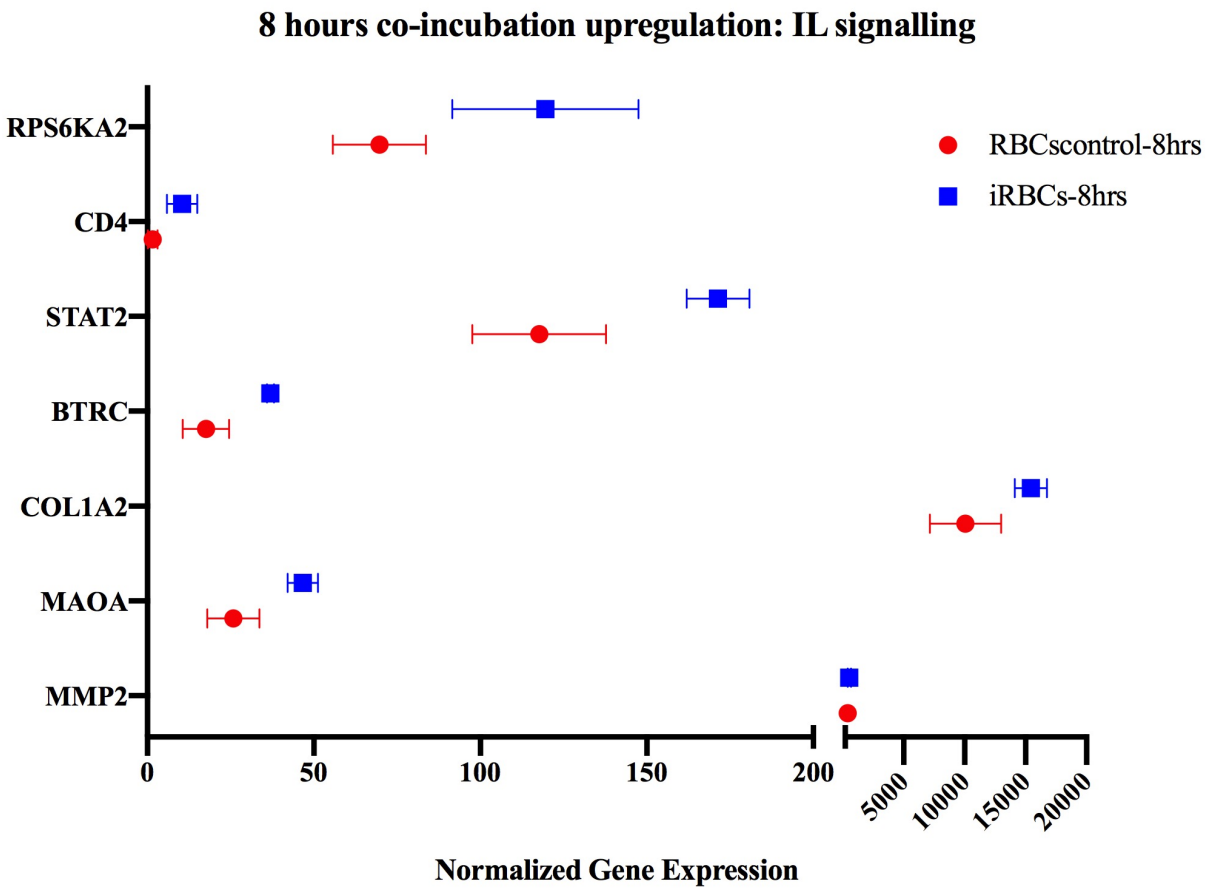

***Figure 3.17 8 hour co-incubation: analysis of up regulated genes – IL signalling*:** Expression levels of 8 hours co-incubation of iRBCs and control RBCs analysed via NGS. The mean expression levels are compared. P-values were adjusted using Holm's method. *: significant

The following table 3.8 displays the exactly analysed values of the normalized expression levels, the fold change and the p-value for MMP2, MAOA, COL1A2, BTRC, STAT2, CD4, and RPS6KA2.

Table 3.8 Up regulated genes in 8 hours co-incubation of iRBCs and PC lungs:

Gene	Normalized expression in control	normalized expression in 4 hrs co-incubation	Fold change	p-value
MMP2	404,4426549	545,597478	1,363648967	0,047878204
MAOA	25,81312134	46,68742181	1,907510431	0,026296807
COL1A2	10065,21122	15435,54763	1,536283426	0,001704952
BTRC	17,59999663	36,94357658	1,879169772	0,049716805
STAT2	117,6774326	171,3711713	1,533709088	0,011097195
GDF5	8,55507272	0,725385055	0,162619295	0,042428272
CD4	1,572152408	10,44413242	4,433954997	0,028102966

Furthermore, 55 of the downregulated genes are involved in the signalling of the cell cycle. The following figure 3.18 displays the normalized expression levels of the 55 downregulated genes.

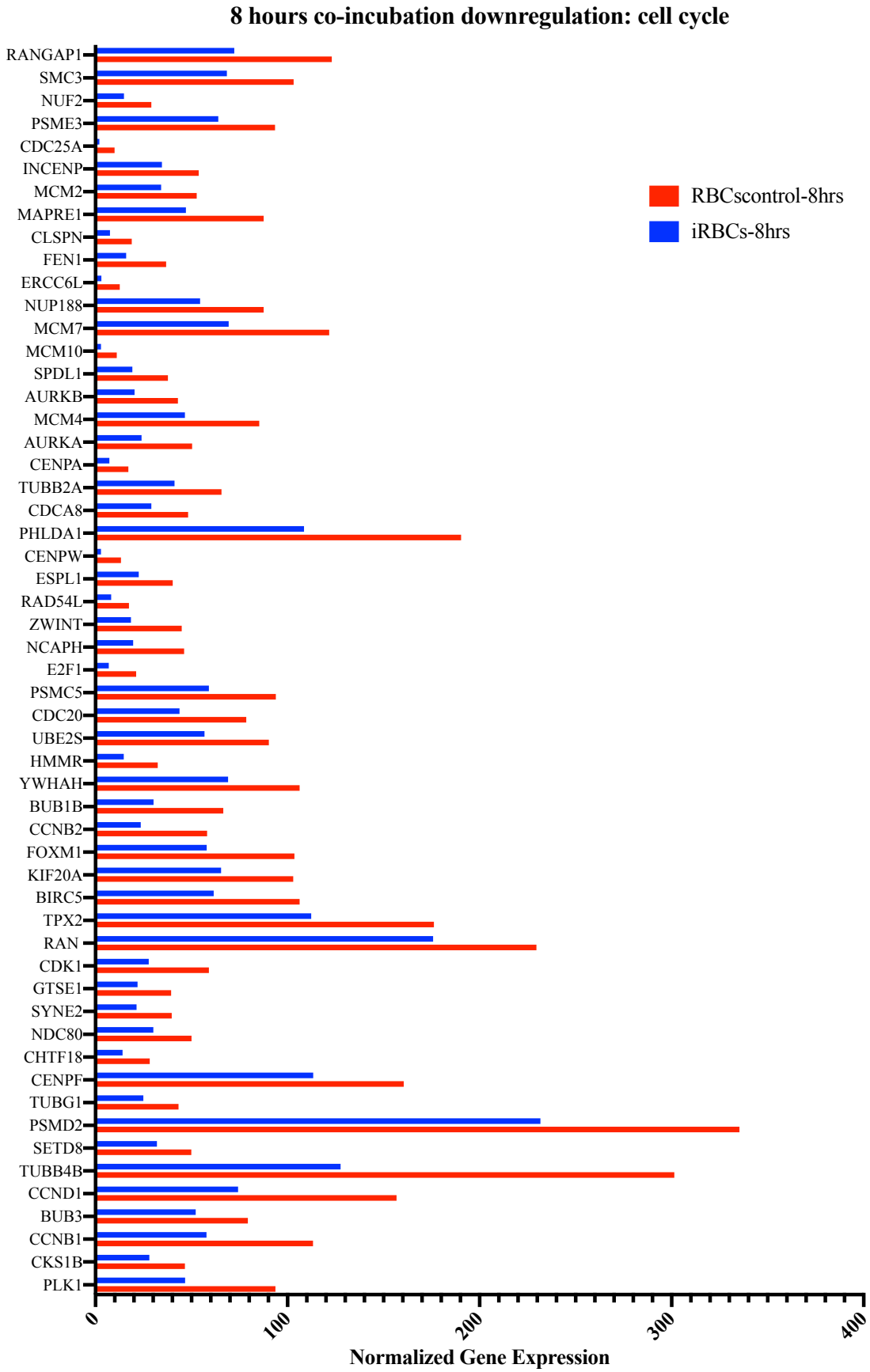

Figure 3.18 8 hours co-incubation: analysis of down regulated genes – cell cycle: Expression levels of 8 hours co-incubation of iRBCs and control RBCs analysed via NGS. The mean expression levels are compared. P-values were adjusted using Holm's method. *: significant

The following table 3.9 displays the exactly analysed values of the normalized expression levels, the fold change and the p-value for the 55 downregulated genes in the 8 hours co-incubation.

Table 3.9 Down regulated genes in 8 hours co-incubation of iRBCs and PC lungs:

Gene	Normalized expression in control	normalized expression in 4 hrs co-incubation	Fold change	p-value
PLK1	93,71732711	46,68831447	0,439629539	0,00092812
CKS1B	46,53509348	27,99489787	0,500208965	0,046603226
CCNB1	113,2772316	57,81303065	0,469588471	0,000626898
BUB3	79,29374633	52,16670034	0,593822621	0,035094147
CCND1	156,7701138	74,22108262	0,474912403	0,000594717
TUBB4B	301,3946962	127,6603308	0,401204347	1,27445E-05
SETD8	49,89898973	31,95069237	0,584605062	0,049347561
PSMD2	335,2978862	231,7282825	0,656452267	0,011153603
TUBG1	43,24763324	24,91398485	0,505840146	0,0339322
CENPF	160,4937951	113,3436815	0,667297644	0,042558282
CHTF18	28,20918969	14,13101647	0,4277542	0,028450599
NDC80	50,00603673	30,12934652	0,557062295	0,041320119
SYNE2	39,73526461	21,33433792	0,470214166	0,023194201
GTSE1	39,35147989	21,89192503	0,483818166	0,028487631
CDK1	59,09943462	27,77090744	0,411678335	0,004013891
RAN	229,5789907	175,8447508	0,727639042	0,048830999
TPX2	176,2350631	112,3466898	0,594022878	0,007905143
BIRC5	106,2602748	61,5882569	0,524279111	0,006170464
KIF20A	102,9788913	65,38297398	0,58107553	0,016368414
FOXM1	103,6095307	57,95129656	0,501163093	0,003264832
CCNB2	58,10325626	23,60557304	0,377996668	0,001749349
BUB1B	66,5445071	30,18197563	0,422178979	0,002406026
YWHAH	106,280594	69,07671594	0,589348804	0,018119902
HMMR	32,43845997	14,68772393	0,433812098	0,026203905

UBE2S	90,29674966	56,78928938	0,546601783	0,032789495
CDC20	78,50098976	43,72285715	0,500225093	0,009983638
PSMC5	93,87871445	59,0127856	0,65034462	0,04493476
E2F1	21,21408719	6,875948513	0,294735302	0,007529869
CENPW	13,25574742	2,823406723	0,252019516	0,025892401
PHLDA1	190,3948004	108,5835595	0,546652855	0,000344771
CDCA8	48,27657198	29,12282282	0,510713214	0,049606345
TUBB2A	65,63837001	41,1073543	0,574844301	0,02665285
CENPW	13,25574742	2,823406723	0,252019516	0,025892401
AURKA	50,35499934	23,9652105	0,408312221	0,004426525
MCM4	85,2373691	46,57415844	0,487380489	0,014248651
AURKB	42,91646727	20,30172782	0,389238068	0,005371856
SPDL1	37,72250434	19,17298815	0,434210333	0,023671469
MCM10	11,05363811	2,834252334	0,229758747	0,025746491
MCM7	121,6704502	69,40199937	0,526088845	0,005748572
NUP188	87,5969517	54,50821489	0,615916518	0,027226722
ERCC6L	12,62813417	3,038549275	0,225920541	0,017847817
FEN1	36,77292859	15,95877575	0,373520573	0,007097217
CLSPN	18,84940748	7,495612605	0,290636731	0,021518704
MAPRE1	87,5988658	47,08453064	0,552482656	0,0177129
MCM2	52,74840825	34,17413109	0,556551958	0,04305783
INCENP	53,69931525	34,58307171	0,578365862	0,047737312
CDC25A	9,955052528	1,916382242	0,219392036	0,031156318
PSME3	93,5098533	63,99042957	0,66072795	0,044342719
NUF2	29,09932659	14,79083586	0,416064755	0,025255538
SMC3	103,1763112	68,46337999	0,657269753	0,032934309
RANGAP1	123,0530847	72,28270237	0,536222995	0,004427983

In addition, the genes that were upregulated or downregulated after 4 hours were checked for their corresponding expression after an 8 hours co-incubation.

From the 12 upregulated genes after the 4 hours co-incubation none was significantly expressed compared to the control after eight hours.

From the 36 downregulated genes after the 4 hours co-incubation five were significantly expressed compared to the control eight hours.

ERRFI1 and HBA2 were downregulated after four hours and after eight hours of co-incubations.

FBLN1, NID1, and PLTP were downregulated after four hours and upregulated after eight hours of co-incubation.
These findings are visualized in figure 3.19 and table 3.10.

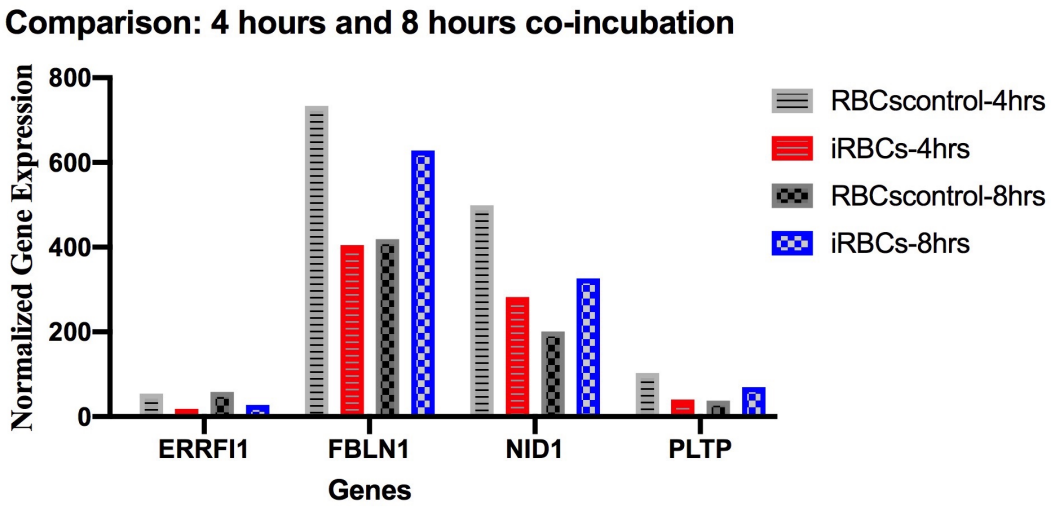

***Figure 3.19 Comparison for genes that are significantly differently expressed in 4 hours and 8 hours co-incubation*:** ERRFI1, FBLN1, NID1, PLTP

***Table 3.10 Comparison for genes that are significantly differently expressed in 4 hours and 8 hours co-incubation*:** ERRFI1, FBLN1, NID1, PLTP:

Genes	Normalized expression in control 4hrs	Normalized expression in 4hrs co-incubation	fold change 4hrs	p-value 4hrs	normalized expression in control 8hrs	normalized expression in 8hrs co-incubation	fold change 8hrs	p-value 8hrs
ERRFI1	54,2544773	18,39224007	0,378516154	0,030421707	58,26525946	27,44698589	0,443709969	0,004319532
FBLN1	733,9310413	404,9346062	0,558918264	0,033056433	419,0825388	628,1551358	1,540818803	0,009890167
NID1	499,2203104	282,2590018	0,57854715	0,045887172	201,2057823	326,1410392	1,673189688	0,000922275
PLTP	102,978204	40,54093962	0,399095231	0,017984097	37,84446903	69,40445536	1,865828686	0,014805891

3.3.3. Gene analysis for co-incubations

In the data analysis, the co-incubations were examined for interleukins (ILs), intercellular adhesion molecules (ICAMs), tumour necrosis factor superfamily (TNFSFs), chemokine ligands (CXCLs), nuclear factor kappa-light-chain-enhancer of activated B cells (NFκBs), REL proto-oncogenes (RELs) and erythropoietin receptor (EPOR).

3.3.3.1. Interleukins

The following figure 3.20 shows the compared normalized gene expression levels for the four and for the eight hours co-incubations for interleukins. The displayed interleukins are IL-6, IL-7, IL-10, IL-11, IL-15, IL-16, IL-18, IL-24, IL-32, IL-33 and IL-34.

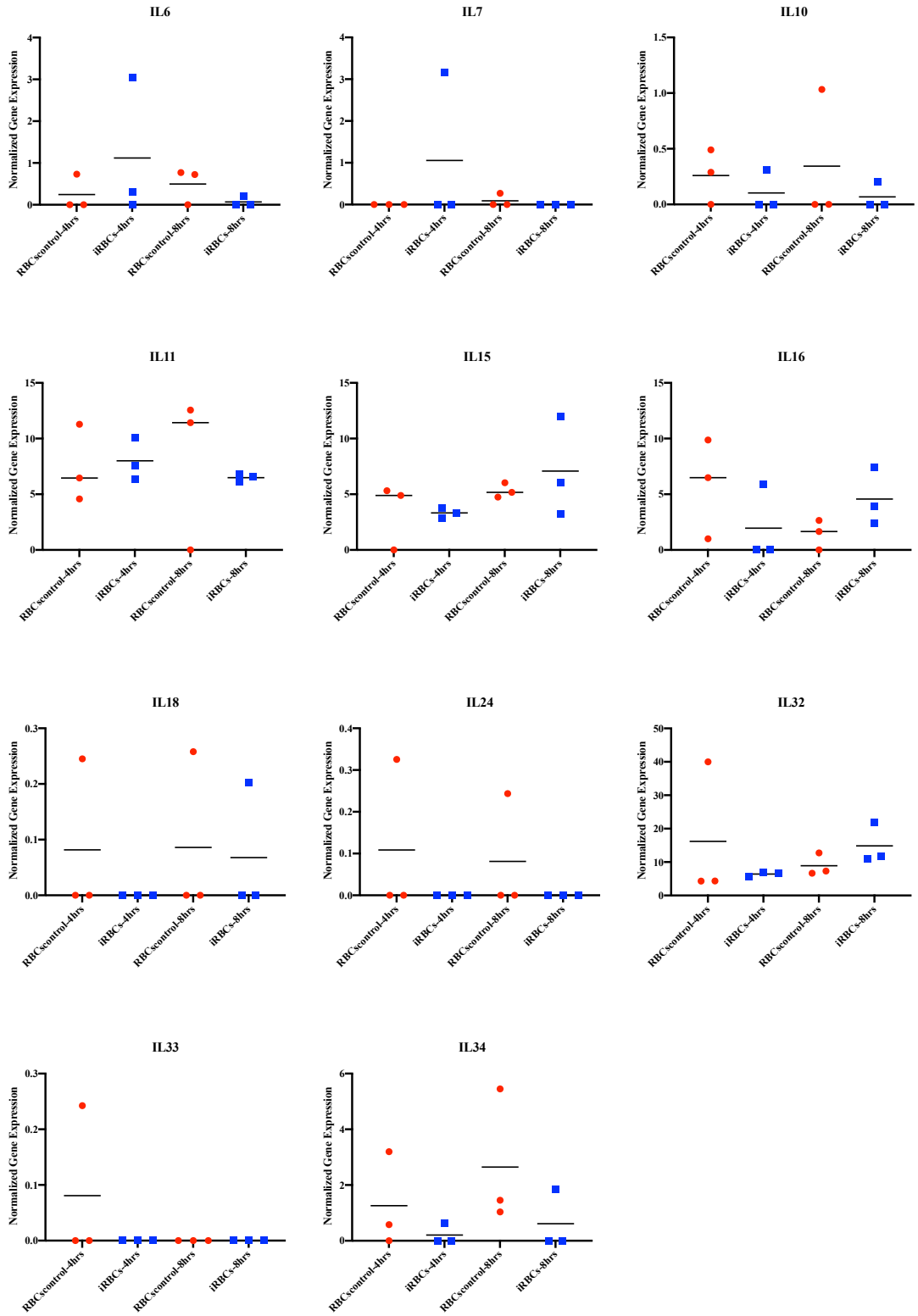

Figure 3.20 Compared normalized expression levels of interleukins after four and after eight hours co-incubations.

3.3.3.2. ICAMs

The figure 3.21 displays the compared normalized gene expression levels for the four and for the eight hours co-incubations for ICAMs. ICAM1, ICAM3, ICAM4 and ICAM5 were analysed.

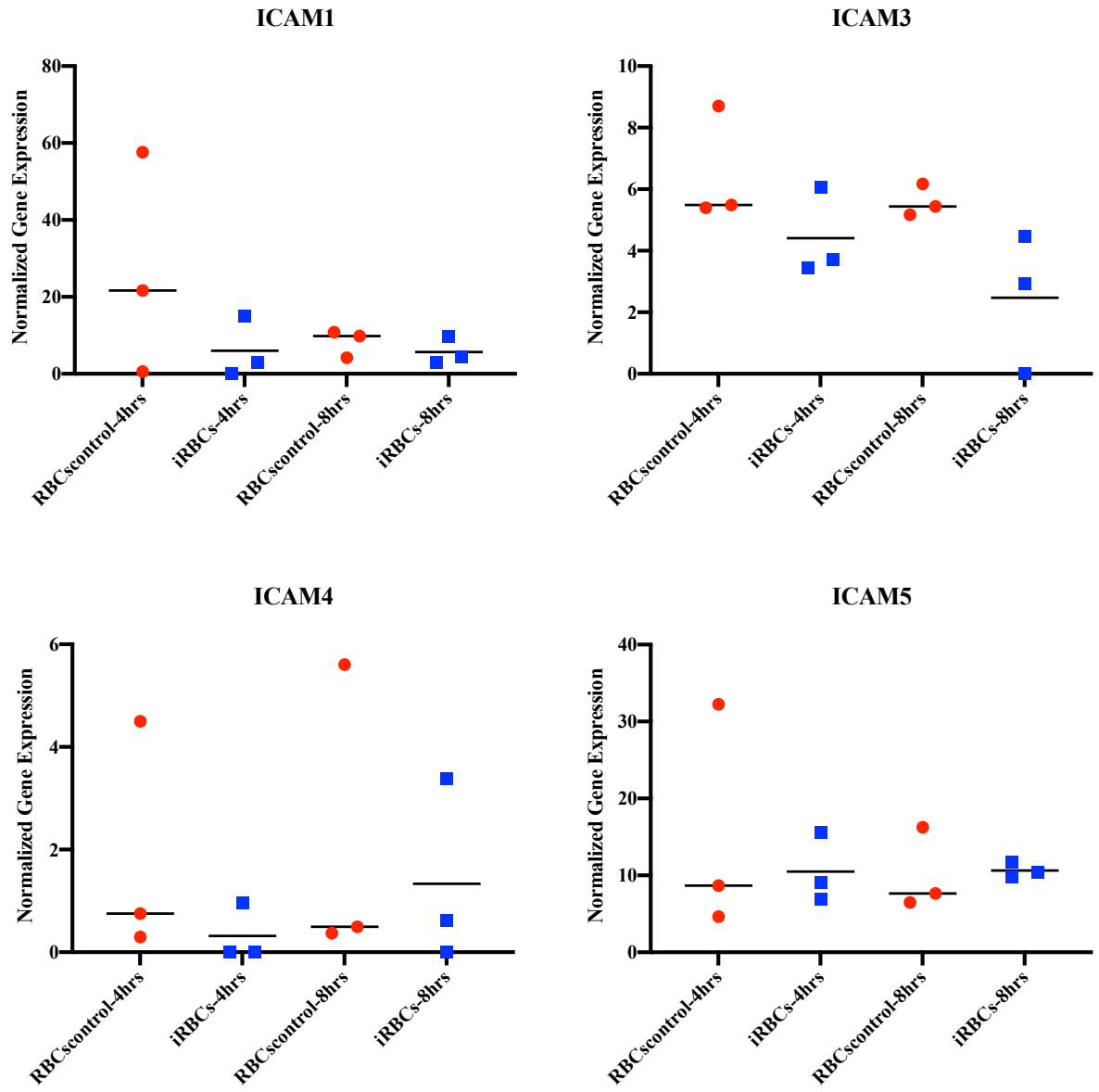

Figure 3.21 Compared normalized expression levels of ICAMs after four and after eight hours co-incubations.

3.3.3.3. TNFSFs

The figure 3.22 illustrates the compared normalized gene expression levels for the four and for the eight hours co-incubations for TNFSFs. The investigated TNFSFs are TNFSF9, TNFSF10, TNFSF12, TNFSF13, TNFSF14, TNFSF15, and TNFSF18.

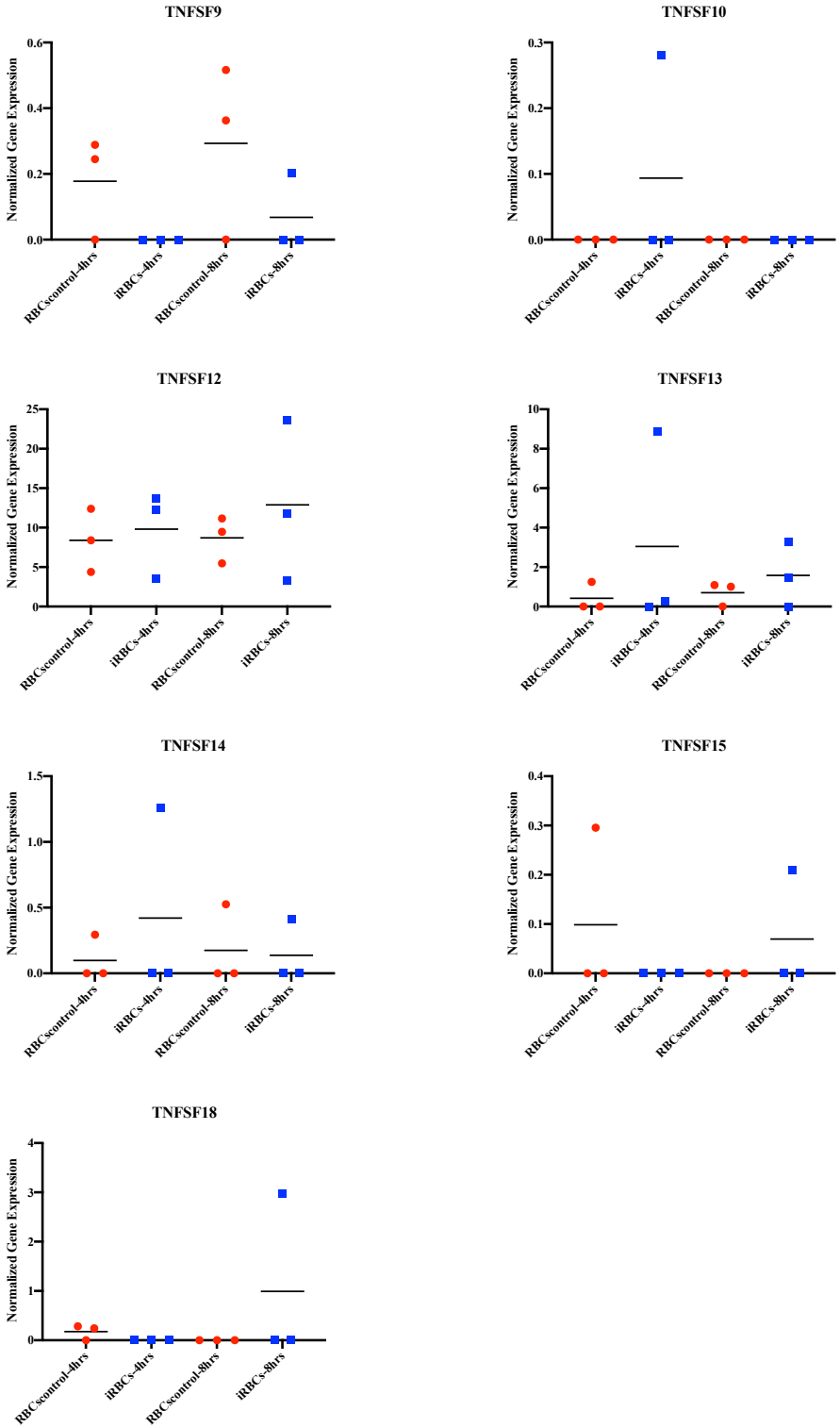

Figure 3.22 Compared normalized expression levels of TNFSFs after four and after eight hours co-incubations.

3.3.3.4. CXCLs

The figure 3.23 features the compared normalized gene expression levels for the four and for the eight hours co-incubations for CXCLs. The investigated CXCLs are CXCL1, CXCL2, CXCL3, CXCL5, CXCL6, CXCL8, CXCL12, and CXCL16.

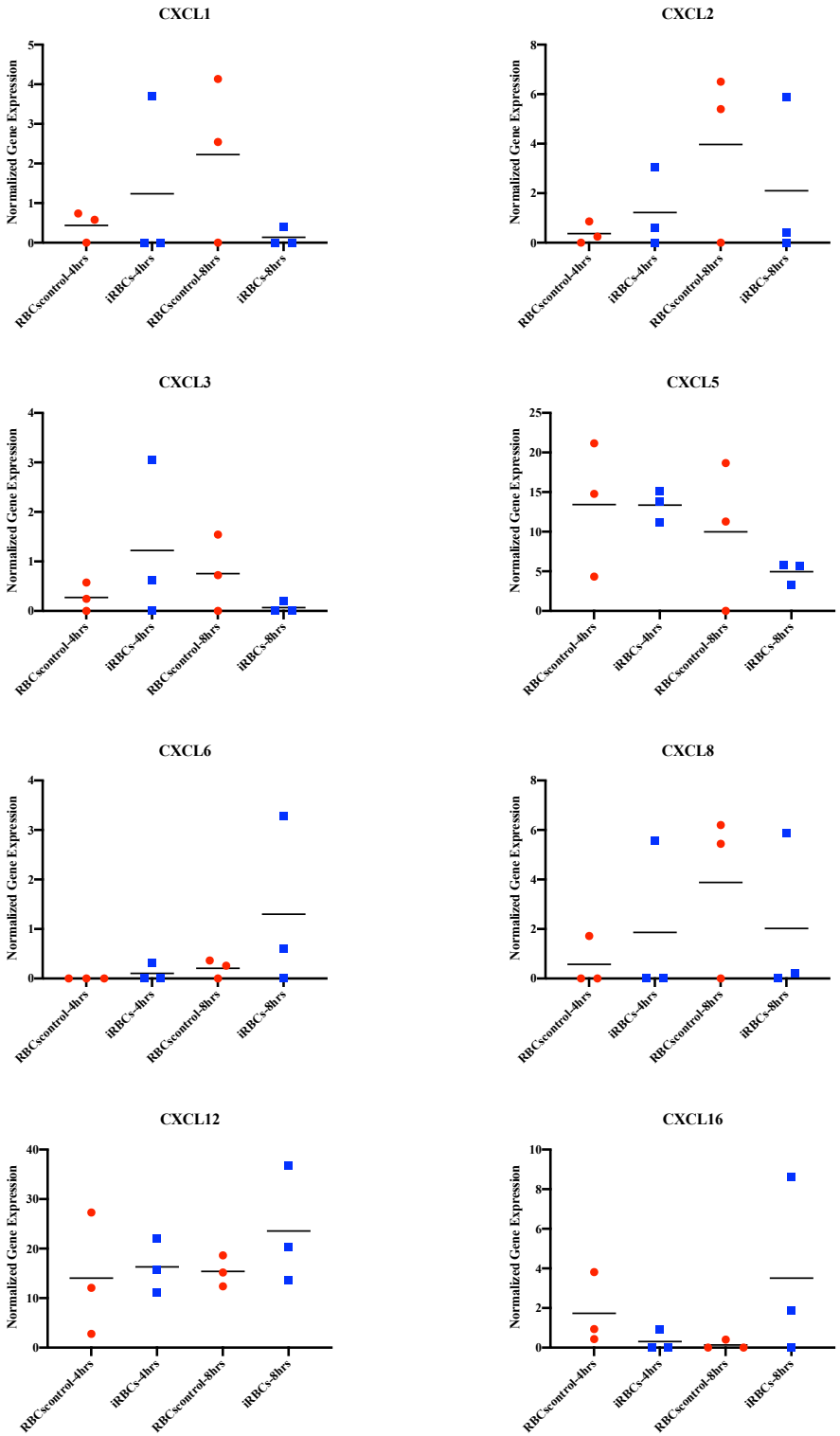

Figure 3.23 Compared normalized expression levels of CXCLs after four and after eight hours co-incubations.

3.3.3.5. NFκBs and RELs

The figure 3.24 shows the compared normalized gene expression levels for the four and for the eight hours co-incubations for NFκBs and RELs. The investigated NFκBs are NFκB1 and NFκB2. The analysed RELs are REL, RELA, and RELB.

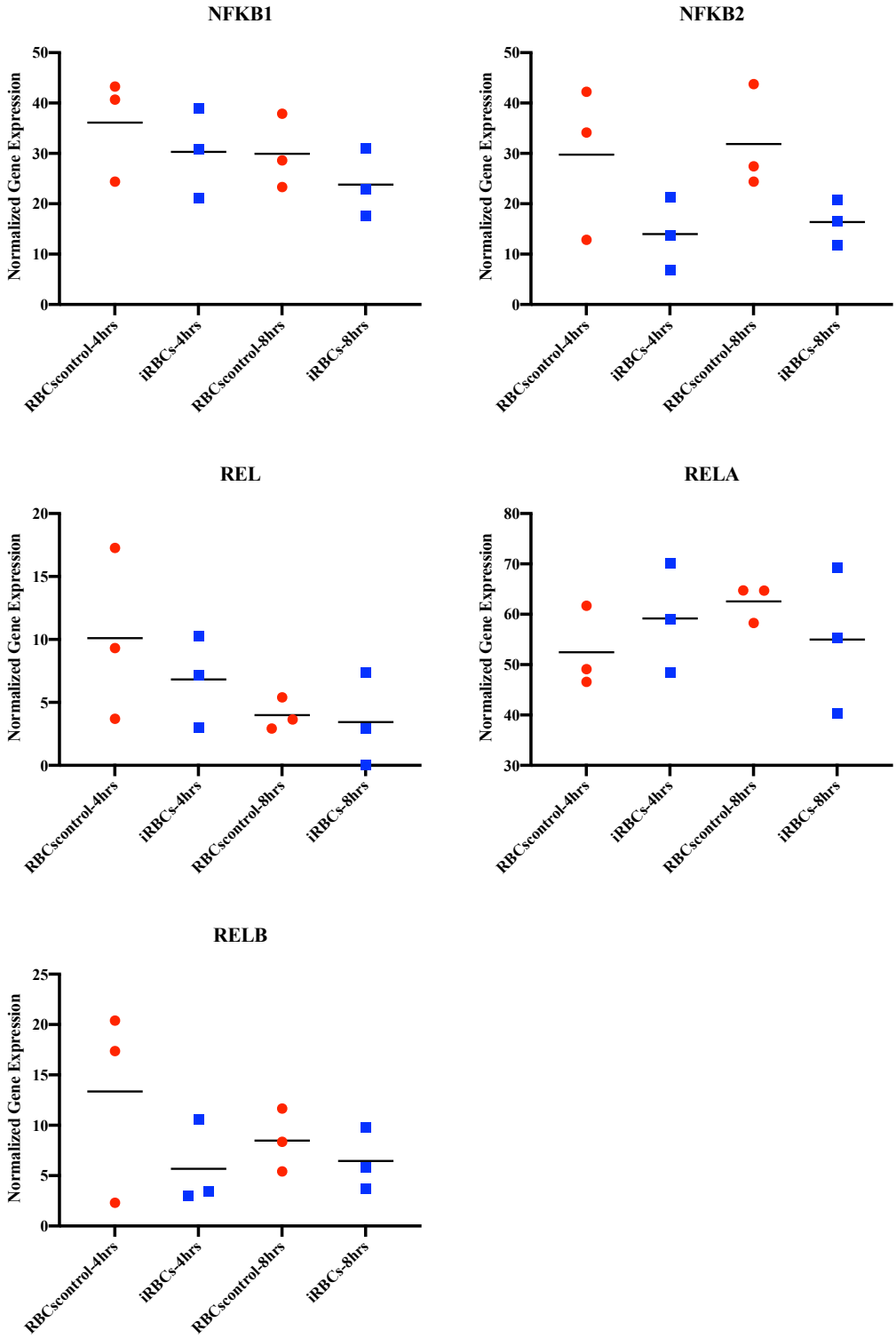

Figure 3.24 Compared normalized expression levels of NFκBs and RELs after four and after eight hours co-incubations.

3.3.3.6. EPOR

The figure 3.25 displays the compared normalized gene expression levels for the four and for the eight hours co-incubations for EPOR.

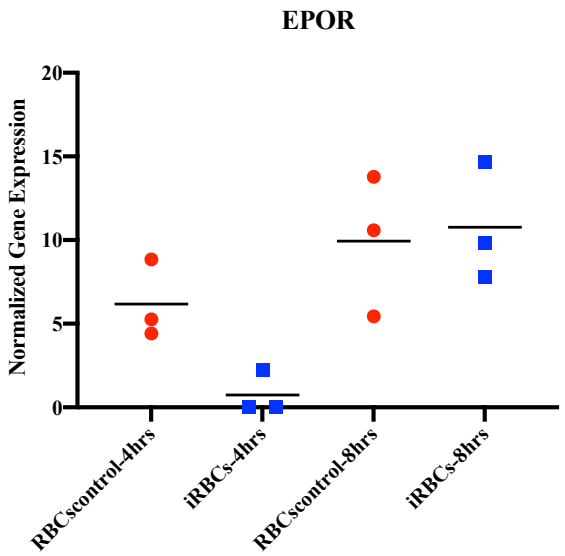

Figure 3.25 Compared normalized expression levels of EPOR after four and after eight hours co-incubations.

3.4. Fluorescence-Activated Cell Sorting of HMVEC-L

Hanifeh Torabi, a colleague from the BNITM, performed FACS on primary lung cells after TNF stimulation to detect the existing amount of CD36, ICAM-1 and CSA receptors. The FACS was performed as described in chapter 2.2.2.4. The corresponding amount is expressed in mean fluorescence intensity (MFI). The MFIs of the marked receptors are compared to a not TNF stimulated control. For each receptor (CD36, ICAM-1 and CSA) three samples were examined with FACS:

- The mean MFI of CD36 is 718 (samples: 448, 455, 1251)
- The mean MFI of ICAM-1 is 21650 (samples: 5039, 2751, 57151)
- The mean MFI of CSA is 32519 (samples: 44983, 7593, 44983)
- The mean MFI of the control is 784 (samples: 444, 435, 1472) and 1181 (samples: 1123, 1217, 1203)

The data is represented in figure 2.26.

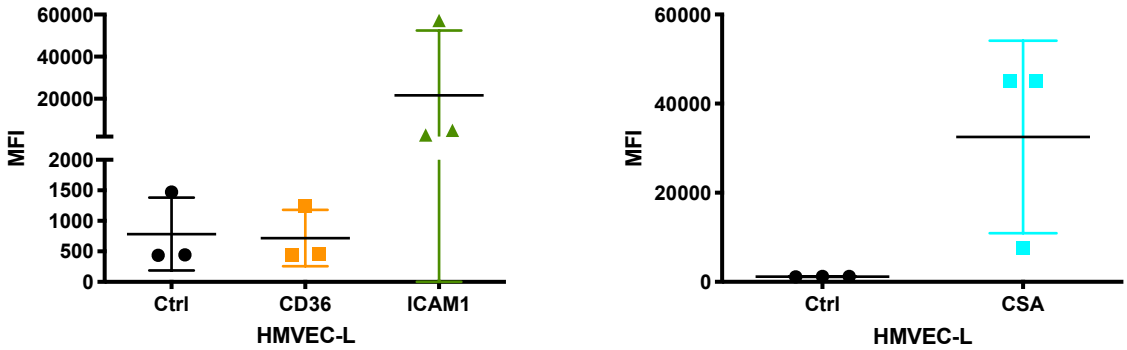

Figure 3.26 FACS of HMVEC-L for CD36, ICAM-1 and CSA after TNF stimulation and not TNF stimulated control.

4. Discussion

The present study is conducted to do justice to the clinical relevance of *Plasmodium falciparum* Malaria worldwide. The focus is placed on lung endothelial cells since lung manifestations are common in uncomplicated malaria. In severe malaria, ALI and ARDS might develop and worsen the patients' prognosis.
The underlying pathomechanism of *P. falciparum* infiltration in the human lungs is not yet fully understood, but there is great interest in the process of cytoadhesion.
Therefore, it was aimed to analyse the cytoadhesion between iRBCs and human lung endothelial cells. The focus was placed on a potential *var* gene antigenic switch of the parasites and on the expressed receptor on the surfaces of infected erythrocytes and lung tissue.
The findings of this research could help to better understand the pathomechanism and to identify potential target points for therapy or vaccination strategies.

4.1. Enrichment of infected erythrocytes over HULEC-5a

4.1.1. *Var* genes

The RNA analysis in 3.1.2.1. showed a significant change in expression rates during the enrichment of infected erythrocytes over HULEC-5a for *Var*04 and *Var*66.
*Var*04 is further known as *Var*2CSA and it was significantly overexpressed. It is linked to placental malaria in pregnant women because it has the ability to bind to chondroitin sulfate A which is expressed on the syncytiotrophoblast surface.
Although research in *Var*2CSA shows great prospect in helping to develop a placental malaria vaccine, there is no known connection to malarial lung cells. Therefore, the gene switch to *var*2CSA was not considered relevant in the setup of the present study.
*Var*66 was significantly underexpressed after the enrichment over HULEC-5a. We could not determine a relevant explanation for this change in expression. Therefore, work with this cell line was not continued.

4.1.2. *Rifin* genes

As presented in 3.1.2.2., seven *rifin* pseudogenes have been significantly expressed in the enriched culture compared to the starting culture.
Especially the *rifin* pseudogenes PfIT_120005900 and PfIT_120060200 were highly overexpressed. PfIT_120005900 was about 185 times overexpressed and PfIT_120060200 was about 208 times higher expressed.
There is research suggesting that *rifin* and *stevor* are expressed in the invasive merozoite and on the surface of the infected erythrocyte. This might implicate them as a relevant parasite virulence factor (Niang et al., 2014).
This could be a potential topic for further scientific research.

4.1.3. *Stevor* genes

The RNA analysis in 3.1.2.3. showed that PfIT_040007000 was expressed about 26 times higher in the enriched culture compared to the starting culture. As mentioned before in 4.1.2., *stevor* genes might play an important role as a virulence factor (Niang et al., 2014).
There should be further research on this topic.

4.2. Enrichment of infected erythrocytes over HMVEC-L

The enrichment of infected erythrocytes over HMVEC-L appeared successful in bare cell count as visualised in figure 3.6.
Unfortunately, we did not perform an RNA analysis with the enriched cells after four rounds of enrichment. We simply continued the work by using the enriched cells for the co-incubations.
Luckily, Hanifeh Torabi, a PhD colleague from the BNITM, performed a similar enrichment of infected erythrocytes over HMVEC-L following the same protocol and the hereby collected RNA was analysed with NGS.
The data showed a significant overexpression for *Var*66, *Var*23, *Var*34, *Var*30, and *Var*03. The corresponding data is attached in the supplements figure 1 and table 1. Interestingly, *var*66 was also significantly differently expressed in our experimental setup with HULEC-5a. So, this var gene might play a relevant role in the adhesion process of infected erythrocytes to

lung tissue. Besides that, there is not yet sufficient investigation of which *var* genes mediate the attachment to human lung cells. Further experiments should be conducted to support or challenge our results and to help better understand the binding mechanism in lung cells.
In addition, two erythrocyte membrane protein-1 like genes have been significantly overexpressed in Torabi's data: PfIT_080005200 and PfIT_110005800 (Supp. Table 2). Further experiments should be carried out here to help better understand the underlying processes.

4.3. Co-Incubation of iRBCs and HMVEC-L

The co-incubations of iRBCs and lung primary cells were performed in order to explore whether there is an effect of cytoadhesion on the cells and their genes after a specific amount of time. The timeframes of four and eight hours were chosen following the established protocol of Yifan Wu, a colleague from the BNITM, who did the same work successfully with brain primary cells (Y. Wu, 2023).

4.3.1. Co-Incubation for four hours

After the four hours co-incubation of iRBCs and HMVEC-L, twelve genes were overexpressed (fig 3.7.). From these genes two spiked the interest, since they are both part of IL signalling and therefore important for the immune reaction: HMOX and EGR1.
Infection by *Plasmodium* leads to haemolysis and the release of haemoglobin from the iRBCs. Seixas et al. postulated that the expression of HMOX in *Plasmodium*-infected mice is essential to their survival and to the restoring of homeostasis. HMOX-deficient mice had a 100% lethality rate due to hepatic failure (Seixas et al., 2009).
So, the overexpression of HMOX after four hours of co-incubation could be a relevant survival mechanism in humans as well and should be further investigated.
Early growth response protein 1 is a transcription factor induced by stress signals to transactivate multiple downstream cascades of cell proliferation and apoptosis regulation. It was found a relevant factor in the process of bacterial adhesion and the outcome of an infection (Banerji & Saroj, 2021; de Klerk et al., 2017).
Therefore, it is particularly interesting that the expression of EGR1 was upregulated during the early stages of co-incubation after four hours. This finding could support the thesis of

Banerji & Saroj (2021) and extend the relevance of EGR1 on bacterial adhesion to include *Plasmodium* adhesion as well.
In the performed experiments in 3.3.2., HMOX and EGR1 both were on normal expression levels after eight hours of co-incubation compared to the control. It is therefore postulated that their main relevance is for an early stage immune response.

After the four hours co-incubation of iRBCs and lung primary cells, 36 genes were downregulated. Six of these underexpressed genes are involved in the construction of the extracellular matrix: LTBP4, FBLN1, MMP2, MMP14, NID1, and GDF5. Their downregulation could be explained by an affected barrier function due to cytoadhesion and a consequently impaired extracellular matrix. But science did not yet connect these genes with lung malaria or malaria in general, so further research could be helpful to assess their relevance.

4.3.2. Co-Incubation for eight hours

After the eight hours co-incubation, 462 genes were significantly differently expressed as outlined in 3.3.2. In comparison, only 48 genes were on different expression levels after four hours. This total difference of 10-fold could mean that some of the processes induced by cytoadhesion are rather slow and need time to show the corresponding change in gene expression.
From the upregulated genes, seven are involved in interleukin signalling: MMP2, MAOA, COL1A2, BTRC, STAT2, CD4, and RPS6KA2.
From these seven genes, two are part of the toll like receptor (TLR) cascade: BTRC and RPS6KA2. TLRs play a key role in the innate immune system and especially TLR9 is postulated to be part of the immune response to Malaria (Naing et al., 2021). So, its upregulation in the present study appears congruent with current science.
Interestingly, the three genes FBLN1, NID1, and PLTP have been downregulated after four hours, but upregulated after eight hours. FBLN1 and NID1 both encode proteins of the extracellular matrix that have been shown to interact with each other: fibogen-1 and nidogen-1 (Adam et al., 1997). Their change in expression levels could be explained following 4.3.1.: After four hours, the genes are downregulated due to an impaired extracellular matrix in early cytoadhesion. In response to the impairment, the genes are then upregulated after eight hours. This postulation should be further investigated.

From the 230 downregulated genes, 55 genes are involved in the signalling of the cell cycle. This supports the hypothesis that cytoadhesion influences the signalling processes in the affected cells.
From the 55 genes, two are downregulated after four hours and still downregulated after eight hours: ERRFI1 and HBA2. ERRFI1 is a cytoplasmic protein linked with cell signalling and the interferon pathway (J. Wu et al., 2015). This finding supports the previously mentioned hypothesis as well.

4.3.3. Gene analysis for co-incubations

4.3.3.1. Interleukins

Interleukins are a class of cytokines produced by different body cells. They are essential for the activation and differentiation of immune cells. In humans, there are 36 known families of interleukins with different effects on the immune system, some pro-inflammatory and some anti-inflammatory effects. They can enable a big spectrum of reactions in cells and tissues by binding to high-affinity receptors on cell surfaces (Justiz Vaillant & Qurie, 2022).
Some pro-inflammatory cytokines have been related to clinical malaria or severe malaria such as: IL-6, IL-8, IL-10, IL-11, IL-12, IL-13, IL-31, and IL-33 (Ayimba et al., 2011; Lyke et al., 2004; Oyegue-Liabagui et al., 2017).
In the present study, the expression levels of interleukins after four and eight hours co-incubation were compared to the controls in 3.3.3.1. The compared interleukins IL-6, IL-7, IL-10, IL-11, IL-15, IL-16, IL-18, IL.24, IL-32, IL-33, and IL-34 did not present with any significant change in expression levels. It is therefore postulated that the process of cytoadhesion does not affect the interleukins. The known relevance of interleukins in infection with plasmodium can't be explained by the present study and might arise out of a different process of interaction. Further research is needed to support this hypothesis.

4.3.3.2. ICAMs

Intercellular adhesion molecules (ICAMs) belong to the immunoglobulin superfamily and play a vital role in inflammation, immune response, and intracellular signalling. There are five known members of the ICAM family, ICAM-1 to ICAM-5 (Hayflick et al., 1998). Especially

ICAM-1 has been determined to play a central role in the binding of iRBCs. *Pf*EMP1 was found to bind to ICAM-1 and thereby achieve the adhesion between iRBC and vasculature (Chakravorty & Craig, 2005; Lennartz et al., 2019).
Therefore, it was of interest in the present study whether the expression levels of ICAMs changed during the co-incubation with iRBCs. The figure 3.21 in 3.3.3.2. shows that the expression levels of ICAM-1, ICAM-3, ICAM-4, and ICAM-5 did not change significantly with the co-incubations of four and eight hours. It appears that cytoadhesion itself does not lead to the expression of ICAMs.
This finding goes hand in hand with the work of BNITM colleague Yifan Wu who performed similar experiments with primary brain cells: The expression levels of ICAMs did not change after co-incubation of four and eight hours between iRBCs and primary brain cells (Y. Wu, 2023).

4.3.3.3. TNFSFs

The tumour necrosis factor superfamily (TNFSF) is a protein superfamily whose 19 members function as cytokines and promote different cell function such as immune response, inflammation, proliferation, and apoptosis (Aggarwal et al., 2012).
In the human body, TNF family members have been recognized to both promote malaria parasite eradication, but also to add to the development of severe malaria (Cruz et al., 2016; Randall & Engwerda, 2010).
Thus, in the present study, it was considered relevant whether the expression levels of TNFSFs would change after co-incubation. In 3.3.3.3. the expression levels of TNFSF9, TNFSF10, TNFSF12, TNFSF13, TNFSF14, TNFSF15, and TNFSF18 were analysed after four and eight hours co-incubations. None of these TNFSF genes were significantly differently expressed in the co-incubations compared to their controls. It is therefore postulated, that cytoadhesion does not lead to the increased or decreased expression of TNFSFs.

4.3.3.4. CXCLs

CXC chemokines belong to the chemokine superfamily. They are secreted molecules that act in leukocyte trafficking and activation. There are 16 known members of the CXCL family (Zlotnik & Yoshie, 2000).
Two CXCLs have been discovered in association with severe malaria syndromes in case-control studies: CXCL8 and CXCL9 (Ayimba et al., 2011). In addition, in vitro studies showed the ability of iRBCs to induce CXCL1, CXCL2, CXCL6, and CXCL8 production (Viebig et al., 2005).
In the present study in 3.3.3.4., the expression levels of CXCL1, CXCL2, CXCL3, CXCL5, CXCL6, CXCL8, CXCL12, and CXCL16 have been compared between co-incubations with iRBCs and controls after four and eight hours. None of the CXCLs showed a significant change in expression with co-incubations for these time frames. The current hypothesis is that cytoadhesion by itself does not lead to the changed expression of CXCLs.

4.3.3.5. NFκBs and RELs

Nuclear factor 'kappa-light-chain-enhancer' of activated B-cells (NFκB) is a specific transcription factor that is vital for the regulation of immune response, cell proliferation, and apoptosis. It has effects on all stages of immune system functioning from the development of lymphoid tissues, through haematopoiesis, to recognition of Pathogen-Associated Molecular Patterns. Its family consists of five proteins that form NF-κB complexes: NFκB1, NFκB2, RelA, RelB, and c-Rel (Hayden & Ghosh, 2011; Zhou et al., 2021).
NFκB was identified as an important player of immune response during Plasmodium infections. After in vitro exposure of human brain endothelial cells to *P.falciparum* infected erythrocytes, NFκB was induced and the NFκB cascade was upregulated (Bąska & Norbury, 2022).
In the present study in 3.3.3.5., the expression levels of NFκB1, NFκB2, RelA, RelB, and c-Rel in HMVEC-L after four and eight hours of co-incubations with iRBCs were assessed. None of the five genes was significantly upregulated. So, it appears that cytoadhesion does not affect the expression of NFκB.

4.3.3.6. EPOR

The erythropoietin receptor is a receptor in immune cells that is activated upon binding of erythropoietin (EPO). EPO is the central erythropoietic regulator and it provides the necessary signal for RBC progenitors to compensate for anaemia and hypoxia. In addition to the bone marrow, also parenchymal, neuronal, immune, and neoplastic cells seem to be EPO-responsive. In immune cells, such as macrophages, the EPO-EPOR mechanism interacts with activation of NFκB and formation of TNF-α and IL-6. With a big range of induced signal cascades, EPO has pro-inflammatory and anti-inflammatory effects. Its precise function is yet to be investigated (Liu et al., 2006; Nairz et al., 2011, 2012).
In the present study in 3.3.3.6., the expression level of EPOR was not significantly upregulated compared to the controls. It is postulated that the effect of cytoadhesion during co-incubation does not lead to the expression of EPOR.

4.4. FACS of HMVEC-L

With the Fluorescence-Activated Cell Sorting, it was aimed to identify the number of expressed receptors on primary lung cells (HMVEC-L) after TNF stimulation in comparison to a not TNF stimulated control. Hanifeh Torabi from the BNITM who performed the experiment checked for CD36, ICAM-1, and CSA since they have been described to play a role in *Plasmodium* cytoadhesion.
CD36 is a multifunctional receptor that was found to serve as a receptor for *Pf*EMP1 on iRBCs' surface. The iRBCs are hereby enabled to adhere to endothelia and to sequester in host organs to avoid their own clearance. In addition, CD36 is discussed to mediate a CD36-dependent immune response which helps to reduce parasite numbers and mortality by malaria (K. P. Day et al., 1998; Thylur et al., 2017).
As discussed in 4.3.3.2., ICAM-1 similarly functions as a receptor for *Pf*EMP1 and enables cytoadhesion of iRBCs (Chakravorty & Craig, 2005; Lennartz et al., 2019).
Chrondroitin-4-sulfate (CSA) is part of the proteoglycan matrix of microvasculature in the circulatory system of lung, brain, and placenta. But so far, it was only proven that *P.falciparum* cytoadheres in great numbers to placental CSA via *var*2CSA (*var*04) and therefore promoting placental malaria (Rieger et al., 2015). Rieger et al. discussed that the

specificity of *Pf*EMP1 to placental CSA might be explained by the distance between CSA chains in membranes, which is lower in placenta compared to other tissues.

In the performed experiments of Torabi, visualized in Fig. 3.26., CD36 was not significantly expressed on HMVEC-L surfaces. CD36 expression does not appear to be stimulated by TNF. In the FACS, ICAM-1 was highly expressed on the sorted lung primary cells. ICAM-1 expression might be induced by TNF stimulation and could be part of the activation of endothelial cells in infection.
Finally, CSA was highly expressed on the examined lung cells. Since it has been shown in experiments that *Pf*EMP1 was not able to bind to lung CSA, the high expression of CSA in TNF stimulated HMVEC-L could, in contrary, protect the tissue and suppress the stimulation of the immune system.
It would be helpful to repeat the experiment with cell lines from a different donor and confirm or challenge the results.

4.5. Conclusion

Lung manifestations play a central role in severe malaria and they not only limit the clinical management, but also increase malaria mortality rates especially in the highly burdened tropical and subtropical countries.

The present work aimed to help better understand the influence of cytoadhesion of *P. falciparum* infected erythrocytes on human lung endothelial cells.

In the first part, the performed enrichment assays aimed to recognize a potential antigenic switch of *var* genes after contact with lung cells. In HULEC-5a, the results were not conclusive and work with this cell line was not continued. In HMVEC-L, the lung primary cells, five *var* genes were predominant after enrichment: *Var*66, *Var*23, *Var*34, *Var*30, and *Var*03.

In the second part, the *P. falciparum* infected erythrocytes were co-incubated for four and eight hours over lung primary cells and afterwards the RNA of the iRBCs was analysed for the expression levels compared to the corresponding controls. It was shown that multiple genes were significantly overexpressed and significantly underexpressed after four and after eight hours. From notable interest were the overexpression of HMOX and EGR1 after four hours since these genes are involved in IL signalling. However, the overall analysis demonstrated that the relevant gene families such as interleukins, ICAMs, TNFSFs, CXCLs, NFκBs, and EPOR were not stimulated by co-incubation. Since we know that the experimental setup worked before and the immune system was stimulated in comparable experiments with primary brain cells by Torabi from BNITM, the absence of stimulation in this study cannot be adequately explained by an insufficient method. The absence of stimulation might be due to a protection of lung tissue by high CSA expression, but the clinical relevance of lung manifestations and as well former studies suggest the relevant presence of cytoadhesion and sequestration in vivo. Therefore, it would be advisable to repeat the experiments with cells from another donor to continue the in vitro work with primary lung cells and to confirm or contradict the present study results.

In the third and final part, FACS was performed with primary lung cells after stimulation with TNF in order to quantify the numbers of expressed receptors on the surface. ICAM-1 and CSA were highly expressed on the stimulated cells. This leads to the hypothesis that ICAM-1 is part of activation of lung tissue in infection while CSA might attempt the protection of the lung tissue from infection, as already mentioned above in the second part of the conclusion. This postulation should be challenged in repetitions of the experimental set up with cell lines from different donors.

5. Summary

Malaria is one of the most relevant infectious diseases around the world and *P. falciparum* is its most relevant causing parasite with high mortality rates especially in risk groups such as pregnant women and young children. *P. falciparum* has the skillset to evade the immune system and to cytoadhere and to sequester in endothelial cells of vital organs such as brain and lungs. In the lungs, the parasite can cause oedema and lead to ARDS with poor clinical outcome. The cytoadhesion relies on the interaction between a parasite ligand and its corresponding human endothelial receptor. The main parasite ligand that has been identified so far is *Pf*EMP1 which is encoded by the *var* genes, a family of about 60 genes. The parasite has been shown to perform an antigenic switch to a mutually expressed *var* gene to evade the human immune system and to adapt its binding mechanisms via *Pf*EMP1. There are multiple important corresponding human endothelial receptors yet described such as ICAM-1, CD36, and EPCR. The affected blood vessels and the lung tissue react to the infection with *P. falciparum* with a stimulation of the immune system, an unsettled homeostasis, and an endothelial dysfunction. This study aimed at helping in better understanding the influence of cytoadhesion of *P. falciparum* infected erythrocytes on human lung endothelial cells. In order to achieve this aim, three steps were performed: First, *P. falciparum* infected erythrocytes were enriched over HULEC-5a and HMVEC-L and their transcriptome was analysed for the antigenic *var* gene switch. The results were inconclusive for HULEC-5a. For HMVEC-L five *var* genes were significantly overexpressed after enrichment. Second, lung primary cells (HMVEC-L) were co-incubated with iRBCs for four or eight hours and their isolated RNA was sequenced for changes in gene expression levels. The results showed changed levels for numerous genes and indicated immune activation by elevated expression of EGR1 and HMOX1, but overall the relevant gene families of interleukins, ICAMs, TNFSFs, CXCLs, NFκBs, and EPOR were not significantly stimulated by co-incubation. Third, the lung primary cells were stimulated with TNF and the expressed receptors were examined via FACS. Here, the results showed high numbers of ICAM-1, which is a potential activated ligand in inflammation and high numbers of CSA, which is a potential protector of lung tissue. In conclusion, the experimental setup appeared successful while some of the results were inconclusive. The experiments should be repeated with cell lines from another donor to confirm or challenge the outlined results and to continue the important investigation in the pathomechanism of lung malaria.

6. Zusammenfassung

Malaria ist eine der relevantesten Infektionskrankheiten weltweit und *Plasmodium falciparum* ist ihr wichtigster Erreger. *P. falciparum* Malaria verursacht hohe Sterblichkeitsraten, besonders in Risikogruppen wie Schwangere und Kleinkinder. *P. falciparum* kann dem Immunsystem ausweichen und an Endothelzellen in wichtigen Organen binden und in die Zellen sequestrieren. In den Lungen kann der Parasit ein Lungenödem und ein akutes Atemnotsyndrom verursachen. Die Bindung von infizierten Erythrozyten an Endothelzellen wird durch einen Parasitenliganden und seinen humanen Endothelrezeptor vermittelt. Der wichtigste bisher erforschte parasitäre Ligand ist *Pf*EMPF1, welcher von der *var* Genfamilie kodiert wird. Es konnte gezeigt werden, dass *P. falciparum* in der Lage ist einen Antigenwechsel zu einem einzigen exprimierten *var* Gen durchzuführen, um auf diese Weise dem Immunsystem zu entkommen und die Bindung mittels *Pf*EMP1 anzupassen. Wichtige dazu passende humane Gewebsrezeptoren sind unter anderem ICAM-1, CD36 und EPCR. Die Blutgefäße und das Lungengewebe reagieren auf die Infektion mit einer Aktivierung des Immunsystems, einer gestörten Homöostase und einer endothelialen Dysfunktion. Die hier präsentierte Studie strebt ein besseres Verständnis über die Wirkung der Zytoadhäsion von mit *P. falciparum* infizierten Erythrozyten an humanen Lungenendothelzellen an. Hierfür wurden drei Versuchsschritte durchgeführt: Als Erstes wurden mit *P. falciparum* infizierte Erythrozyten über HULEC-5a und HMVEC-L angereichert und deren Transkriptom auf einen Antigenwechsel des *var* Gens hin untersucht. Für die HULEC-5a Zellreihe waren die Ergebnisse nicht aussagekräftig. Bei der HMVEC-L Zellreihe zeigten sich fünf *var* Gene in ihrer Expression signifikant erhöht. Als Zweites wurden HMVEC-L gemeinsam mit infizierten Erythrozyten für vier bzw. acht Stunden inkubiert und anschließend deren isolierte RNA sequenziert, um Veränderungen in den Genexpressionslevels zu untersuchen. Die Ergebnisse zeigten veränderte Expressionslevels für viele Gene und eine Immunsystemaktivierung deutete sich durch erhöhte Expressionen von EGR1 und HMOX1 an. Allerdings wurden relevante Genfamilien wie Interleukine, ICAMs, TNFSFs, CXCLs, NFκBs und EPOR durch die gemeinsame Inkubation nicht signifikant stimuliert. Als Drittes wurden HMVEC-L mit TNF stimuliert und die exprimierten Rezeptoren mittels FACS identifiziert. Hier zeigten die Ergebnisse einerseits eine hohe Anzahl von ICAM-1, was ein möglicher Ligand bei Entzündungsprozessen in den Lungen ist und andererseits auch eine hohe Anzahl von CSA, was möglicherweise ein protektiver Faktor für die Lunge ist. Abschließend betrachtet erscheint der Versuchsaufbau erfolgreich, wobei einige Ergebnisse nicht beweiskräftig waren. Die Experimente sollten mit Zellen von einem anderen Spender wiederholt werden, um so die hier präsentierten Ergebnisse zu überprüfen und die wichtige Erforschung des Pathomechanismus von Malaria in der Lunge fortzusetzen.

7. Abbreviations

ACT	Artemisine based combination therapy
ALI	acute lung injury
ALS2CR12	amyotrophix lateral scleoris 2 chromosome region, candidate 12
Ang2	Angiopoietin-2
ARDS	acute respiratory distress syndrome
BNITM	Bernhard Nocht Institute for Tropical Medicine
BTRC	beta-transducin repeat containing E3 ubiquitin protein ligase
CACNA2D1	Calcium voltage-gated channel auxiliary subunit alpha2delta 1
CARD-19	caspase recruitment domain family member 19
cDNA	complimentary DNA
CD4	cluster of differentiation 4
CHMI	Controlled Human Malaria Infection
CM	Cerebral Malaria
COL5A3	Collagen type V alpha 3 chain
COLIA2	Collagen type I alpha 2 chain
CSA	chondroitin sulfate A
CSP	Circumsporozoite protein
CXCL	chemokine ligand
DENND2C	DENN domain containing 2C
EGR1	Early growth response protein 1
EPCR	endothelial protein C receptor
EPOR	erythropoietin receptor
ER	endoplasmic reticulum
ERRFI1	ERBB receptor feedback inhibitor 1
FACS	fluorescence activated cell sorting
FBLN1	fibulin-1
FV	food vacuole
FST	Follistatin
GDF5	growth differentiation factor 5
HBA2	haemoglobin subunit alpha 2
HMOX1	Heme oxygenase 1 gene
HMVEC-L	Human Lung Microvascular Endothelial Cells

HS	human serum
HULEC-5a	Human Lung Microvascular Endothelium Cell line-5a
ICAM	intracellular adhesion molecule
IE	infected erythrocytes
IMC	inner membrane complex
IL	interleukine
iRBC	infected red blood cell
KAHRP	knob-associated histidine-rich protein
LTBP4	latent-transforming growth factor beta-binding protein 4
MA-ARDS	malaria-associated acute respiratory distress syndrome
MAOA	monoamine oxidase A
MFI	mean fluorescence intensity
MFS	malaria freezing solution
MMVC	Multi-Stage Malaria Vaccine Consortium
MMP2	matrix metalloproteinase-2
MMP14	matrix metalloproteinase-14
MSP	Merozoite surface protein
MTIX	Metaxin 1
MTS	malaria thawing solution
NFκB	nuclear factor kappa-light-chain-enhancer of activated B cells
NID1	Nidogen-1
PA	posteroanterior
PBS	phosphate buffered saline
PC	primary cells
PAMVAC	pregnancy associated malaria vaccine
PECAM1	platelet endothelial cell adhesion molecule 1
P. falciparum	*Plasmodium falciparum*
*Pf*EBA	*Plasmodium falciparum* erythrocyte binding antigen
*Pf*EMP1	*Plasmodium falciparum* erythrocyte membrane protein 1
*Pf*RH	*Plasmodium falciparum* reticulocyte binding protein homologue
*Pf*SPZ	*Plasmodium falciparum* sporozoites
PC	Primary cells
PCR	polymerase chain reaction
PLTP	phospholipid transfer protein

POSTN	Periostin
PVM	parasitophorous vacuole membrane
RBC	red blood cell
REL	REL proto oncogene
RESA	ring infected erythrocyte surface protein
RNA	ribonucleic acid
RPMI	roswell park memorial institute
RPS6KA2	ribosomal protein S6 kinase A2
RT qPCR	real-time quantitative polymerase chain reaction
SEAQUAMAT	South East Asian Quinine Artesunate Malaria Trial
SEPT5-GP1BB	septin5 – glycoprotein 1b
SM	Severe Malaria
SMN2	survival of motor neuron 2
STAT2	signal transducer and activator of transcription 2
TBV	transmission blocking vaccine
TM	thrombomodulin
TNFSF	tumor necrosis factor superfamily
TSP	thrombospondin
TVM	tubovesicular membrane
UM	Uncomplicated Malaria
VCAM1	vascular cell adhesion molecule 1
VSA	Variant surface antigen
VWF	Von Willebrand factor
WHO	World Health Organisation
x *g*	gravity
µg	microgram
µl	microliter
µm	micrometer

8. Lists of Tables and Figures

8.1. List of Figures

Figure 1.1 Map of malaria case incidence rate 5
Figure 1.2 The major clinical complications associated with adult severe malaria and paediatric severe malaria 7
Figure 1.3 P. falciparum life cycle 12
Figure 1.4 The P. falciparum blood stages 16
Figure 1.5 Stages I - V of sexual development in P. falciparum parasites 18
Figure 1.6 The pathogenesis of severe malaria 19
Figure 1.7 Gene families coding for molecules associated with the surface of iRBCs 22
Figure 2.1 Lung endothelial primary cells 39
Figure 3.1 Plan of performed experiments 50
Figure 3.2 Selection and Enrichment of IT4 infected erythrocytes over HULEC-5a lung endothelial cells 52
Figure 3.3 var genes expression levels of IT4 culture enriched over HULEC-5a and control IT4 starting culture 54
Figure 3.4 rifin genes expression levels of IT4 culture enriched over HULEC-5a and control IT4 starting culture 56
Figure 3.5 stevor genes expression levels of IT4 culture enriched over HULEC-5a and control IT4 starting culture 57
Figure 3.6 Selection and Enrichment of IT4 infected erythrocytes over HMVEC-L lung endothelial primary cells. 59
Figure 3.7 4 hours co-incubation: up regulated genes 61
Figure 3.8 4 hours co-incubation: down regulated genes 62
Figure 3.9 4 hours co-incubation: analysis of up regulated genes – IL signalling 64
Figure 3.10 4 hours co-incubation: analysis of down regulated genes –Extracellular matrix . 65
Figure 3.11 normalized gene expression of up regulated genes after 8 hours co-incubation (1/3) 67
Figure 3.12 normalized gene expression of up regulated genes after 8 hours co-incubation (2/3) 68
Figure 3.13 normalized gene expression of up regulated genes after 8 hours co-incubation (3/3) 69
Figure 3.14 normalized gene expression of down regulated genes after 8 hours co-incubation (1/3) 70
Figure 3.15 normalized gene expression of down regulated genes after 8 hours co-incubation (2/3) 71
Figure 3.16 normalized gene expression of down regulated genes after 8 hours co-incubation (3/3) 72
Figure 3.17 8 hour co-incubation: analysis of up regulated genes – IL signalling 73
Figure 3.18 8 hours co-incubation: analysis of down regulated genes – cell cycle 75
Figure 3.19 Comparison for genes that are significantly differently expressed in 4 hours and 8 hours co-incubation 78
Figure 3.20 Compared normalized expression levels of interleukins after four and after eight hours co-incubations 80
Figure 3.21 Compared normalized expression levels of ICAMs after four and after eight hours co-incubations 81
Figure 3.22 Compared normalized expression levels of TNFSFs after four and after eight hours co-incubations 82

Figure 3.23 Compared normalized expression levels of CXCLs after four and after eight hours co-incubations 83
Figure 3.24 Compared normalized expression levels of NFκBs and RELs after four and after eight hours co-incubations 84
Figure 3.25 Compared normalized expression levels of EPOR after four and after eight hours co-incubations 85
Figure 3.26 FACS of HMVEC-L for CD36, ICAM-1 and CSA after TNF stimulation and not TNF stimulated control 86

8.2. List of Tables

Table 1.1 IT4 PfEMP1 variants 24
Table 1.2 Diagnosing criteria of ALI and ARDS 26
Table 2.1 Technical devices 29
Table 2.2 Software 30
Table 2.3 Labware and disposables 30
Table 2.4 Kits 31
Table 2.5 Chemical and biological reagents 31
Table 2.6 RPMI-HS 32
Table 2.7 5% D-Sorbitol 33
Table 2.8 Binding medium 33
Table 2.9 Malaria freezing solution 33
Table 2.10 Malaria thawing solution 34
Table 2.11 10% Giemsa stain 34
Table 2.12 HULEC-5a cell culture 34
Table 2.13 Lung primary cells culture medium 35
Table 2.14 Lung primary cells cryo solution 35
Table 2.15 Oligonucleotides used for RT qPCR 48
Table 2.16 Program qPCR LightCycler 480 49
Table 3.1 Significantly expressed var genes after five enrichment rounds of IT4 culture over HULEC-5a 53
Table 3.2 Significantly expressed rifin genes after five enrichment rounds of IT4 culture over HULEC-5a 55
Table 3.3 Significantly expressed stevor genes after five enrichment rounds of IT4 culture over HULEC-5[a] 57
Table 3.4 Up regulated genes in 4 hours co-incubation 61
Table 3.5 Down regulated genes in 4 hours co-incubation 63
Table 3.6 Upregulated genes in 4 hours co-incubation involved in IL signalling 64
Table 3.7 Downregulated genes in 4 hours co-incubation involved in extracellular matrix 65
Table 3.8 Up regulated genes in 8 hours co-incubation of iRBCs and PC lungs 74
Table 3.9 Down regulated genes in 8 hours co-incubation of iRBCs and PC lungs 76
Table 3.10 Comparison for genes that are significantly differently expressed in 4 hours and 8 hours co-incubation 78

9. References

Abu Bakar, N., Klonis, N., Hanssen, E., Chan, C., & Tilley, L. (2010). Digestive-vacuole genesis and endocytic processes in the early intraerythrocytic stages of Plasmodium falciparum. *Journal of Cell Science*, *123*(Pt 3), 441–450. https://doi.org/10.1242/jcs.061499

Adam, S., Göhring, W., Wiedemann, H., Chu, M.-L., Timpl, R., & Kostka, G. (1997). Binding of fibulin-1 to nidogen depends on its C-terminal globular domain and a specific array of calcium-binding epidermal growth factor-like (EG) modules 11Edited by I. B. Holland. *Journal of Molecular Biology*, *272*(2), 226–236. https://doi.org/10.1006/jmbi.1997.1244

Aggarwal, B. B., Gupta, S. C., & Kim, J. H. (2012). Historical perspectives on tumor necrosis factor and its superfamily: 25 years later, a golden journey. *Blood*, *119*(3), 651–665. https://doi.org/10.1182/blood-2011-04-325225

Ahiboh, H., Oga, A. S., Yapi, H. F., Kouakou, G., Boua, K. D., Edjeme, N., & Monnet, D. (2008). [Anaemia, iron index status and acute phase proteins in malaria (Abidjan, Côte d'Ivoire)]. *Bulletin De La Societe De Pathologie Exotique (1990)*, *101*(1), 25–28.

Aikawa, M., Miller, L. H., Rabbege, J. R., & Epstein, N. (1981). Freeze-fracture study on the erythrocyte membrane during malarial parasite invasion. *The Journal of Cell Biology*, *91*(1), 55–62. https://doi.org/10.1083/jcb.91.1.55

Alister, G. C., Mohd Fadzli Mustaffa, K., & Pradeep, R. P. (2012). Cytoadherence and Severe Malaria. *The Malaysian Journal of Medical Sciences : MJMS*, *19*(2), 5–18.

Angchaisuksiri, P. (2014). Coagulopathy in malaria. *Thrombosis Research*, *133*(1), 5–9. https://doi.org/10.1016/j.thromres.2013.09.030

Anstey, N. M., Jacups, S. P., Cain, T., Pearson, T., Ziesing, P. J., Fisher, D. A., Currie, B. J., Marks, P. J., & Maguire, G. P. (2002). Pulmonary manifestations of uncomplicated falciparum and vivax malaria: Cough, small airways obstruction, impaired gas transfer, and increased pulmonary phagocytic activity. *The Journal of Infectious Diseases*, *185*(9), 1326–1334. https://doi.org/10.1086/339885

Arama, C., & Troye-Blomberg, M. (2014). The path of malaria vaccine development: Challenges and perspectives. *Journal of Internal Medicine*, *275*(5), 456–466. https://doi.org/10.1111/joim.12223

Aursudkij, B., Wilairatana, P., Vannaphan, S., Walsh, D. S., Gordeux, V. R., & Looareesuwan, S. (1998). Pulmonary edema in cerebral malaria patients in Thailand. *The Southeast Asian Journal of Tropical Medicine and Public Health*, *29*(3), 541–545.

Avril, M., Tripathi, A. K., Brazier, A. J., Andisi, C., Janes, J. H., Soma, V. L., Sullivan, D. J., Bull, P. C., Stins, M. F., & Smith, J. D. (2012). A restricted subset of var genes mediates adherence of Plasmodium falciparum-infected erythrocytes to brain endothelial cells. *Proceedings of the National Academy of Sciences of the United States of America*, *109*(26), E1782-1790. https://doi.org/10.1073/pnas.1120534109

Ayimba, E., Hegewald, J., Ségbéna, A. Y., Gantin, R. G., Lechner, C. J., Agosssou, A., Banla, M., & Soboslay, P. T. (2011). Proinflammatory and regulatory cytokines and chemokines in infants with uncomplicated and severe Plasmodium falciparum malaria.

Clinical and Experimental Immunology, *166*(2), 218–226. https://doi.org/10.1111/j.1365-2249.2011.04474.x

Banerji, R., & Saroj, S. D. (2021). Early growth response 1 (EGR1) activation in initial stages of host-pathogen interactions. *Molecular Biology Reports*, *48*(3), 2935–2943. https://doi.org/10.1007/s11033-021-06305-0

Bannister, L. H., Hopkins, J. M., Fowler, R. E., Krishna, S., & Mitchell, G. H. (2000). A brief illustrated guide to the ultrastructure of Plasmodium falciparum asexual blood stages. *Parasitology Today (Personal Ed.)*, *16*(10), 427–433. https://doi.org/10.1016/s0169-4758(00)01755-5

Bartoloni, A., & Zammarchi, L. (2012). Clinical Aspects of Uncomplicated and Severe Malaria. *Mediterranean Journal of Hematology and Infectious Diseases*, *4*(1). https://doi.org/10.4084/MJHID.2012.026

Bąska, P., & Norbury, L. J. (2022). The Role of Nuclear Factor Kappa B (NF-κB) in the Immune Response against Parasites. *Pathogens*, *11*(3), 310. https://doi.org/10.3390/pathogens11030310

Beeson, J. G., Drew, D. R., Boyle, M. J., Feng, G., Fowkes, F. J. I., & Richards, J. S. (2016). Merozoite surface proteins in red blood cell invasion, immunity and vaccines against malaria. *FEMS Microbiology Reviews*, *40*(3), 343–372. https://doi.org/10.1093/femsre/fuw001

Boes, A., Spiegel, H., Voepel, N., Edgue, G., Beiss, V., Kapelski, S., Fendel, R., Scheuermayer, M., Pradel, G., Bolscher, J. M., Behet, M. C., Dechering, K. J., Hermsen, C. C., Sauerwein, R. W., Schillberg, S., Reimann, A., & Fischer, R. (2015). Analysis of a Multi-component Multi-stage Malaria Vaccine Candidate—Tackling the Cocktail Challenge. *PloS One*, *10*(7), e0131456. https://doi.org/10.1371/journal.pone.0131456

Buffet, P. A., Safeukui, I., Deplaine, G., Brousse, V., Prendki, V., Thellier, M., Turner, G. D., & Mercereau-Puijalon, O. (2011). The pathogenesis of Plasmodium falciparum malaria in humans: Insights from splenic physiology. *Blood*, *117*(2), 381–392. https://doi.org/10.1182/blood-2010-04-202911

Carter, R., Mendis, K. N., Miller, L. H., Molineaux, L., & Saul, A. (2000). Malaria transmission-blocking vaccines—How can their development be supported? *Nature Medicine*, *6*(3), 241–244. https://doi.org/10.1038/73062

Castelli, F., Tomasoni, L. R., & Matteelli, A. (2012). Advances in the treatment of malaria. *Mediterranean Journal of Hematology and Infectious Diseases*, *4*(1), e2012064. https://doi.org/10.4084/MJHID.2012.064

Chakravorty, S. J., & Craig, A. (2005). The role of ICAM-1 in Plasmodium falciparum cytoadherence. *European Journal of Cell Biology*, *84*(1), 15–27. https://doi.org/10.1016/j.ejcb.2004.09.002

Charoenpan, P., Indraprasit, S., Kiatboonsri, S., Suvachittanont, O., & Tanomsup, S. (1990). Pulmonary edema in severe falciparum malaria. Hemodynamic study and clinicophysiologic correlation. *Chest*, *97*(5), 1190–1197. https://doi.org/10.1378/chest.97.5.1190

Christensen, D. (2016). Vaccine adjuvants: Why and how. *Human Vaccines & Immunotherapeutics*, *12*(10), 2709–2711. https://doi.org/10.1080/21645515.2016.1219003

Claessens, A., Hamilton, W. L., Kekre, M., Otto, T. D., Faizullabhoy, A., Rayner, J. C., & Kwiatkowski, D. (2014). Generation of Antigenic Diversity in Plasmodium falciparum by Structured Rearrangement of Var Genes During Mitosis. *PLOS Genetics*, *10*(12), e1004812. https://doi.org/10.1371/journal.pgen.1004812

Coatney, R. G., William E Collins, Mc Wilson Warren, & Peter G Contacos. (1971). *The primate malarias*.

Cowman, A. F., Berry, D., & Baum, J. (2012). The cellular and molecular basis for malaria parasite invasion of the human red blood cell. *The Journal of Cell Biology*, *198*(6), 961–971. https://doi.org/10.1083/jcb.201206112

Cowman, A. F., & Crabb, B. S. (2006). Invasion of red blood cells by malaria parasites. *Cell*, *124*(4), 755–766. https://doi.org/10.1016/j.cell.2006.02.006

Cox, F. E. (2010). History of the discovery of the malaria parasites and their vectors. *Parasites & Vectors*, *3*(1), 5. https://doi.org/10.1186/1756-3305-3-5

Cruz, L. N., Wu, Y., Ulrich, H., Craig, A. G., & Garcia, C. R. S. (2016). Tumor necrosis factor reduces Plasmodium falciparum growth and activates calcium signaling in human malaria parasites. *Biochimica et Biophysica Acta*, *1860*(7), 1489–1497. https://doi.org/10.1016/j.bbagen.2016.04.003

Cunnington, A. J., Riley, E. M., & Walther, M. (2013). Stuck in a rut? Reconsidering the role of parasite sequestration in severe malaria syndromes. *Trends in Parasitology*, *29*(12). https://doi.org/10.1016/j.pt.2013.10.004

Day, K. P., Hayward, R. E., Smith, D., & Culvenor, J. G. (1998). CD36-dependent adhesion and knob expression of the transmission stages of Plasmodium falciparum is stage specific. *Molecular and Biochemical Parasitology*, *93*(2), 167–177. https://doi.org/10.1016/s0166-6851(98)00040-1

Day, N. P., Hien, T. T., Schollaardt, T., Loc, P. P., Chuong, L. V., Chau, T. T., Mai, N. T., Phu, N. H., Sinh, D. X., White, N. J., & Ho, M. (1999). The prognostic and pathophysiologic role of pro- and antiinflammatory cytokines in severe malaria. *The Journal of Infectious Diseases*, *180*(4), 1288–1297. https://doi.org/10.1086/315016

de Klerk, N., Saroj, S. D., Wassing, G. M., Maudsdotter, L., & Jonsson, A.-B. (2017). The Host Cell Transcription Factor EGR1 Is Induced by Bacteria through the EGFR-ERK1/2 Pathway. *Frontiers in Cellular and Infection Microbiology*, *7*, 16. https://doi.org/10.3389/fcimb.2017.00016

Dondorp, A. M., Fanello, C. I., Hendriksen, I. C., Gomes, E., Seni, A., Chhaganlal, K. D., Bojang, K., Olaosebikan, R., Anunobi, N., Maitland, K., Kivaya, E., Agbenyega, T., Nguah, S. B., Evans, J., Gesase, S., Kahabuka, C., Mtove, G., Nadjm, B., Deen, J., … White, N. J. (2010). Artesunate versus quinine in the treatment of severe falciparum malaria in African children (AQUAMAT): An open-label, randomised trial. *The Lancet*, *376*(9753), 1647–1657. https://doi.org/10.1016/S0140-6736(10)61924-1

Dondorp, A. M., Pongponratn, E., & White, N. J. (2004). Reduced microcirculatory flow in severe falciparum malaria: Pathophysiology and electron-microscopic pathology. *Acta Tropica*, *89*(3), 309–317. https://doi.org/10.1016/j.actatropica.2003.10.004

Dzikowski, R., & Deitsch, K. (2006). Antigenic variation by protozoan parasites: Insights from Babesia bovis. *Molecular Microbiology*, *59*(2), 364–366. https://doi.org/10.1111/j.1365-2958.2005.05007.x

Eksi, S., Morahan, B. J., Haile, Y., Furuya, T., Jiang, H., Ali, O., Xu, H., Kiattibutr, K., Suri, A., Czesny, B., Adeyemo, A., Myers, T. G., Sattabongkot, J., Su, X., & Williamson, K. C. (2012). Plasmodium falciparum gametocyte development 1 (Pfgdv1) and gametocytogenesis early gene identification and commitment to sexual development. *PLoS Pathogens*, *8*(10), e1002964. https://doi.org/10.1371/journal.ppat.1002964

El-Moamly, A. A., & El-Sweify, M. A. (2023). Malaria vaccines: The 60-year journey of hope and final success—lessons learned and future prospects. *Tropical Medicine and Health*, *51*, 29. https://doi.org/10.1186/s41182-023-00516-w

Epstein, J. E., Paolino, K. M., Richie, T. L., Sedegah, M., Singer, A., Ruben, A. J., Chakravarty, S., Stafford, A., Ruck, R. C., Eappen, A. G., Li, T., Billingsley, P. F., Manoj, A., Silva, J. C., Moser, K., Nielsen, R., Tosh, D., Cicatelli, S., Ganeshan, H., … Hoffman, S. L. (2017). Protection against Plasmodium falciparum malaria by PfSPZ Vaccine. *JCI Insight*, *2*(1), e89154. https://doi.org/10.1172/jci.insight.89154

Fanelli, V., & Ranieri, V. M. (2015). Mechanisms and Clinical Consequences of Acute Lung Injury. *Annals of the American Thoracic Society*, *12*(Supplement 1), S3–S8. https://doi.org/10.1513/AnnalsATS.201407-340MG

Farrar, J., Hotez, P. J., Junghanss, T., Kang, G., Lalloo, D., & White, N. J. (2013). *Manson's Tropical Diseases E-Book*. Elsevier Health Sciences.

Fonager, J., Pasini, E. M., Braks, J. A. M., Klop, O., Ramesar, J., Remarque, E. J., Vroegrijk, I. O. C. M., van Duinen, S. G., Thomas, A. W., Khan, S. M., Mann, M., Kocken, C. H. M., Janse, C. J., & Franke-Fayard, B. M. D. (2012). Reduced CD36-dependent tissue sequestration of Plasmodium-infected erythrocytes is detrimental to malaria parasite growth in vivo. *The Journal of Experimental Medicine*, *209*(1), 93–107. https://doi.org/10.1084/jem.20110762

Fried, M., & Duffy, P. E. (2015). Designing a VAR2CSA-based vaccine to prevent placental malaria. *Vaccine*, *33*(52), 7483–7488. https://doi.org/10.1016/j.vaccine.2015.10.011

Fried, M., & Duffy, P. E. (2017). Malaria during Pregnancy. *Cold Spring Harbor Perspectives in Medicine*, *7*(6). https://doi.org/10.1101/cshperspect.a025551

Genton, B. (2023). R21/Matrix-M^{TM} malaria vaccine: A new tool to achieve WHO's goal to eliminate malaria in 30 countries by 2030? *Journal of Travel Medicine*, *30*(8), taad140. https://doi.org/10.1093/jtm/taad140

Grüring, C., Heiber, A., Kruse, F., Ungefehr, J., Gilberger, T.-W., & Spielmann, T. (2011). Development and host cell modifications of Plasmodium falciparum blood stages in four dimensions. *Nature Communications*, *2*, 165. https://doi.org/10.1038/ncomms1169

Guizetti, J., & Scherf, A. (2013). Silence, activate, poise and switch! Mechanisms of antigenic variation in Plasmodium falciparum. *Cellular Microbiology*, *15*(5), 718–726. https://doi.org/10.1111/cmi.12115

Guttery, D. S., Holder, A. A., & Tewari, R. (2012). Sexual Development in Plasmodium: Lessons from Functional Analyses. *PLoS Pathogens*, *8*(1). https://doi.org/10.1371/journal.ppat.1002404

Hanson, J., Lam, S. W. K., Mahanta, K. C., Pattnaik, R., Alam, S., Mohanty, S., Hasan, M. U., Hossain, A., Charunwatthana, P., Chotivanich, K., Maude, R. J., Kingston, H., Day, N. P., Mishra, S., White, N. J., & Dondorp, A. M. (2012). Relative contributions of macrovascular and microvascular dysfunction to disease severity in falciparum

malaria. *The Journal of Infectious Diseases*, *206*(4), 571–579. https://doi.org/10.1093/infdis/jis400

Hanssen, E., Goldie, K. N., & Tilley, L. (2010). Ultrastructure of the asexual blood stages of Plasmodium falciparum. *Methods in Cell Biology*, *96*, 93–116. https://doi.org/10.1016/S0091-679X(10)96005-6

Hatz, C. F. R. (2004). *Prophylaxe und Therapie der Malaria in der Praxis*. https://link.springer.com/article/10.1007/s00108-004-1198-3

Hawking, F., Wilson, M. E., & Gammage, K. (1971). Evidence for cyclic development and short-lived maturity in the gametocytes of Plasmodium falciparum. *Transactions of the Royal Society of Tropical Medicine and Hygiene*, *65*(5), 549–559. https://doi.org/10.1016/0035-9203(71)90036-8

Hayden, M. S., & Ghosh, S. (2011). NF-κB in immunobiology. *Cell Research*, *21*(2), 223–244. https://doi.org/10.1038/cr.2011.13

Hayflick, J. S., Kilgannon, P., & Gallatin, W. M. (1998). The intercellular adhesion molecule (ICAM) family of proteins. *Immunologic Research*, *17*(3), 313–327. https://doi.org/10.1007/BF02786454

Hviid, L. (2007). Development of vaccines against Plasmodium falciparum malaria: Taking lessons from naturally acquired protective immunity. *Microbes and Infection*, *9*(6), 772–776. https://doi.org/10.1016/j.micinf.2007.02.008

Idro, R., Jenkins, N. E., & Newton, C. R. J. C. (2005). Pathogenesis, clinical features, and neurological outcome of cerebral malaria. *The Lancet. Neurology*, *4*(12), 827–840. https://doi.org/10.1016/S1474-4422(05)70247-7

Ishizuka, A. S., Lyke, K. E., DeZure, A., Berry, A. A., Richie, T. L., Mendoza, F. H., Enama, M. E., Gordon, I. J., Chang, L.-J., Sarwar, U. N., Zephir, K. L., Holman, L. A., James, E. R., Billingsley, P. F., Gunasekera, A., Chakravarty, S., Manoj, A., Li, M., Ruben, A. J., … Seder, R. A. (2016). Protection against malaria at 1 year and immune correlates following PfSPZ vaccination. *Nature Medicine*, *22*(6), 614–623. https://doi.org/10.1038/nm.4110

Jäschke, A., Coulibaly, B., Remarque, E. J., Bujard, H., & Epp, C. (2017). Merozoite Surface Protein 1 from Plasmodium falciparum Is a Major Target of Opsonizing Antibodies in Individuals with Acquired Immunity against Malaria. *Clinical and Vaccine Immunology: CVI*, *24*(11). https://doi.org/10.1128/CVI.00155-17

Josling, G. A., & Llinás, M. (2015). Sexual development in Plasmodium parasites: Knowing when it's time to commit. *Nature Reviews. Microbiology*, *13*(9), 573–587. https://doi.org/10.1038/nrmicro3519

Justiz Vaillant, A. A., & Qurie, A. (2022). Interleukin. In *StatPearls*. StatPearls Publishing. http://www.ncbi.nlm.nih.gov/books/NBK499840/

Kim, H., Higgins, S., Liles, W. C., & Kain, K. C. (2011). Endothelial activation and dysregulation in malaria: A potential target for novel therapeutics. *Current Opinion in Hematology*, *18*(3), 177–185. https://doi.org/10.1097/MOH.0b013e328345a4cf

L H Bannister, J M Hopkins, R E Fowler, S Krishna, & G H Mitchell. (2000). *A brief illustrated guide to the ultrastructure of Plasmodium falciparum asexual blood stages*.

Labbé, A.-C., Loutfy, M. R., & Kain, K. C. (2001). Recent advances in the prophylaxis and treatment of malaria. *Current Infectious Disease Reports*, *3*(1), 68–76. https://doi.org/10.1007/s11908-001-0061-0

Lauer, S. A., Rathod, P. K., Ghori, N., & Haldar, K. (1997). A membrane network for nutrient import in red cells infected with the malaria parasite. *Science (New York, N.Y.)*, *276*(5315), 1122–1125. https://doi.org/10.1126/science.276.5315.1122

Lennartz, F., Smith, C., Craig, A. G., & Higgins, M. K. (2019). Structural insights into diverse modes of ICAM-1 binding by Plasmodium falciparum-infected erythrocytes. *Proceedings of the National Academy of Sciences of the United States of America*, *116*(40), 20124–20134. https://doi.org/10.1073/pnas.1911900116

Lewis, C. A., & Martin, G. S. (2004). Understanding and managing fluid balance in patients with acute lung injury. *Current Opinion in Critical Care*, *10*(1), 13–17. https://doi.org/10.1097/00075198-200402000-00003

Liu, Y., Pop, R., Sadegh, C., Brugnara, C., Haase, V. H., & Socolovsky, M. (2006). Suppression of Fas-FasL coexpression by erythropoietin mediates erythroblast expansion during the erythropoietic stress response in vivo. *Blood*, *108*(1), 123–133. https://doi.org/10.1182/blood-2005-11-4458

Looareesuwan, S., White, N. J., Karbwang, J., Turner, R. C., Phillips, R. E., Kietinun, S., Rackow, C., & Warrell, D. A. (1985). QUININE AND SEVERE FALCIPARUM MALARIA IN LATE PREGNANCY. *The Lancet*, *326*(8445), 4–8. https://doi.org/10.1016/S0140-6736(85)90056-X

Lyke, K. E., Burges, R., Cissoko, Y., Sangare, L., Dao, M., Diarra, I., Kone, A., Harley, R., Plowe, C. V., Doumbo, O. K., & Sztein, M. B. (2004). Serum Levels of the Proinflammatory Cytokines Interleukin-1 Beta (IL-1β), IL-6, IL-8, IL-10, Tumor Necrosis Factor Alpha, and IL-12(p70) in Malian Children with Severe Plasmodium falciparum Malaria and Matched Uncomplicated Malaria or Healthy Controls. *Infection and Immunity*, *72*(10), 5630–5637. https://doi.org/10.1128/IAI.72.10.5630-5637.2004

Maguire, G. P., Handojo, T., Pain, M. C. F., Kenangalem, E., Price, R. N., Tjitra, E., & Anstey, N. M. (2005). Lung Injury in Uncomplicated and Severe Falciparum Malaria: A Longitudinal Study in Papua, Indonesia. *The Journal of Infectious Diseases*, *192*(11), 1966–1974. https://doi.org/10.1086/497697

Maknitikul, S., Luplertlop, N., Grau, G. E. R., & Ampawong, S. (2017). Dysregulation of pulmonary endothelial protein C receptor and thrombomodulin in severe falciparum malaria-associated ARDS relevant to hemozoin. *PLOS ONE*, *12*(7), e0181674. https://doi.org/10.1371/journal.pone.0181674

Marsh, K. (1992). Malaria-a neglected disease? *Parasitology*, *104*(S1), S53–S69. https://doi.org/10.1017/S0031182000075247

Matuschewski. (2006). *Getting infectious: Formation and maturation of Plasmodium sporozoites in the Anopheles vector*.

McCormick, C. J., Craig, A., Roberts, D., Newbold, C. I., & Berendt, A. R. (1997). Intercellular adhesion molecule-1 and CD36 synergize to mediate adherence of Plasmodium falciparum-infected erythrocytes to cultured human microvascular endothelial cells. *The Journal of Clinical Investigation*, *100*(10), 2521–2529. https://doi.org/10.1172/JCI119794

Metzger, W. G., Sulyok, Z., Theurer, A., & Köhler, C. (2020). Entwicklung von Impfstoffen gegen Malaria – aktueller Stand. *Bundesgesundheitsblatt, Gesundheitsforschung, Gesundheitsschutz*, *63*(1), 45–55. https://doi.org/10.1007/s00103-019-03070-1

Mohanty, S., Mishra, S. K., Pati, S. S., Pattnaik, J., & Das, B. S. (2003). Complications and mortality patterns due to Plasmodium falciparum malaria in hospitalized adults and children, Rourkela, Orissa, India. *Transactions of the Royal Society of Tropical Medicine and Hygiene*, *97*(1), 69–70. https://doi.org/10.1016/s0035-9203(03)90027-7

Mordmüller, B., Sulyok, M., Egger-Adam, D., Resende, M., de Jongh, W. A., Jensen, M. H., Smedegaard, H. H., Ditlev, S. B., Soegaard, M., Poulsen, L., Dyring, C., Calle, C. L., Knoblich, A., Ibáñez, J., Esen, M., Deloron, P., Ndam, N., Issifou, S., Houard, S., … Nielsen, M. A. (2019). First-in-human, Randomized, Double-blind Clinical Trial of Differentially Adjuvanted PAMVAC, A Vaccine Candidate to Prevent Pregnancy-associated Malaria. *Clinical Infectious Diseases: An Official Publication of the Infectious Diseases Society of America*, *69*(9), 1509–1516. https://doi.org/10.1093/cid/ciy1140

Mota, M. M., Pradel, G., Vanderberg, J. P., Hafalla, J. C., Frevert, U., Nussenzweig, R. S., Nussenzweig, V., & Rodríguez, A. (2001). Migration of Plasmodium sporozoites through cells before infection. *Science (New York, N.Y.)*, *291*(5501), 141–144. https://doi.org/10.1126/science.291.5501.141

Moxon, C. A., Wassmer, S. C., Milner, D. A., Chisala, N. V., Taylor, T. E., Seydel, K. B., Molyneux, M. E., Faragher, B., Esmon, C. T., Downey, C., Toh, C.-H., Craig, A. G., & Heyderman, R. S. (2013). Loss of endothelial protein C receptors links coagulation and inflammation to parasite sequestration in cerebral malaria in African children. *Blood*, *122*(5), 842–851. https://doi.org/10.1182/blood-2013-03-490219

Mueller, A.-K., Labaied, M., Kappe, S. H. I., & Matuschewski, K. (2005). Genetically modified Plasmodium parasites as a protective experimental malaria vaccine. *Nature*, *433*(7022), 164–167. https://doi.org/10.1038/nature03188

Müller, O., Tozan, Y., & Becher, H. (2015). RTS,S/AS01 malaria vaccine and child mortality. *Lancet (London, England)*, *386*(10005), 1736. https://doi.org/10.1016/S0140-6736(15)00694-7

Naing, C., Wong, S. T., & Aung, H. H. (2021). Toll-like receptor 9 and 4 gene polymorphisms in susceptibility and severity of malaria: A meta-analysis of genetic association studies. *Malaria Journal*, *20*(1), 302. https://doi.org/10.1186/s12936-021-03836-6

Nairz, M., Schroll, A., Moschen, A. R., Sonnweber, T., Theurl, M., Theurl, I., Taub, N., Jamnig, C., Neurauter, D., Huber, L. A., Tilg, H., Moser, P. L., & Weiss, G. (2011). Erythropoietin Contrastingly Affects Bacterial Infection and Experimental Colitis by Inhibiting Nuclear Factor-κB-Inducible Immune Pathways. *Immunity*, *34*(1), 61–74. https://doi.org/10.1016/j.immuni.2011.01.002

Nairz, M., Sonnweber, T., Schroll, A., Theurl, I., & Weiss, G. (2012). The pleiotropic effects of erythropoietin in infection and inflammation. *Microbes and Infection / Institut Pasteur*, *14*(3), 238–246. https://doi.org/10.1016/j.micinf.2011.10.005

Nayak, K. C., Mohini, null, Kumar, S., Tanwar, R. S., Kulkarni, V., Gupta, A., Sharma, P., Sirohi, P., & Ratan, P. (2011). A study on pulmonary manifestations in patients with malaria from northwestern India (Bikaner). *Journal of Vector Borne Diseases*, *48*(4), 219–223.

Ngwa, C. J., Scheuermayer, M., Mair, G. R., Kern, S., Brügl, T., Wirth, C. C., Aminake, M. N., Wiesner, J., Fischer, R., Vilcinskas, A., & Pradel, G. (2013). Changes in the

transcriptome of the malaria parasite Plasmodium falciparum during the initial phase of transmission from the human to the mosquito. *BMC Genomics*, *14*, 256. https://doi.org/10.1186/1471-2164-14-256

Niang, M., Bei, A. K., Madnani, K. G., Pelly, S., Dankwa, S., Kanjee, U., Gunalan, K., Amaladoss, A., Yeo, K. P., Bob, N. S., Malleret, B., Duraisingh, M., & Preiser, P. R. (2014). The variant STEVOR protein of Plasmodium falciparum is a red cell binding protein important for merozoite invasion and rosetting. *Cell Host & Microbe*, *16*(1), 81–93. https://doi.org/10.1016/j.chom.2014.06.004

Oh, S. S., Voigt, S., Fisher, D., Yi, S. J., LeRoy, P. J., Derick, L. H., Liu, S., & Chishti, A. H. (2000). Plasmodium falciparum erythrocyte membrane protein 1 is anchored to the actin-spectrin junction and knob-associated histidine-rich protein in the erythrocyte skeleton. *Molecular and Biochemical Parasitology*, *108*(2), 237–247. https://doi.org/10.1016/s0166-6851(00)00227-9

Olotu, A., Urbano, V., Hamad, A., Eka, M., Chemba, M., Nyakarungu, E., Raso, J., Eburi, E., Mandumbi, D. O., Hergott, D., Maas, C. D., Ayekaba, M. O., Milang, D. N., Rivas, M. R., Schindler, T., Embon, O. M., Ruben, A. J., Saverino, E., Abebe, Y., … Hoffman, S. L. (2018). Advancing Global Health through Development and Clinical Trials Partnerships: A Randomized, Placebo-Controlled, Double-Blind Assessment of Safety, Tolerability, and Immunogenicity of PfSPZ Vaccine for Malaria in Healthy Equatoguinean Men. *The American Journal of Tropical Medicine and Hygiene*, *98*(1), 308–318. https://doi.org/10.4269/ajtmh.17-0449

Oyegue-Liabagui, S. L., Bouopda-Tuedom, A. G., Kouna, L. C., Maghendji-Nzondo, S., Nzoughe, H., Tchitoula-Makaya, N., Pegha-Moukandja, I., & Lekana-Douki, J.-B. (2017). Pro- and anti-inflammatory cytokines in children with malaria in Franceville, Gabon. *American Journal of Clinical and Experimental Immunology*, *6*(2), 9–20.

Payne, R. O., Silk, S. E., Elias, S. C., Miura, K., Diouf, A., Galaway, F., de Graaf, H., Brendish, N. J., Poulton, I. D., Griffiths, O. J., Edwards, N. J., Jin, J., Labbé, G. M., Alanine, D. G., Siani, L., Di Marco, S., Roberts, R., Green, N., Berrie, E., … Draper, S. J. (2017). Human vaccination against RH5 induces neutralizing antimalarial antibodies that inhibit RH5 invasion complex interactions. *JCI Insight*, *2*(21). https://doi.org/10.1172/jci.insight.96381

Petter, M., & Duffy, M. F. (2015). Antigenic Variation in Plasmodium falciparum. *Results and Problems in Cell Differentiation*, *57*, 47–90. https://doi.org/10.1007/978-3-319-20819-0_3

Pham, T.-T., Punsawad, C., Glaharn, S., De Meyer, S. F., Viriyavejakul, P., & Van den Steen, P. E. (2019). Release of endothelial activation markers in lungs of patients with malaria-associated acute respiratory distress syndrome. *Malaria Journal*, *18*. https://doi.org/10.1186/s12936-019-3040-3

Portugal, S., Drakesmith, H., & Mota, M. M. (2011). Superinfection in malaria: Plasmodium shows its iron will. *EMBO Reports*, *12*(12), 1233–1242. https://doi.org/10.1038/embor.2011.213

Preiser, P., Kaviratne, M., Khan, S., Bannister, L., & Jarra, W. (2000). The apical organelles of malaria merozoites: Host cell selection, invasion, host immunity and immune evasion. *Microbes and Infection*, *2*(12), 1461–1477. https://doi.org/10.1016/s1286-4579(00)01301-0

Prudêncio, M., Rodriguez, A., & Mota, M. M. (2006). The silent path to thousands of merozoites: The Plasmodium liver stage. *Nature Reviews. Microbiology*, *4*(11), 849–856. https://doi.org/10.1038/nrmicro1529

Purcell, L. A., Wong, K. A., Yanow, S. K., Lee, M., Spithill, T. W., & Rodriguez, A. (2008). Chemically attenuated Plasmodium sporozoites induce specific immune responses, sterile immunity and cross-protection against heterologous challenge. *Vaccine*, *26*(38), 4880–4884. https://doi.org/10.1016/j.vaccine.2008.07.017

Randall, L. M., & Engwerda, C. R. (2010). TNF family members and malaria: Old observations, new insights and future directions. *Experimental Parasitology*, *126*(3), 326–331. https://doi.org/10.1016/j.exppara.2010.04.016

Rask, T. S., Hansen, D. A., Theander, T. G., Pedersen, A. G., & Lavstsen, T. (2010). Plasmodium falciparum Erythrocyte Membrane Protein 1 Diversity in Seven Genomes – Divide and Conquer. *PLOS Computational Biology*, *6*(9), e1000933. https://doi.org/10.1371/journal.pcbi.1000933

Reeder, J. C., Cowman, A. F., Davern, K. M., Beeson, J. G., Thompson, J. K., Rogerson, S. J., & Brown, G. V. (1999). The adhesion of Plasmodium falciparum-infected erythrocytes to chondroitin sulfate A is mediated by P. falciparum erythrocyte membrane protein 1. *Proceedings of the National Academy of Sciences of the United States of America*, *96*(9), 5198–5202.

Reinsch, F. (2018). *Analysis of Protein Translocation at the Interface between the Malaria Parasite Plasmodium falciparum and its Host Cell* [doctoralThesis, Staats- und Universitätsbibliothek Hamburg Carl von Ossietzky]. https://ediss.sub.uni-hamburg.de/handle/ediss/7859

Rénia, L., Grüner, A. C., Mauduit, M., & Snounou, G. (2013). Vaccination using normal live sporozoites under drug treatment. *Methods in Molecular Biology (Clifton, N.J.)*, *923*, 567–576. https://doi.org/10.1007/978-1-62703-026-7_39

Richard Carter, K. N. M. (2002). *Evolutionary and historical aspects of the burden of malaria*.

Rieger, H., Yoshikawa, H. Y., Quadt, K., Nielsen, M. A., Sanchez, C. P., Salanti, A., Tanaka, M., & Lanzer, M. (2015). Cytoadhesion of Plasmodium falciparum–infected erythrocytes to chondroitin-4-sulfate is cooperative and shear enhanced. *Blood*, *125*(2), 383–391. https://doi.org/10.1182/blood-2014-03-561019

Ross, R. (1897). Observations on a Condition Necessary to the Transformation of the Malaria Crescent. *British Medical Journal*, *1*(1883), 251–255.

Rossati, A., Bargiacchi, O., Kroumova, V., Zaramella, M., Caputo, A., & Garavelli, P. L. (2016). Climate, environment and transmission of malaria. *Le Infezioni in Medicina*, *24*(2), 93–104.

Rowe, J. A., Claessens, A., Corrigan, R. A., & Arman, M. (2009). Adhesion of Plasmodium falciparum-infected erythrocytes to human cells: Molecular mechanisms and therapeutic implications. *Expert Reviews in Molecular Medicine*, *11*. https://doi.org/10.1017/S1462399409001082

Scherf, A., Lopez-Rubio, J. J., & Riviere, L. (2008). Antigenic Variation in Plasmodium falciparum. *Annual Review of Microbiology*, *62*(1), 445–470. https://doi.org/10.1146/annurev.micro.61.080706.093134

Seixas, E., Gozzelino, R., Chora, A., Ferreira, A., Silva, G., Larsen, R., Rebelo, S., Penido, C., Smith, N. R., Coutinho, A., & Soares, M. P. (2009). Heme oxygenase-1 affords protection against noncerebral forms of severe malaria. *Proceedings of the National Academy of Sciences of the United States of America*, *106*(37), 15837–15842. https://doi.org/10.1073/pnas.0903419106

Senczuk, A. M., Reeder, J. C., Kosmala, M. M., & Ho, M. (2001). Plasmodium falciparum erythrocyte membrane protein 1 functions as a ligand for P-selectin. *Blood*, *98*(10), 3132–3135. https://doi.org/10.1182/blood.v98.10.3132

Shute. (1945). *An investigation into the number of sporozoites found in the salivary glands of Anopheles mosquitoes*.

Sidjanski, S., & Vanderberg, J. P. (1997). Delayed migration of Plasmodium sporozoites from the mosquito bite site to the blood. *The American Journal of Tropical Medicine and Hygiene*, *57*(4), 426–429. https://doi.org/10.4269/ajtmh.1997.57.426

Sissoko, M. S., Healy, S. A., Katile, A., Omaswa, F., Zaidi, I., Gabriel, E. E., Kamate, B., Samake, Y., Guindo, M. A., Dolo, A., Niangaly, A., Niaré, K., Zeguime, A., Sissoko, K., Diallo, H., Thera, I., Ding, K., Fay, M. P., O'Connell, E. M., … Duffy, P. E. (2017). Safety and efficacy of PfSPZ Vaccine against Plasmodium falciparum via direct venous inoculation in healthy malaria-exposed adults in Mali: A randomised, double-blind phase 1 trial. *The Lancet. Infectious Diseases*, *17*(5), 498–509. https://doi.org/10.1016/S1473-3099(17)30104-4

Slomianny, C. (1990). Three-dimensional reconstruction of the feeding process of the malaria parasite. *Blood Cells*, *16*(2–3), 369–378.

Smith, J. D., Rowe, J. A., Higgins, M. K., & Lavstsen, T. (2013). Malaria's Deadly Grip: Cytoadhesion of Plasmodium falciparum Infected Erythrocytes. *Cellular Microbiology*, *15*(12). https://doi.org/10.1111/cmi.12183

South East Asian Artesuante Malaria Trial (SEAQUAMAT) group. (2005). Artesunate versus quinine for treatment of severe falciparum malaria: A randomised trial. *The Lancet*, *366*(9487), 717–725. https://doi.org/10.1016/S0140-6736(05)67176-0

Spielmann, T., Hawthorne, P. L., Dixon, M. W. A., Hannemann, M., Klotz, K., Kemp, D. J., Klonis, N., Tilley, L., Trenholme, K. R., & Gardiner, D. L. (2006). A cluster of ring stage-specific genes linked to a locus implicated in cytoadherence in Plasmodium falciparum codes for PEXEL-negative and PEXEL-positive proteins exported into the host cell. *Molecular Biology of the Cell*, *17*(8), 3613–3624. https://doi.org/10.1091/mbc.e06-04-0291

Sturm, A., Amino, R., van de Sand, C., Regen, T., Retzlaff, S., Rennenberg, A., Krueger, A., Pollok, J.-M., Menard, R., & Heussler, V. T. (2006). Manipulation of host hepatocytes by the malaria parasite for delivery into liver sinusoids. *Science (New York, N.Y.)*, *313*(5791), 1287–1290. https://doi.org/10.1126/science.1129720

Talman, A. M., Domarle, O., McKenzie, F. E., Ariey, F., & Robert, V. (2004). Gametocytogenesis: The puberty of Plasmodium falciparum. *Malaria Journal*, *3*, 24. https://doi.org/10.1186/1475-2875-3-24

Taylor, W. R. J., Cañon, V., & White, N. J. (2006). Pulmonary Manifestations of Malaria. *Treatments in Respiratory Medicine*, *5*(6), 419–428. https://doi.org/10.2165/00151829-200605060-00007

Theisen, M., Adu, B., Mordmüller, B., & Singh, S. (2017). The GMZ2 malaria vaccine: From concept to efficacy in humans. *Expert Review of Vaccines*, *16*(9), 907–917. https://doi.org/10.1080/14760584.2017.1355246

Thylur, R. P., Wu, X., Gowda, N. M., Punnath, K., Neelgund, S. E., Febbraio, M., & Gowda, D. C. (2017). CD36 receptor regulates malaria-induced immune responses primarily at early blood stage infection contributing to parasitemia control and resistance to mortality. *The Journal of Biological Chemistry*, *292*(22), 9394–9408. https://doi.org/10.1074/jbc.M117.781294

Tougan, T., Edula, J. R., Takashima, E., Morita, M., Shinohara, M., Shinohara, A., Tsuboi, T., & Horii, T. (2018). Molecular Camouflage of Plasmodium falciparum Merozoites by Binding of Host Vitronectin to P47 Fragment of SERA5. *Scientific Reports*, *8*(1), 5052. https://doi.org/10.1038/s41598-018-23194-9

Tse, E. G., Korsik, M., & Todd, M. H. (2019). The past, present and future of anti-malarial medicines. *Malaria Journal*, *18*(1), 93. https://doi.org/10.1186/s12936-019-2724-z

Turner, L., Lavstsen, T., Berger, S. S., Wang, C. W., Petersen, J. E. V., Avril, M., Brazier, A. J., Freeth, J., Jespersen, J. S., Nielsen, M. A., Magistrado, P., Lusingu, J., Smith, J. D., Higgins, M. K., & Theander, T. G. (2013). Severe malaria is associated with parasite binding to endothelial protein C receptor. *Nature*, *498*(7455), 502–505. https://doi.org/10.1038/nature12216

van den Brand, J. M. A., Haagmans, B. L., van Riel, D., Osterhaus, A. D. M. E., & Kuiken, T. (2014). The Pathology and Pathogenesis of Experimental Severe Acute Respiratory Syndrome and Influenza in Animal Models. *Journal of Comparative Pathology*, *151*(1), 83–112. https://doi.org/10.1016/j.jcpa.2014.01.004

Viebig, N. K., Wulbrand, U., Förster, R., Andrews, K. T., Lanzer, M., & Knolle, P. A. (2005). Direct Activation of Human Endothelial Cells by Plasmodium falciparum-Infected Erythrocytes. *Infection and Immunity*, *73*(6), 3271–3277. https://doi.org/10.1128/IAI.73.6.3271-3277.2005

Vinnemeier, C., & Rolling, T. (2018). Prophylaxe und Therapie der Malaria: Aktuelle Empfehlungen. *DMW - Deutsche Medizinische Wochenschrift*, *143*(07), 472–475. https://doi.org/10.1055/s-0044-100818

Wang, R., Smith, J. D., & Kappe, S. H. I. (2009). Advances and challenges in malaria vaccine development. *Expert Reviews in Molecular Medicine*, *11*, e39. https://doi.org/10.1017/S1462399409001318

Warrell, D. A., & Gilles, H. M. (2017). *Essential Malariology, 4Ed*. CRC Press.

Wassmer, S. C., Taylor, T. E., Rathod, P. K., Mishra, S. K., Mohanty, S., Arevalo-Herrera, M., Duraisingh, M. T., & Smith, J. D. (2015). Investigating the Pathogenesis of Severe Malaria: A Multidisciplinary and Cross-Geographical Approach. *The American Journal of Tropical Medicine and Hygiene*, *93*(3_Suppl), 42–56. https://doi.org/10.4269/ajtmh.14-0841

WHO. (2015). *Guidelines for the Treatment of Malaria. Third Edition*. World Health Organization.

WHO. (2023). *World malaria report 2023*. https://www.who.int/teams/global-malaria-programme/reports/world-malaria-report-2023

World Health Organization. (2000). Severe falciparum malaria. *Transactions of The Royal Society of Tropical Medicine and Hygiene*, *94*(Supplement_1), 1–90. https://doi.org/10.1016/S0035-9203(00)90300-6

Wright, G. J., & Rayner, J. C. (2014). Plasmodium falciparum erythrocyte invasion: Combining function with immune evasion. *PLoS Pathogens*, *10*(3), e1003943. https://doi.org/10.1371/journal.ppat.1003943

Wu, J., Cai, B., Sun, W., Huang, R., Liu, X., Lin, M., Pattaradilokrat, S., Martin, S., Qi, Y., Nair, S. C., Bolland, S., Cohen, J. I., Austin, C. P., Long, C. A., Myers, T. G., Wang, R., & Su, X. (2015). Genome-Wide Interactions of Mouse-Plasmodium yoelii Parasite and Identification of Regulators of Type I Interferon Response. *Cell Reports*, *12*(4), 661–672. https://doi.org/10.1016/j.celrep.2015.06.058

Wu, Y. (2023). *The role of human endothelium and microRNAs as active participants in the immune response and pathogenesis during malaria* [doctoralThesis, Staats- und Universitätsbibliothek Hamburg Carl von Ossietzky]. https://ediss.sub.uni-hamburg.de/handle/ediss/10442

Yipp, B. G., Hickey, M. J., Andonegui, G., Murray, A. G., Looareesuwan, S., Kubes, P., & Ho, M. (2007). Differential roles of CD36, ICAM-1, and P-selectin in Plasmodium falciparum cytoadherence in vivo. *Microcirculation (New York, N.Y.: 1994)*, *14*(6), 593–602. https://doi.org/10.1080/10739680701404705

Zhou, J., Zhou, Q., Zhang, T., & Fan, J. (2021). C7ORF41 Regulates Inflammation by Inhibiting NF-κB Signaling Pathway. *BioMed Research International*, *2021*, 7413605. https://doi.org/10.1155/2021/7413605

Zlotnik, A., & Yoshie, O. (2000). Chemokines: A new classification system and their role in immunity. *Immunity*, *12*(2), 121–127. https://doi.org/10.1016/s1074-7613(00)80165-x

10. Supplements

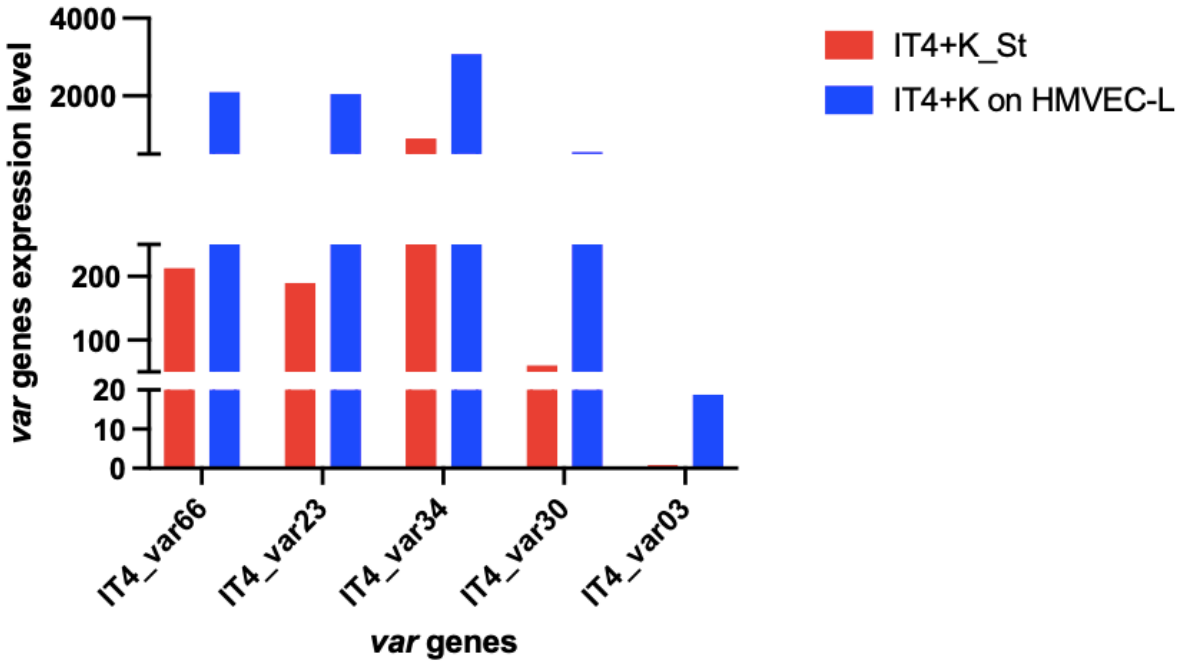

Supp. figure 1 significantly overexpressed var genes after enrichment of IT4 culture over HMVEC-L.

Supp. table 1 significantly overexpressed var genes after enrichment of IT4 culture over HMVEC-L:

gene ID	*var* gene	baseMeanControl	baseMeanEnriched	foldChange	UPS
PfIT_040025500	IT4_var66	212,9159874	2096,206535	9,85425625	C1
PfIT_040017000	IT4_var23	189,4527361	2048,128204	10,81987364	C1
PfIT_080014100	IT4_var34	897,0294768	3080,546184	3,434971422	C1
PfIT_040025800	IT4_var30	60,03153009	554,7280266	9,236676561	
PfIT_140006400	IT4_var03	0,827155256	18,78032914	23,01674346	A3

Supp. table 2 significantly overexpressed erythrocyte membrane protein 1-like after enrichment of IT4 culture over HMVEC-L:

gene ID	*var* gene	baseMeanControl	baseMeanEnriched	foldChange
PfIT_080005200	no name	0	8,8328135	57,24119094
PfIT_110005800	no name	0	3,383855615	22,4830787

11. Acknowledgements

Ich widme diese Arbeit meiner Mutter Ilona Weber-Schell.
Ich wünschte, du wärest nicht nur bei Beginn, sondern auch bei Abschluss der Arbeit an meiner Seite gewesen.

Die Vollendung der Dissertation wäre alleine nicht möglich gewesen und so möchte ich mich an dieser Stelle bei allen bedanken, die mich auf dem Weg unterstützt haben:

Ich danke Prof. Dr. Iris Bruchhaus für die großartige Betreuung und die Hilfe in allen Lebenslagen.

Ich danke Prof. Dr. Jürgen May für die unkomplizierte und herzliche Betreuung.

Ich danke Dr. Nahla Galal Metwally für die stete Unterstützung tagtäglich im Labor und weit darüber hinaus.

Ich danke allen aktuellen und ehemaligen Mitgliedern der AG Wirt-Parasit-Interaktion. Danke Susann, Jerry, Yifan, Max, Philip, Torben, Barbara und Hanifeh.

Ich danke meiner Familie für den Rückhalt, die Geduld und die Liebe.
Danke Lutz und Toni, ihr seid mein Glück.

12. Curriculum Vitae

Entfällt aus datenschutzrechtlichen Gründen.

13. Declaration on Oath

Eidesstaatliche Versicherung

Ich versichere ausdrücklich, dass ich die Arbeit selbständig und ohne fremde Hilfe verfasst, andere als die von mir angegebenen Quellen und Hilfsmittel nicht benutzt und die aus den benutzten Werken wörtlich oder inhaltlich entnommenen Stellen einzeln nach Ausgabe (Auflage und Jahr des Erscheinens), Band und Seite des benutzten Werkes kenntlich gemacht habe.
Ferner versichere ich, dass ich die Dissertation bisher nicht einem Fachvertreter an einer anderen Hochschule zur Überprüfung vorgelegt oder mich anderweitig um Zulassung zur Promotion beworben habe.
Ich erkläre mich einverstanden, dass meine Dissertation vom Dekanat der Medizinischen Fakultät mit einer gängigen Software zur Erkennung von Plagiaten überprüft werden kann.

Unterschrift: _____